An Investigation of Photodynamic Inactivation of Gram-positive and Gram-negative Bacteria for Water Disinfection Using a Cationic Porphyrin

A thesis submitted to Dublin City University in fulfilment of the requirements for the award of the degree of Doctor of Philosophy

by

Thayse Marques Passos, B.Sc., M.Sc.

School of Biotechnology

Dublin City University,

Dublin 9,

Ireland.

Research supervisors:

Dr. Bríd Quilty
Emeritus Professor
School of Biotechnology
Dublin City University,
Dublin 9,
Ireland.

Dr. Mary Pryce
Associate Professor
School of Chemical Sciences
Dublin City University,
Dublin 9,
Ireland.

January 2018

I hereby certify that this material, which I now submit for assessment on the programme of study leading to the award of Ph.D. is entirely my own work, and that I have exercised reasonable care to ensure that the work is original, and does not to the best of my knowledge breach any law of copyright, and has not been taken from the work of others save and to the extent that such work has been cited and acknowledged within the text of my work.

Signed: _____

ID No.: _____

Date: _____

Acknowledgments

I am grateful to my family. Despite the distance, they always tried to be understanding and supportive regarding my decision to pursue a new life abroad. A special thank you to my mom, who encouraged me to pursue my dreams and to be very dedicated to everything I do. You have inspired me to be strong and persevere in the most difficult times.

I would like to express my sincere appreciation to my supervisors, Dr. Bríd Quilty and Dr. Mary Pryce, for the all the guidance, patience, motivation, and immense knowledge transmitted throughout the last four years.

To my colleagues from the School of Biotechnology and the School of Chemical Sciences, thank you for all the support, friendship and parties. A special thanks to my laboratory colleague, Declan McGlade, for the experiences shared and entertainment in the lab. Huge thanks to my friend and colleague, Flávio Ferreira, with whom I learned and shared invaluable things throughout the last years.

I would like to thank my friends, who made this journey lighter and joyful. With special thanks to my beloved Rafael, Mariana, Míriam and Aoibheann.

To Declan Smith, thank you for all the care and support, especially in the last few months.

To all the members of staff from the School of Biotechnology and the School of Chemical Sciences, thank you for the technical assistance and for all the help and support in the teaching labs. With special mention to Allison Tipping, Monica McGorgam, Kasia Zdrojewska, Deirdre Curtin, David Cunningham, Aisling McCarthy and Una Prendergast.

I gratefully acknowledge the funding received towards my PhD from Coordenação de Aperfeiçoamento de Pessoal de Nível Superior – CAPES – Science Without Boarders (SWB) PhD fellowship.

Table of Contents

List of abbreviations 1
List of Tables 3
List of Figures 5
Abstract 9
1. Introduction 10
1.1 Water supply and quality 11
1.2 Water treatment 13
1.2.1 Chlorination 15
1.2.2. Ozonation 17
1.2.3. Hydrogen Peroxide 17
1.2.4 Phototreatments 18
1.3 Photodynamic inactivation 21
1.3.1 Photosensitisers 24
1.3.2 Light source 27
1.3.3 Antimicrobial photodynamic inactivation 27
1.3.2.1 Effect of photosensitisers on bacterial cells 35
Cytoplasmic membrane 36
Proteins 37
Nucleic acids 37
1.4 Photodynamic inactivation for water disinfection 37
1.5 Aim and objectives of the project 43
2. Materials and Methods 44
2.1 Materials 45
2.1.1 Photosensitiser 45
2.1.2 Bacteria 45
2.1.3 Buffer 47
2.1.4 Growth media 47
2.1.5 Chemicals 47
2.1.6 Lamps 48
2.2 Methods 49
2.2.1 Experimental System 49
2.2.1.1 Medium 49
2.2.1.2 Porphyrin 50
Extinction coefficient calculation 50
Ultraviolet-visible spectroscopy 50
Reactive oxygen species (ROS) production 50
Near-infrared spectroscopy - singlet oxygen generation 51
Evaluation of TMPyP mutagenicity– Ames test 52
2.2.1.3 Vessels 53

96-well plates 53
Glass petri dishes 54
2.2.1.4 Light dose calculation 54
2.2.2 Inoculum preparation 56
2.2.3 Methods used to monitor the response of the bacteria to PDI. 56
Streak plate technique 56
Drop plate technique 56
Pour plate technique 57
Inactivation rate 57
2.2.4 Antibiotic profile of the bacteria 57
Kirby-Bauer disc diffusion method 57
Minimum Inhibitory Concentration 59
2.2.5 Pigment production measurement 59
2.2.6 Bacterial cell aggregation measurement 60
Settling method 60
Microscopic method 60
2.2.7 Porphyrin immobilisation 61
Glass bead coating 61
Polymeric matrix incorporation 62
Monitoring TMPyP leaching 63
2.2.8 PDI with immobilised porphyrin 63
PDI with hydrogels 63
PDI with glass beads 63
2.2.9 Data Analysis 64
3. Results 65
3.1 Development of the experimental system 66
3.1.1 The porphyrin TMPyP 66
3.1.1.1 UV-visible spectroscopy 67
3.1.1.2 Extinction coefficient calculation 67
3.1.1.3 Reactive oxygen species (ROS) production 68
3.1.1.4 NIR-spectroscopy 69
3.1.1.5 Evaluation of TMPyP mutagenicity – Ames test 70
3.1.2 Medium 71
3.1.3 The experimental vessel 71
Experiments in 96-well-plates 71
3.2 Investigating the response of Gram-negative and Gram-positive bacteria to PDI . 78
Monochromatic lamp (λ=525nm) 78
Multichromatic lamp (λ>400nm) 79
Dichromatic lamp (λ= 430 and 660nm) 80
3.2.1 Gram-negative bacteria 80
3.2.2 Gram-positive Bacteria 87

3.2.3 Antibiotic profile of the bacteria 90
3.2.3.1 Kirby-Bauer disc diffusion method 90
3.2.3.2 Minimum Inhibitory Concentration 92
3.3 A study of factors influencing the response of E. coli and Pseudomonas species to PDI 93
3.3.1 Pigment production measurement 93
3.3.2 Aggregation and settling of bacterial cells 96
3.3.3 Studies with cocultures 98
PDI with cocultures 98
MIC of cocultures 101
3.3.4 PDI with the immobilised porphyrin 103
3.3.4.1 PDI with Glass beads 103
3.3.4.2 PDI with hydrogels 104
3.3.4.3 TMPyP leaching in the medium 107
4. Discussion 109
4.1 Development of the experimental system 110
4.2 Response of bacteria to PDI 115
4.3 Factors governing environmental resistance 124
4.4 Factors influencing the practical application of PDI 129
4.5 Immobilisation of the porphyrin 131
5. Conclusions and Future Work 133
6. References 135
Appendix I 160
Appendix II 164

List of abbreviations

ATP	Adenosine Triphosphate
ARB	Antibiotic resistant bacteria
BPO	Benzoyl peroxide
CFU	Colony Forming Unities
CLSM	confocal laser scanning microscope
DBP	Disinfection by product
DNA	Deoxyribonucleic Acid
DO	Dissolved oxygen
DPBF	1,3-Diphenylisobenzofuran
DSM	German Collection of Microorganisms and Cell Cultures
EGDMA	ethylene glycol dimethacrylate
EPA	Environmental protection agency
EPS	Extracellular polymeric substances
EU	European Union
GC	Gas Chromatography
HEMA	2-Hydroxyethyl methacrylate
HOMO	Highest occupied molecular orbital
IC	Internal conversion
ISC	Intersystem crossing
J	Joules
LED	Light-Emitting Diode
LPS	Lipopolysaccharides
LUMO	Lowest occupied molecular orbital
MAA	Methacrylic acid
MIC	Minimum Inhibitory Concentration
MS	Mass Spectrometry
mW	MilliWatts
OD	Optical Density
PBS	Phosphate Buffer Saline
PDT	Photodynamic Therapy
PDI	Photodynamic Inactivation
PI	Propidium Iodide
PS	Photosensitiser
RNA	Ribonucleic Acid
ROS	Reactive Oxygen Specie

RPM	Rotations per minute
TLC	Thin Layer Chromatography
TMPyP	5,10,15,20-Tetrakis(N-methyl-4-pyridyl)-21,23H-porphyrin tetratosylate
UNICEF	United Nations Children's Emergency Fund
UV	Ultraviolet
UVA	Long Wave Ultraviolet
UVC	Short Wave Ultraviolet
W	Watts
WHO	World Health Organization

List of Tables

Table 1.1 - EU Drinking Water Directive (98/83/EEC) microbiological parameters..... 13
Table 1.2 – Waterborne pathogens relative resistance to chlorine and infectivity (Adapted from WHO, 2008). 16
Table 1.3 – Microorganisms investigated through the photoinactivation processes. ... 30
Table 2.1 - Properties of the porphyrin TMPyP. 45
Table 2.2 - Bacterial strains used in the study. 46
Table 2.3. Growth media used in the different experiments. 47
Table 2.4 – Chemicals used in this study. 48
Table 2.5 – Antibiotic discs used for the antimicrobial susceptibility test. 58
Table 3.1 – Average number of revertant wells per sample analysed. 71
Table 3.2 – The response of E. coli T37-1 and P. putida DSM 6125 to TMPyP (0, 0.625, 1.25, 2.5, 5, 10 and 20 μM) under the irradiation of the monochromatic lamp (λ=525nm). 72
Table 3.3 – The response of E. coli T37-1 and P. putida DSM 6125 to TMPyP (0, 0.625, 1.25, 2.5, 5, 10 and 20 μM) under the irradiation of the multichromatic lamp (λ≥400nm). 73
Table 3.4. Length of time/dosage necessary for a 3-log reduction and total deactivation of bacteria under exposure to the monochromatic multi-LED lamp (λ=525nm). ... 77
Table 3.5. Length of time/dosage necessary for a 5-log reduction and total deactivation of bacteria from Enterobacteriaceae family, under exposure to the Dichromatic lamp (430 and 660 nm) with TMPyP at 3.65μM. 83
Table 3.6. Length of time/dosage necessary for a 5-log reduction and total deactivation of Pseudomonads, under exposure to the Dichromatic lamp (430 and 660 nm) with TMPyP at 3.65μM. 86
Table 3.7. Length of time/dosage necessary for a 5-log reduction and total deactivation of Gram-positive bacteria, under exposure to the Dichromatic lamp (430 and 660 nm) with TMPyP at 3.65μM. 89
Table 3.8 – Zone of inhibition (mm) for the antibiotics disc of: imipenem (10μg); ampicillin (10μg); ciprofloxacin (10μg); cefotaxime (30μg); tetracycline (30μg); erytromycin (30μg); and vancomycin (30μg) against 12 different bacterial strains. 91
Table 3.9 – Minimum Inhibitory Concentration of the antibiotics Tetracycline and Ampicillin against 12 different bacterial strains. 92
Table 3.10. Length of time/dose necessary for a 5-log reduction and total deactivation of E. coli T37-1 and P. fluorescens DSM 50090, under exposure to the dichromatic lamp (430 and 660 nm) with TMPyP coated glass beads. 104

Table 3.11. Length of time/dose necessary for a 5-log reduction and total deactivation of E. coli T37-1 and P. fluorescens DSM 50090, under exposure to the Dichromatic lamp (430 and 660 nm) with TMPyP incorporated to hydrogels at 3.65, 5 and 10μM. 106
Table AI – TMPyP absorbance and respective concentration in PBS at 422nm. 162

List of Figures

Figure 1.1 – Water cycle, from precipitation to usage and disposal (RobecoSAM, 2015). 13
Figure 1.2 – Typical drinking water treatment plant (Source: University of Alberta - http://srwp.ualberta.ca/Research-Areas/Drinking-Water-Treatment). 14
Figure 1.3 – Example of a wastewater treatment plant (Source: The water treatments). 15
Figure 1.4 – Visible and ultraviolet light spectrum. 18
Figure 1.5 – Chart illustrating the application of SODIS for household water disinfection (McGuigan et al., 2012). 19
Figure 1.6 – Illustration of the mechanism of photocatalytic disinfection with TiO_2 irradiated by UV light (Wang et al., 2013). 20
Figure 1.7- Jablonski diagram showing the photochemical mechanisms involved in the photodynamic action (Hamblin and Abrahamse, 2016). 22
Figure 1.8 – Basic chemical structure of a natural porphyrin (A) and a synthetic porphyrin (B) (Stojiljkovic et al., 2001). 25
Figure 1.9 - Typical UV-visible spectrum of a porphyrin with an insert showing enlargement of the Q- band region between 480-720 nm (Giovanetti, 2012). 25
Figure 1.10 - Schematic representation of some of PDI advantages over antibiotics, in the deactivation of microorganisms (Dai et al., 2009). 28
Figure 1.11 - Schematic representation of the different cellular envelopes of Gram-negative bacteria (A) and Gram-positive bacteria (B) (Yin et al., 2016). 34
Figure 1.12 - Example of a photosensitiser mechanism of action on the cytoplasmic membrane of S. aureus cells (Komagoe et al., 2011). 35
Figure 1.13 - Circulating water photoreactor system used by Bonnet et al., 2006. a—membrane; b—water jacket, continuous flow, infra-red filter; c—light source; d—air pump; e—bacterial air filter; f—3-way tap/pressure release; g—2-way taps; h—frit for aeration; j—peristaltic pump; k—reservoir. 42
Figure 2.1 – Chemical structure of the porphyrin TMPyP. 45
Figure 2.2 – Lamps used for the PDI experiments. (A) Monochromatic 525nm LED lamp (B) Visible light (400 -700 nm) LED (C) Dichromatic (460 and 630 nm) LED lamp. 49
Figure 2.3 – Schematic representation of the graph for the integrated emission calculation. 52
Figure 2.4 – Representation of the 96-well plate with the treatments distribution in the central area. 54

Figure 2.5 – Representation of the light incidence, from the monochromatic 525nm LED lamp and the visible (λ ≥400nm) LED lamp over the 96-well plates. 55
Figure 2.6 – Representation of the light incidence, from the dichromatic (430 and 660nm) lamp over the petri dishes. 55
Figure 2.7 – Halo of inhibition from the Kirby-Bauer disc diffusion method. 58
Figure 2.8 - 96 well-plate set up for MIC determination. Two-fold dilutions were carried out in series, from the left to the right. 59
Figure 2.9 – TMPyP coated glass beads (5mm). 61
Figure 2.11 – TMPyP immobilised into a hydrogel polymeric matrix. A – hydrogel inside the Petri dish mould and B – hydrogel film. 63
Figure 3.1 – UV-visible spectrum of the wavelength absorbance for the porphyrin TMPyP in PBS. Insert shows the four Q-bands. 67
Figure 3.2 – Calibration curve of TMPyP absorbance versus its concentration at 422nm (y=71541x+0.0087, with R^2 = 0.9989). 68
Figure 3.3. ROS production by the porphyrin TMPyP at the concentrations 0, 3.65, 5 and 10μM. Hydrogen peroxide (H_2O_2) was used as a positive control. 69
Figure 3.5– 96-well plate showing the revertant (yellow) and non-revertant (purple) wells observed in AMES-MOD ISO™ test. 70
Figure 3.6. Logarithmic reduction in the number of bacteria treated with porphyrin TMPyP (10μM solution) following 60 minutes of exposure to the monochromatic lamp (λ=525nm). 75
Figure 3.7. Logarithmic reduction in the number of bacteria treated with porphyrin TMPyP (20μM solution) following 60 minutes of exposure to the monochromatic lamp (λ=525nm). 76
Figure 3.8– Cell concentration, in logarithmic scale, of 8 bacteria after 180 minutes of exposure to the monochromatic lamp (λ=525nm). 79
Figure 3.9 – Cell concentration, in logarithmic scale, of 8 bacteria after 180 minutes of exposure to the multichromatic lamp (λ≥400nm). 79
Figure 3.10 – Logarithmic reduction in the number of 5 Enterobacteriaceae bacteria following exposure to the Dichromatic lamp with TMPyP at 3.65 (a) 5 (b) and 10μM (c) 82
Figure 3.11 – Logarithmic reduction in the cell concentration of Pseudomonas spp. bacteria after exposure to the Dichromatic lamp with TMPyP at 3.65μM (a), 5μM (b) and 10μM (c). 85
Figure 3.12 – Logarithmic reduction in the cell concentration of B. subtilis DSM 10 and S. aureus DSM 799 bacteria after exposure to the dichromatic lamp with TMPyP at 3.65μM (a), 5μM (b) and 10μM (c). 88

Figure 3.13 - UV–Visible spectra of the supernatant of the four different Pseudomonas strains grown in Luria-Bertani (LB) medium. 94
Figure 3.14 - UV–Visible spectra of the supernatant of the four different Pseudomonas strains grown in M9 medium. 94
Figure 3.15 - UV–Visible spectra of the supernatant of the four different Pseudomonas strains grown in King A medium. 95
Figure 3.16 - UV–Visible spectra of the supernatant of the four different Pseudomonas strains grown in King B medium. 95
Figure 3.17 - UV–Visible spectra of the supernatant of the four different Pseudomonas strains grown in nutrient broth. 96
Figure 3.18 – Percentage reduction in optical density after 60 min due to aggregation/settling of bacterial cells. 97
Figure 3.19 - CLSM micrographs (x100) of P. putida CP1 (left) and P. putida DSM 6125 (right) planktonic cells after overnight growth in nutrient broth. 97
Figure 3.20 - CLSM micrographs (Z-stack – 100x) of P. fluorescens DSM 50090 (left) and P. aeruginosa PAO1 (right) agglomerates after overnight growth in nutrient broth. 98
Figure 3.21 - Logarithmic reduction in the cell concentration of a coculture (grown together) of E. coliT37-1 and P. aeruginosa PAO1 after exposure to the dichromatic lamp with TMPyP at 3.65μM. The orange line shows the numbers for the total counts and the red line shows the numbers for E. coliT37-1 only. The dotted line shows the possible numbers P. aeruginosa PAO1, obtained by subtracting the total count in NA by the McConkey agar counts. 99
Figure 3.22 - Logarithmic reduction in the cell concentration of a co-culture (grown separately) of E. coliT37-1 and P. aeruginosa PAO1 after exposure to the Dichromatic lamp with TMPyP at 3.65μM. The orange line shows the numbers for the total counts and the red line shows the numbers for E. coliT37-1 only. The dotted line shows the possible numbers P. aeruginosa PAO1, obtained by subtracting the total count in NA by the McConkey agar counts. 100
Figure 3.23. CLSM micrographs (x100) of the co-culture of P. aeruginosa PAO1 and E. coliT37-1 after growing together overnight in nutrient broth and stained with SYTO9. 100
Figure 3.24 - Logarithmic reduction in the cell concentration of E. coli T37-1 and P. fluorescens DSM50090 after exposure to the dichromatic lamp with the TMPyP glass beads. 103
Figure 3.25 - Logarithmic reduction in the cell concentration of E. coli T37-1 after exposure to the Dichromatic lamp with the polymer immobilised TMPyP at the concentrations of 3.65, 5 and 10μM. 104

For P. fluorescens (Fig. 3.27), the lowest concentration of TMPyP immobilised to the hydrogel, 3.65 105
Figure 3.26 - Logarithmic reduction in the cell concentration of P. fluorescens DSM50090 after exposure to the Dichromatic lamp with the polymer immobilised TMPyP at the concentrations of 3.65, 5 and 10μM. 105
Figure 3.27 – UV-vis spectra of the PBS suspension during PDI with the hydrogel at 10μM. 107
Figure 3.28 – UV-vis spectra of the PBS suspension during PDI with the glass beads. 108

Abstract

An Investigation of Photodynamic Inactivation of Gram-Positive and Gram-Negative Bacteria for Water Disinfection Using a Cationic Porphyrin

Thayse Marques Passos, School of Biotechnology, Dublin City University

The photodynamic inactivation of bacteria in water has been gaining interest in recent years. The process involves using a light source, which can be sunlight, to activate a photosensitiser. The reactive oxygen species generated can kill bacterial cells. A laboratory scale system was developed to investigate the photodynamic inactivation of Gram-positive and Gram-negative bacteria in water using as photosensitiser the porphyrin 5,10,15,20-tetrakis(N-methyl-4-pyridyl)-21H, 23H-porphine (TMPyP). Preliminary investigations were performed in 96-well plates. Later experiments were carried out in 60x15 mm glass Petri dishes. The light sources used were light-emitting diode (LED) lamps with wavelengths in the range 400 – 700nm. TMPyP (3.65uM – 10uM) in PBS was evaluated against the Gram-negative bacteria *Escherichia coli* T37-1, *Escherichia coli* DSM 498, *Escherichia coli* DSM 1103, *Shigella sonnei* DSM 5570, *Salmonella enterica* DSM 17058, *Pseudomonas putida CP1*, *Pseudomonas putida* DSM 6125, *Pseudomonas fluorescens* DSM 50090*, Pseudomonas aeruginosa PAO1,* and *Enterobacter aerogenes* DSM 30053 and the Gram-positive bacteria *Staphylococcus aureus* DSM 799 *and Bacillus subtilis* DSM 10. The inoculum size in all cases was 10^5 CFU/ml. The response of the bacteria was monitored using the plate count technique. The time required to kill the bacteria ranged from 30 minutes to 90 minutes depending on the organism and the concentration of TMPyP. Increased resistance observed with *Pseudomonas* species was attributed to cell aggregation. Mixed culture studies showed that when aggregating strains of *Pseudomonas* were co-cultured with *E. coli*, the resistance of *E. coli* to the treatment was increased. The incorporation of TMPyP onto glass beads and a polymeric matrix of methacrylate was investigated to enhance the application of the technology for water disinfection. The response showed the potential of this system as an alternative environmentally friendly approach for water disinfection.

1. Introduction

1.1 Water supply and quality

The availability of safe water is of major importance for public health, being essential for drinking, food production, domestic use, industrial and recreational purposes. The United Nations General Assembly, in 2010, recognised access to water and sanitation as a human right, meaning that every human being has the right to access safe, sufficient and affordable water for household and personal uses (Resolution A/RES/64/292, UN, 2010).

Access to safe drinking-water is extremely important not only for health, but also for the development of a community. Research has shown that investments in the improvement of water supplies and sanitation of a region can lead to a series of economic benefits, since the reduction in the costs associated with health, counterbalances the costs of undertaking the basic sanitation interventions (WHO, 2011).

However, given the global increase in demand for water, we rely on effective treatment systems to ensure a safe supply for domestic and industrial use. We also rely on effective wastewater treatment to ensure that our water supply is sustained and that water contamination is minimised. Modern age water treatment technologies are well established, however, water contamination continues to be a problem, for a variety of reasons.

Overpopulation, lack of hygiene and sanitation, industrial development and the expansion of the consumer society are the major contributors to increased contamination of water systems. A large proportion of the world's population still have no sustainable access to basic sanitation. The World Health Organization (WHO) and the United Nations Children`s Fund (UNICEF) Joint Monitoring Program (JMP) reported that in 2010, in the whole world, only 12% of rural residents had their sanitation facilities linked to sewers. While in urban areas the number went up to 60%, summing up to 2.5 billion people who still use unimproved sanitation facilities or have to defecate in the open. This is a major and alarming problem since different types of diseases, such as diarrhea, cholera, dysentery, typhoid and guinea worm infection can be transmitted via contaminated water (WHO/UNICEF, 2010).

Generally, the major microbial risks are related to the consumption of water that is contaminated with faeces from humans or animals, since the faecal matter can contain pathogenic bacteria, viruses, protozoa and helminths. Peaks in the concentration of pathogens in water can increase the risk of disease incidence, and therefore trigger outbreaks of waterborne disease. These outbreaks should be avoided since they can result in the simultaneous infection of a large number of people and consequently a high proportion of the community (Medema *et al.*, 2003)

Every year, over 200 million people around the world suffer with water related diarrheal illness, and it leads to 2.1 million deaths (WHO, 2011; Gray, 2014). Scientists have reported that this is not an exclusive problem of developing nations, since waterborne diseases are also affecting a considerable number of developed countries (Schoenen, 2002; Baldursson and Karanis, 2011).

Since the majority of waterborne diseases are transmitted by pathogenic microorganisms, it is crucial to guarantee the microbial safety of drinking-water supplies. The first step to prevent the contamination is based on the use of multiple barriers, from catchment (water resources) to user (distribution systems), in order to prevent the contamination or reduce the contamination of potable to levels unharmful to health (Davison *et al.*, 2002).

In order to provide safe potable water, there are standard approaches used to verify the water quality. Safe water should be free from pathogenic microorganisms. According to The European Communities (Drinking Water) (No. 2) Regulations, 2009, *Escherichia coli* and *Enterococci*, bacteria, which are indicators of faecal pollution, must be absent from 100ml sample of drinking water (see Table 1.1). Under certain circumstances, additional indicators may be considered, for example the spore former *Clostridium perfringens*, which needs to be measured in cases where the water source is surface water or influenced by surface water (EPA, 2010).

Control of these bacteria in effluent from wastewater treatment systems will also be required depending on the location of the discharge e.g. if the effluent is being discharged to bathing water and/or fisheries.

Table 1.1 also shows the parameters that are taken into account when analysing water sold into bottles or containers. In this case, the legislation is more strict, and different parametric values and an additional indicator are considered. *E. coli, Enterococci and P. aeruginosa* should be absent in 250ml of bottled water.

The microbial quality of water should be verified in the best way possible (frequency, location, indicators) to ensure the detection of contamination. For this reason, when sampling, the potential variations of water quality in the distribution system should be considered (i.e. location, rainfall) (WHO, 2011; WHO, 2017).

Table 1.1 - EU Drinking Water Directive (98/83/EEC) microbiological parameters.

Parameter	Parametric value
Escherichia coli	0/100ml
Enterococci	0/100ml
Colony count 22 °C	No abnormal change
Colony count 37 °C	20/100ml
*Escherichia coli**	0/250ml
*Enterococci**	0/250ml
*Pseudomonas aeruginosa**	0/250ml

*water offered for sale in bottles or containers.

1.2 Water treatment

There are two main types of water treatment systems. Systems that treat surface or ground water stocks, prior to use, in order to provide safe drinking water; and systems that treat wastewater (sewage), after use, in order to provide safe water for disposal. Figure 1.1 illustrates the water cycle, from precipitation to usage and disposal.

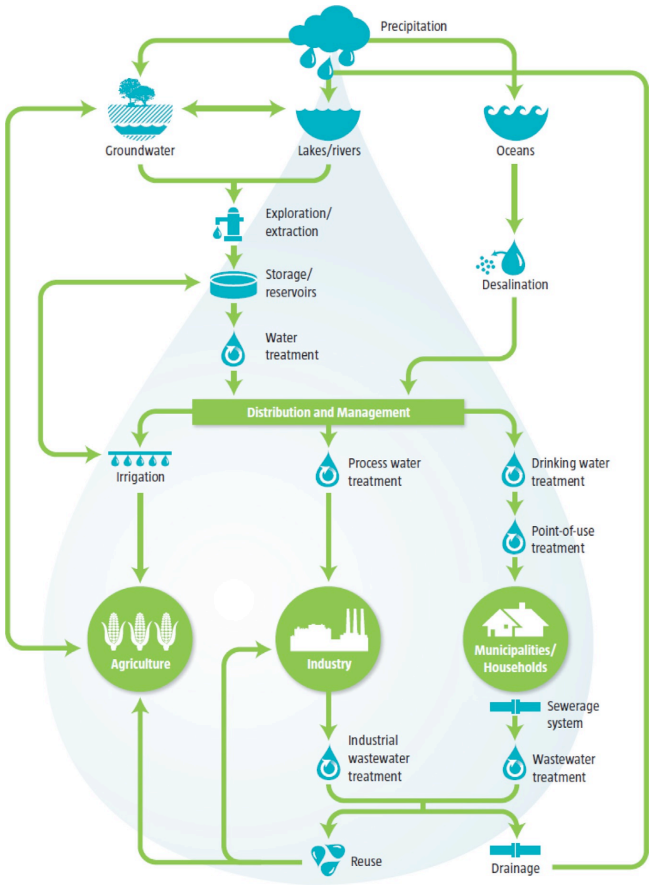

Figure 1.1 – Water cycle, from precipitation to usage and disposal (RobecoSAM, 2015).

For effective water treatment, water has to pass to a series of processes in order to guarantee its purity. For drinking water, the treatment is simpler than for wastewater. It typically happens in a chemically-assisted filtration plant, and the steps included are (EPA, 2002):

- a pre-treatment, where large material can be easily removed by passing the water through a bar screen;
- coagulation and flocculation, where chemicals added to the water will lead to the flocculation of the impurities (i.e. organic matter) present in it;
- sedimentation, where the flocs formed will settle and separate from the water body;
- filtration, where the water free from the sediments will pass through a filter (i.e. sand, charcoal) which will remove smaller particles that were not retained by the flocks; and
- disinfection, for the removal of any pathogenic bacteria that may still be present.

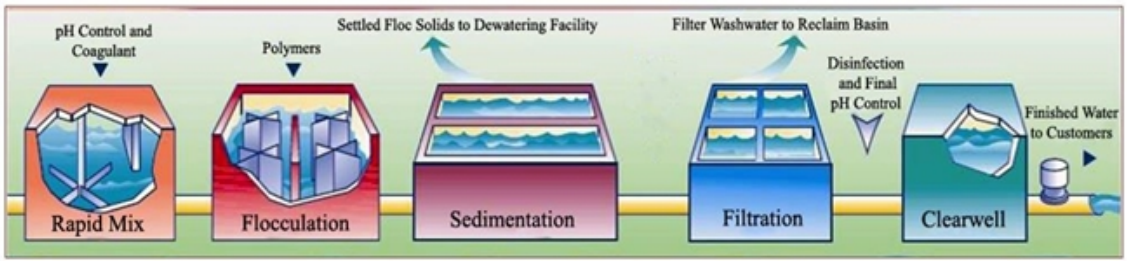

Figure 1.2 – Typical drinking water treatment plant (Source: University of Alberta - http://srwp.ualberta.ca/Research-Areas/Drinking-Water-Treatment).

For wastewater, the treatment process includes physical and chemical steps (Figure 1.3), which generally involves three stages: primary, secondary, and tertiary, as shown in Figure 1.2. The primary treatment involves the removal of suspended solids and organic matter, usually by sedimentation; the secondary includes aeration and activated sludge for the removal of biodegradable organic matter and nutrients; and the final tertiary step is mainly responsible for the water disinfection and pH adjustment (Leslie Grady *et al.,* 2011).

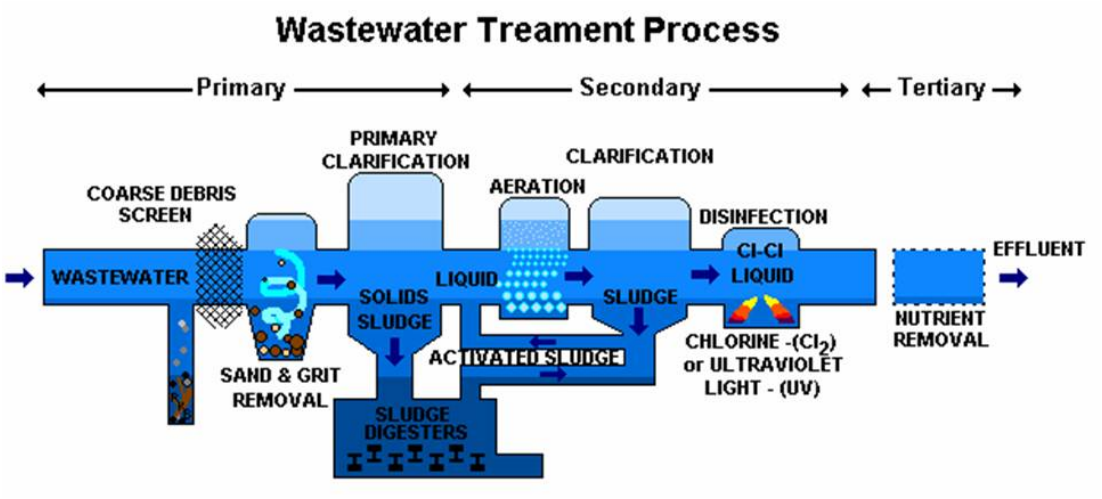

Figure 1.3 – Example of a wastewater treatment plant (Source: The water treatments).

An additional step, called the disinfection step or polishing step, is normally used in water treatment plants. This step is responsible for inactivating waterborne pathogenic microorganisms, like bacteria, viruses, and fungi. The selection of the disinfection technique to be used relies on important factors, such as the effectiveness of the antimicrobial agent in inactivating the pathogens; the formation of toxic disinfection by-products (DPBs); the quality of the water to be treated; and the health and safety implications of the disinfectant and the overall cost of the process.

Traditional water treatment methods are becoming insufficient in the modern age, and it has been pointed out by the Irish Environmental Protection Agency that the improvement of the disinfection standards is urgent and necessary (EPA, 2013).

Existing polishing steps for water treatment includes the use of chlorine, hydrogen peroxide, ozone and ultraviolet light (UV) (MWH, 2005; EPA, 2011).

1.2.1 Chlorination

In the early 1900s chlorine, a waste product from the manufacture of sodium hydroxide, was used for water disinfection, after Robert Koch had proved its efficacy in killing *Vibrio cholera.* Chlorine reacts with water molecules, forming HOCl (hypochlorous acid) and OCl^- (hypochlorite ions), which are harmful to the microbial cell membrane and to intracellular vital organelles (Gray, 2014).

Chlorination is the most widely used disinfection method nowadays, mainly due to its effectiveness and low cost, however, this is likely to change in the near future, because of its down sides. Among the problems caused by its use is the formation of disinfection by-products. These products, for example trihalomethanes (THM) and haloacetic acids (HAA), are formed due to the reaction between chlorine and natural organic matter

present in the water pollutants. They are of great concern due to their effect on human health, since they can be genotoxic and/or carcinogenic (Richardson et. 2007; Hansen *et al.*, 2016).

In addition to that, some pathogens have been found to present resistance to the treatment with chlorine. Table 1.2 shows pathogenic bacteria which can be transmitted through contaminated drinking-water (confirmed by epidemiological studies and case histories). These microorganisms are diverse in characteristics, behaviour and resistance to chlorine, presenting different levels of health significance (impact when an outbreak occurs) and infectivity (WHO, 2008). However, the fact that they can resist to chlorination is worrying, making this method an unreliable option for the disinfection of water.

Table 1.2 – Waterborne pathogens relative resistance to chlorine and infectivity (Adapted from WHO, 2008).

Pathogen	**Health significance**	**Persistence in water supplies**	**Resistance to chlorine***	**Relative infectivity****
Escherichia coli	high	moderate	low	Low
Pseudomonas aeruginosa	moderate	may multiply	moderate	low
Salmonella spp.	high	moderate	low	low
Shigella spp	high	short	low	high
Yersinia enterocolitica	moderate	long	low	low
Campylobacter spp.	high	moderate	low	moderate
Vibrio cholera	high	short to long	low	low
Mycobacterium spp.	low	may multiply	high	low

Note: This table contains pathogens for which there is some evidence of health significance related to their occurrence in drinking-water supplies. Health significance relates to the severity of impact, including association with outbreaks. Detection period for infective stage in water at 20° C: short, up to 1 week; moderate, 1 week to 1 month; long, over 1 month. * When the infective

stage is freely suspended in water treated at conventional doses and contact times and pH between 7 and 8. Low means 99% inactivation at 20° C generally in 30 min. **From experiments with human volunteers, from epidemiological evidence and from animal studies. High means infective doses can be 1–102 organisms or particles, moderate 102 –104 and low >104 (WHO, 2008).

1.2.2. Ozonation

The use of ozone (O_3) for drinking-water disinfection started in 1893, in the Netherlands, and the practice has been improved and spread across Europe since then. Ozone gas can react directly with water, through molecular ozone, or indirectly, where hydroxyl radicals are formed during ozone auto-decomposition, and act as an oxidizing agent. Usually, both mechanisms occur at the same time (Staehelin and Hoigné, 1985). The microbial inactivation occurs through a reaction with the oxidising agent, where the double bond of the cell wall and membrane lipids are damaged, with subsequent inactivation of the nucleic acids (Giese and Christensen, 1954).

This technique is also efficient in removing colour, odour and taste caused by the contaminants, however, the use of ozonation for water disinfection has some down sides, such as high electricity consumption and the need for production onsite, which makes it very expensive. Additionally, it also leads to the production of unwanted disinfection by-products (i.e. bromate) due to its reaction with natural organic matter (NOM) (Magara *et al.*, 1995; Black and Veatch Corporation, 2010; Gray, 2014).

1.2.3. Hydrogen Peroxide

Among the chemicals used for water disinfection, hydrogen peroxide is the least used due to limitations such as its instability when stored and problems when preparing concentrated solutions. It is able to deactivate microbial cells through oxidation; however, its efficacy is questionable. For this reason, it is normally applied in conjunction with other approaches, like ozone or UV light, enhancing the production of hydroxyl radicals. (USEPA, 1999).

Peroxone is the name of the process where hydrogen peroxide is added to ozonated water. This process increases the oxidation rate by increasing the decomposition rate of ozone, and it is effective in removing NOM and microorganisms present in water. However, the fact that peroxone is highly reactive makes its use inappropriate for drinking water treatment (Wolfe *et al.,* 1989; EPA, 2011).

1.2.4 Phototreatments

The use of light (Figure 1.4) in water treatment is not a novelty. While ultraviolet (UV) light has been used for at least 100 years, studies investigating the use of the visible part of the light spectra, as well as the combination of the visible and ultraviolet parts (SODIS) only started around the 1970's and 1980's, respectively (Henry *et al.*, 1910, Gerba *et al,* 1977, Acra *et al.,* 1984).

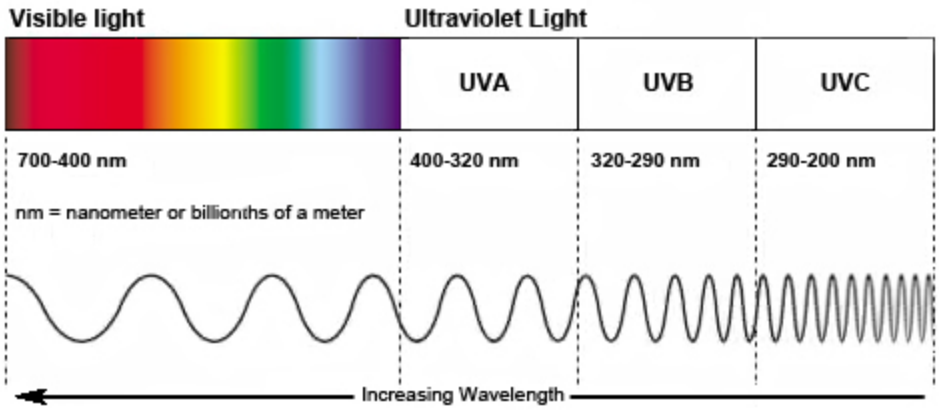

Figure 1.4 – Visible and ultraviolet light spectrum.

The application of UV light in water disinfection, also called photodisinfection was first used commercially in 1910, in a treatment plant in Marseille, France (Henry *et al.*, 1910). The ultraviolet (UV) is the region of the electromagnetic spectrum between the wavelengths 200 to 400 nm. It can be divided into three bands (see Figure 1.4), known as UVC (200–280 nm), UVB (280–320 nm) and UVA (320–400 nm). UVC has the shortest and most energetic wavelength radiation, with enormous potential for biological damage, since DNA absorbs the UV light intensively around 230 and 260 nm (Pattison and Davies, 2006; Hijnen *et al* 2006).

UV radiation induces biological death *via* two different mechanisms which are based on the damage caused to the nucleic acids (DNA/RNA) and to the proteins of the organism. The first mechanism is based on the direct absorption of UV photons by the nucleic acids (or proteins) which can lead to the formation of thymine dimers, and other photoproducts that inhibit transcription and replication of nucleic acids, making the microorganisms sterile (von Sonntag *et al.*, 2004). The second mechanism is based on a photosensitisation process, where the UV light is absorbed by a sensitiser leading to the formation of free radicals or reactive oxygen species (ROS) that can damage vital cellular components. (Pattison and Davies, 2006; Rizzo *et al.,* 2013).

Nevertheless, some microorganisms irradiated with UV light are able to repair their damage caused by this method, through a mechanism called photoreactivation, which occurs in the presence or absence of light, thus decreasing the efficiency of the process and increasing the microbial risk after UV disinfection (Linden *et al.*, 2002; Hijnen *et al.*, 2006; Guo *et al.*, 2011). The formation of disinfection by-products is also of concern when using UV radiation, since the reaction of UV at wavelengths below 240 nm with organic matter or nitrates in the water, can lead to the generation of aldehydes, carboxylic acid and nitrites (von Sonntag and Schuchmann, 1992).

Another use of light for the disinfection of water is by a technique called SODIS and relies on the disinfection of water by solar light. It was first investigated by Prof. Aftim Acra of the American University, in Beirut, in 1984 and since then, the potential for the technique to inactivate different waterborne pathogens has been researched by several groups (Sommer *et al.*, 1997; Berney *et al.*, 2006; Ubomba-Jaswa *et al.*, 2009). SODIS is a technique used for the photoinactivation of microorganisms using solar light and transparent water bottles. The bottles are placed under the sun for several hours, 6 hours on a sunny day and longer on a cloudy day. Following exposure, the water is ready for consumption (Figure 1.5). The mechanisms behind the inactivation are the radiation in the UV-B and UV-A range (see Figure 1.4), which causes direct or mediated damage (reactive oxygen species in presence of oxygen) to proteins and the DNA; and the heat, which can directly or synergistically affect the pathogenic cells (Berney *et al.* 2006; Bosshard *et al.* 2010; McGuigan *et al.*, 2012).

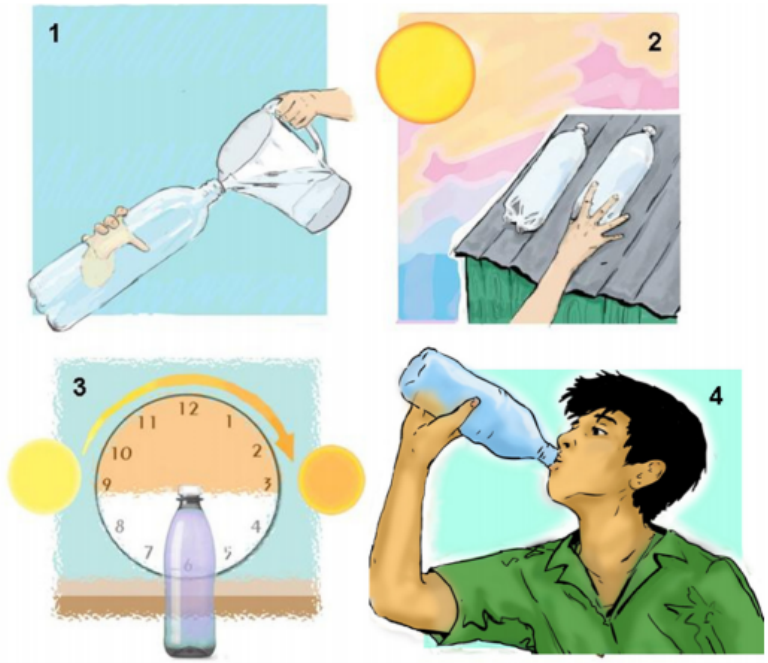

Figure 1.5 – Chart illustrating the application of SODIS for household water disinfection (McGuigan *et al.*, 2012).

A way of enhancing the efficacy of the previous water disinfection methods mentioned, UV and SODIS, is the use of an inorganic photocatalyst, inducing a process called heterogeneous photocatalysis (Liu and Yang, 2003; Seven *et al.*, 2004; Malato *et al.*, 2009; Wang *et al.*, 2013; Abeledo-Lameiro *et al.*, 2017). These catalysts usually require light irradiation in the UV-A (λ < 400 nm) in order to start the photochemical activity. Nevertheless, an artificial UV light source can also be used (Rincon and Pugarin, 2003; Sichel et., 2007; Thandu *et al.,* 2015).

Heterogeneous photocatalysis relies on the application of semiconductor catalysts, like TiO_2, ZnO, Fe_2O_3, CdS, GaP and ZnS for the disinfection of water. Among them, the most used is titanium dioxide (TiO_2) since it is the most stable and most active photocatalyst when irradiated (wavelengths 300-390nm). (Malato *et al.,* 2009; Chong *et al.*, 2010).

The mode of action of the technology relies on the activation of these catalysts by UV light (natural or artificial) (Figure 1.6). The energy from the light source will excite the band gap between the valence band and conduction band of the molecule, forming an electron-hole pair, which is able to oxidise water, leading to the formation of hydroxyl (HO·) and superoxide radicals. These reactive oxygen species can then degrade water contaminates and inactivate microorganisms present in water (Thandu *et al.,* 2015).

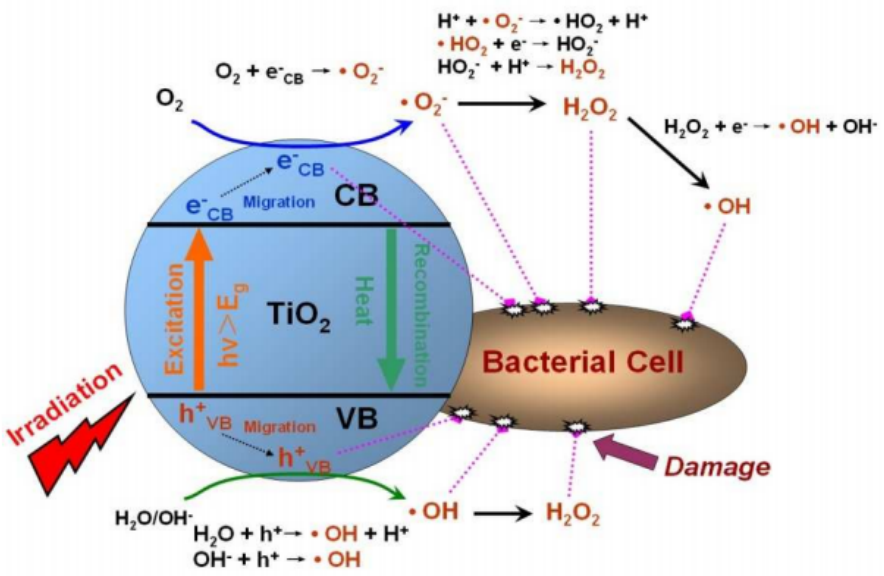

Figure 1.6 – Illustration of the mechanism of photocatalytic disinfection with TiO_2 irradiated by UV light (Wang *et al.*, 2013).

1.3 Photodynamic inactivation

The use of light for therapeutic purposes is not new. First named as “heliotherapy”, the use of solar light for the “restoration of health” was a technique recommended by Herodotes in the 2nd century BC. Later on, this technique started to be called phototherapy, and was applied by Egyptians, Indians and Chinese for over 3000 years, as a tool to treat skin diseases, such as vitiligo, psoriasis, rickets and skin cancer. The phototherapy then relied on the effect of endogenous sensitisers which were responsible for the photodynamic process.

After that, numerous discoveries regarding the use of light for health purposes were reported. Cravin (1815) reported the curing effect of sunlight on ‘scrofula’, rickets, rheumatism, scurvy, paralysis and muscle weakness. After him, Sniadecki (1822) documented the importance of sun exposure for the prevention of rickets. In 1903, Niels Finsen won the Nobel Prize for his work on the use of light radiation for the treatment of diseases like lupus vulgaris, being later acknowledged as the founder of modern phototherapy (Moan and Peng, 2003).

The first thought of using dyes as biological sensitisers arose with a research group from Germany, guided by one of the pioneers of photobiology, Professor Hermann von Tappeiner (director of the Pharmacological Institute of the Ludwig-Maximilians University, in Munich). While one of his students, Oscar Raab, was investigating the toxic effects of acridine on *Paramecia caudatum*, he observed that in one of the experiments, the paramecia survived when incubated with a certain acridine concentration, however, when the experiment was performed again, during a heavy thunderstorm, the organism died (Raab, 1900).

This observation led to the discovery of the photodynamic action. The underlying principle of this technology relies on the activation of a dye or photosensitiser by visible light which then leads to the generation of cytotoxic species, which can kill the cells. The term ‘photodynamic action’ (“*photodynamische Wirkung”*) was created by von Tappeiner and it refers to photosensitised reactions which involves oxygen (Moan and Peng, 2003).

A detailed representation of the principle behind the photodynamic action is illustrated in the Jablonski diagram (Figure 1.7) and explained as follows: the light source (natural or artificial) transfers energy (photons) ($h\nu_{abs}$) to the photosensitiser in the ground state (S_0) which is then excited to the excited singlet state (S_1). In this state, it can lose energy by fluorescence emission ($h\nu_{em}$), returning to S_0 or can go through a process called intersystem crossing (ISC) where it is converted to an excited triplet state. From this state, it can then return to the ground state (S_0) by phosphorescence emission ($h\nu_{em}$) or

go through the two mechanisms involved in photodynamic inactivation (PDI), called Type I and Type II. As phosphorescence involves a spin-inversion which is also spin-forbidden, the triplet state has a relatively longer lifetime (microseconds), allowing its interaction with the substrate (Gollnick, 1968; Sternberg *et al.,* 1998).

When the photosensitiser goes through Type I mechanism it produces reactive oxygen species (ROS) like the superoxide anion, hydrogen peroxide (H_2O_2) and the radical hydroxyl (OH·). In this process, an electron transfer can occur to or from the substrate, mainly when the photosensitiser is in the excited state. It will then produce a reducing electron and an oxidizing hole in the excited state. Another reaction that can happen through the Type I pathway is a hydrogen abstraction, which will generate radical products that can react directly with oxygen giving peroxides or initiating radical chain autoxidation. In the Type II mechanism, the excited triplet state transfers energy to ground state molecular oxygen (O_2), present in the medium, producing singlet oxygen ($^1O_2$) (Foote, 1987). These mechanisms are always competing, and which one will occur depends on factors like oxygen concentration; substrate reactivity and photosensitiser (Gollnick, 1968).

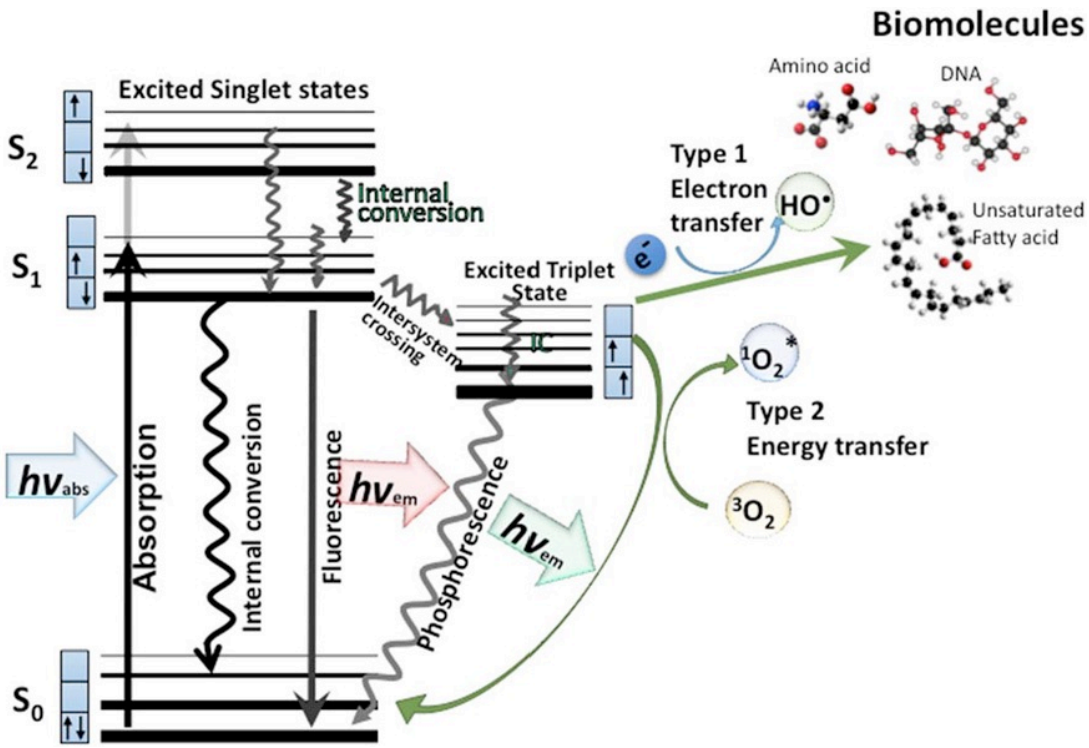

Figure 1.7- Jablonski diagram showing the photochemical mechanisms involved in the photodynamic action (Hamblin and Abrahamse, 2016).

The medium where the photodynamic reaction occurs can directly interfere in the generation and lifetime of the reactive oxygen species, since the molecular oxygen and other substrates present in it are the energy or electron receptors of the system. Singlet oxygen has a lifetime in water of approximately 3–4 μs and its diffusion range is dependent on the medium where it is immersed. When it is produced in pure water, it can diffuse over approximately 1 μm but to only 50 nm in protein-rich lipid layers (Moan, 1990; Sharman *et al.*, 2000; Bronshtein *et al.*, 2004).

These reactive oxygen species generated through the Type I and II mechanism are cytotoxic and, when in contact with living cells, they can cause irreversible damage to its vital components (proteins, nucleic acids and lipids) leading to its death (Girotti, 2001). Due to its multi-target nature, photodynamic inactivation is a very advantageous process, being effective in oxidising various biomolecules leading to the deactivation of different cell types (Alves *et al.*, 2015).

From the beginning of the 1960's, photodynamic inactivation started to be considered as a promising new modality for cancer treatment, then called photodynamic therapy. These studies were led by R. L. Lipson and S. Schwartz at the Mayo Clinic, where they observed that the injection of hematoporphyrin (crude preparations) to neoplastic lesions generated fluorescence, helping in tumour localisation during surgery. After this discovery, several studies have focused in the photodynamic action of photosensitisers in eukaryotic cells, focusing mainly on the treatment of cancer, ophthalmological disorders, and dermatology (Reddi *et al.*, 1981, Dougherty, *et al.*, 1998).

However, due to the complexity of eukaryotic cells, a large variety of potential biding sites had to be considered and investigated in order to elucidate the mechanism of action of the photodynamic process. For this reason, in 1982, Bertolini and his group decided to study the photodynamic action of hematoporphyrin (HP) using bacterial and yeast cells. These cells have a simple structural organisation, being an interesting experimental model with high reproductivity (Bertoloni *et al.*, 1982). Since then, this technology has gained more interest every year and its spectrum of activity is being investigated by different researchers around the world.

To date, photodynamic inactivation has been shown to be effective in inactivating organisms like: human cells (Dougherty, *et al.*, 1998), viruses (Perlin *et al.*, 1987; Casteel *et al.*,2004), bacteria (Nitzan *et al.*, 1994; Alves *et al.*, 2014), molds (Luksiene *et al.*, 2004; Preuβ *et al.*, 2014), yeasts (Luksiene *et al.*, 2004b, Alvarez *et al.*, 2014), protozoa (Giese, 1953; Kassab *et al.*, 2002), helminths (Goble and Boyd, 1959) and insects (Tosk *et al.*, 1986, Amor *et al.*, 1998).

1.3.1 Photosensitisers

Photosensitisers (PS) are a group of UV-visible absorbing molecules which exhibit characteristics such as high absorption coefficients in the spectral region of the excitation light; a triplet state of appropriate energy to allow for efficient energy transfer to ground state oxygen; high quantum yield of the triplet state and a long triplet state lifetime (the photosensitiser efficiency depend on the photophysical properties of its lowest excited triplet state). With regard to PDI, the ideal photosensitiser should present characteristics like absence of dark toxicity; absence of mutagenicity at lower concentrations; and high photostability (Derosa and Crutchley, 2002; Plaetzer *et al.*, 2009, Castano *et al.*, 2014).

Phenothiazine photosensitisers are largely used in cancer and antimicrobial PDI. They have good photodynamic properties, with a reasonable yield of singlet oxygen and light absorption between 600—900 nm. Among them, the most commonly used compounds are the cationic methylene blue and toluidine blue O. However, the commercially available phenothiazine dyes present the disadvantages of inherent dark toxicity (Wainwright *et al.,* 1999).

Another group of photosensitisers that is widely studied are the phthalocyanines (PC), which have their most intense absorption band at > 650 nm and contain four phenyl groups in their chemical structure. Due to the presence of these groups they have solubility and aggregation problems. In order to provide water solubility, they have to be prepared with sulfonic acid groups and atoms in the centre. Asymmetrically substituted disulfonic acids have been reported to be more effective for the photodynamic process than the mono-, symmetrically di-, tri- and tetra-substituted sulfonic acids (Peng *et al.*, 1990; Fingar *et al.*, 1993).

In recent times, the majority of photosensitisers used both clinically and experimentally, are frequently based on heterocyclic ring structures such as porphyrins, which are formed by four pyrrole rings connected at the α position of through unsaturated methane bridges. The word *porphyrin* came from the Greek word *porphura, which means purple*, as all porphyrins are intensely coloured. They can be divided into two classes, the natural porphyrins (NP) and the synthetic (SP) ones, as displayed in Figure 1.8, according to their origin and structure. In order to create a wide range of physio-chemical characteristics, it is possible to introduce more than 50 different metals into the ring structure (Stojiljkovic *et al.*, 2001).

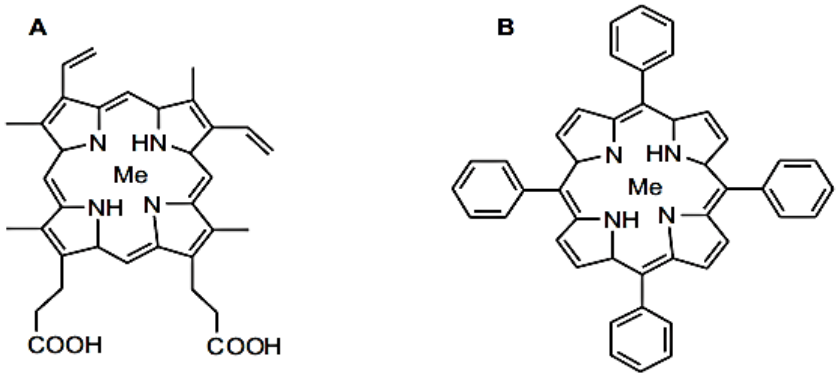

Figure 1.8 – Basic chemical structure of a natural porphyrin (A) and a synthetic porphyrin (B) (Stojiljkovic *et al.*, 2001).

Porphyrins are photosensitisers with excellent photostability and intense absorption in the UV-visible range, having a Soret band (~400nm) and Q-bands (from 450 to 700nm) in the blue and red regions, respectively. Its typical electronic absorption spectrum can be found in Figure 1.9, where the presence of two distinct regions is evident (Derosa and Crutchley, 2002; Giovanetti, 2012; Sampaio *et al.*, 2014).

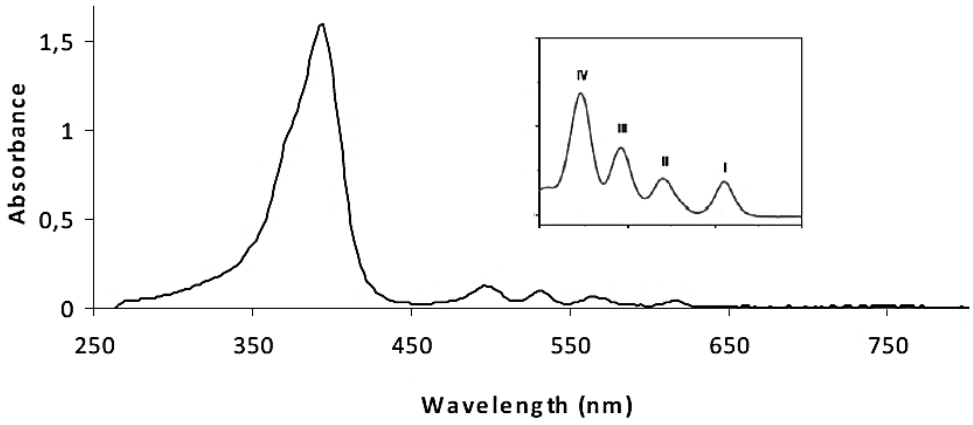

Figure 1.9 - Typical UV-visible spectrum of a porphyrin with an insert showing enlargement of the Q- band region between 480-720 nm (Giovanetti, 2012).

Those two typical regions can be explained in detail by observing the Jablonski diagram (Figure 1.7). The Soret band, also called B band, corresponds to the porphyrin transition from the ground state to the second excited state ($S_0 \rightarrow S_2$). The Q-bands correspond to the weak transition from the ground state to the first excited state ($S_0 \rightarrow S_1$), and appears in the range between 500-750 nm. These specific features of porphyrins are due to their

18 π- electrons conjugation (see Figure 1.8) (Yang *et al.* 2002; Gulino *et al.*, 2005; Paolesse & D'Amico, 2007).

The electron excitation happens through the photons emitted by the light source and absorbed by the photosensitiser molecule. Most of the spectroscopic transitions consider a single photon absorption, by the molecule, at a time. However, simultaneous absorption of more than one photon is possible depending on the light intensity. The single photon absorption relies on the Beer-lambert law, which relates the intensity of the light source, of a specific wavelength (monochromatic), transmitted through a sample to the intensity incident on the sample. The sample absorption coefficient (molar absorptivity in the case of solutions) has to be considered, since it tells how much light can be absorbed by it (Michl, 2006).

The naturally occurring porphyrins are fully conjugated (non-reduced) tetrapyrroles and can vary according to the number and type of side groups (i.e. carboxylic acid groups). Most of them are derived from protoporphyrin IX (PPIX), which is formed by 2 vinyl groups, 2 propionic groups and 4 methyl groups. PPIX and its derivatives (coproporpohyrin, uroporphyrin, etc.) are present in places like tissues, body fluids and faeces of animals (Jori and Spikes, 1984).

Among the synthetic porphyrins, the most common ones are the tetraphenylporphyrins (TPP). They are synthetic heterocyclic compounds that resemble the naturally occurring porphyrins. TPPs are known for their efficacy in localising tumor cells and their capacity to photoinactivate cells has being largely studied since this photosensitiser has a high singlet oxygen yield (Pandey and Zheng, 2000).

Another group of porphyrins that has attracted great attention, since it was described in 1977, is the group of cationic porphyrins (Diamond *et al.*, in 1977). These porphyrins have positive charges which affect their hydrophilicity or lipophilicity, and consequently increase their ability of binding to cells (Merchat *et al.*, 1996; Reddi *et al.*, 2002).

Among this group we find the meso-substituted cationic porphyrin 5,10,15,20-tetrakis-(4-N-methylpyridyl)-porphine (TMPyP or T_4MPyP). This porphyrin possesses properties which makes it particularly attractive for application in photodynamic inactivation of biomolecules. It has relatively high singlet oxygen quantum yields and it remains monomeric in solution even in high concentrations (Villanueva, 1993).

Furthermore, it can be highlighted that at photochemical active doses (micromolar concentrations), porphyrins do not show significant toxicity to most higher organisms, as confirmed by their use in the food industry (Luksiene, 2005), fish farming (Almeida *et al.* 2009) and photodynamic therapy for infectious disease (Hamblin & Hasan 2004).

Photosensitisers can undergo the Type I or the Type II mechanisms in order to generate reactive oxygen species which will cause cell damage. This mechanism depends mainly on the chemical structure of the photosensitiser, however, both mechanisms can occur simultaneously during the photodynamic process. Photosensitisers like methylene blue (MB) or toluidine blue O (TBO) have been reported to function through the Type I pathway, while porphyrin derivatives are prone to the Type II mechanism (Tardivo *et al.*, 2005; Tavares *et al.*, 2011).

1.3.2 Light source

The light source is a key component in the PDI system. The light source used can be natural (sunlight) or artificial (i.e. halogen lamps, xenon arc lamps, LED arrays). The important thing to be considered is the emission wavelength, which should correspond to the photosensitiser high absorption bands (Soret and Q bands), leading to the excitation of its electron from the highest occupied molecular orbital (HOMO), to the lowest unoccupied molecular orbital (LUMO), generating then the unstable and short-lived excited singlet state. As explained before (Jablonski diagram), from there the photosensitiser will undergo the Type I and/or Type II mechanism and produce ROS (Foote, 1991).

The number of photons that are emitted by a lamp, at a specific wavelength, per second, is related to its optical power (Bunce, 1989), therefore, when choosing the light source to be used in PDI, its power (watts) has to be considered. In addition to that, an important variable that also depends on the light power is the fluence rate, which is defined by the radiation power incident in a specific area. It can be measured by a radiometer (or luximeter), and is expressed in Watts (w) per square centimetre (cm^2) (Star, 1990).

For practical reasons, in PDI, the light dose, which is the energy delivered by the light, is calculated. This variable takes into account the irradiation time and is expressed in Joules (J) per square centimetre (cm^2). In addition to that, it is important to note that the distance kept between the lamp and the sample can affect the fluence rate. (Kuznetsova *et al.*, 2007; En-Sheng *et al.*, 2012).

1.3.3 Antimicrobial photodynamic inactivation

Interest in investigating photodynamic inactivation of microbial cells started with Bertoloni *et al.* in 1982. They investigated the photodynamic action of hematoporphyrin (HP) against prokaryotic cells, using Gram-positive and Gram-negative bacteria (*Escherichia coli, Klebsiella pneumoniae, Staphylococcus aureus and Streptococcus faecalis*) and yeasts (*Candida sp*.). Their aim was to investigate the effect of the photoprocess on different strains in order to evaluate the photosensitiser interaction with a variety of

biomolecules, lipopolysaccharides, peptidoglycans, etc., expanding the knowledge regarding the porphyrin mode of action.

Interestingly, they found that the yeast and the Gram-positive bacterial strains were the most susceptible to the treatment, while the Gram-negative bacteria were not sensitive to PDI, indicating that the process efficiency is connected to the cell type.

Following their research, more investigators started to consider the use of PDI for antimicrobial purpose and in recent years it has been proposed as a promising alternative for the treatment of different localised infections. In addition to that, with the advent of drug resistance among a large variety of pathogens, more attention has been brought to the technique, with an increased interest in exploring its applicability (Dai *et al.*, 2009).

A comparison between the application of PDI (here called PDT) and the use of antibiotics for the treatment of microbial infections is shown in Figure 1.10. The photodynamic process has the advantage of being effective against microorganisms that antibiotics cannot eradicate; it has high target selectivity; is cheaper to use and gives results faster (Dai *et al.*, 2009).

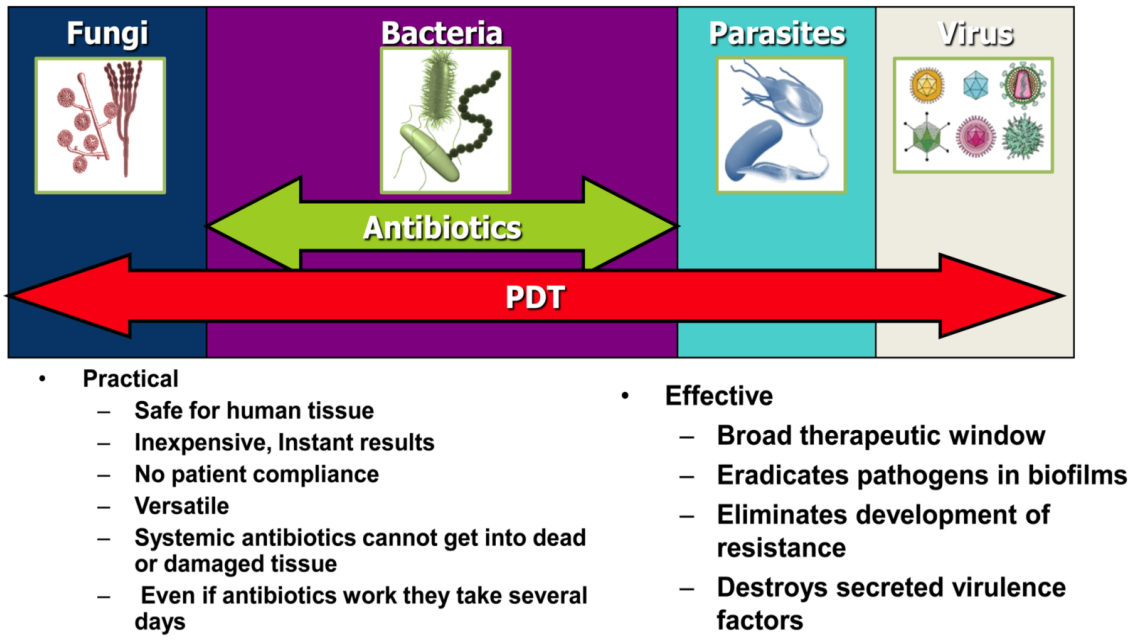

Figure 1.10 - Schematic representation of some of PDI advantages over antibiotics, in the deactivation of microorganisms (Dai *et al.,* 2009).

The effectiveness of PDI on microbial cells depends on a variety of factors which includes the photosensitiser physicochemical properties; the photosensitiser mechanisms of action (type I and/or type II mechanism); the photosensitiser binding site within the cells; the photosensitiser concentration; the light dosage and wavelength; and the organism to

be treated. Among the cell constituents, which can be affected by PDI, are lipids, proteins, carbohydrates, cytoplasmic membrane, cell wall and nucleic acids (Jori, 2006; Alves *et al.*, 2014).

A summary of the microorganisms that have been investigated in PDI experiments, including fungi, bacteria, protozoa and viruses, is presented in Table 1.3. The majority of the work to date has focused on the clinical area, for the treatment of bacterial infections (Demidova and Hamblin, 2005; Nisnevitch *et al.*,2009, Rossoni *et al.,* 2010, Junqueira *et al.,* 2010; Hegge *et al.*, 2012; Dastgheyb *et al.*,2013; Mamone *et al.*, 2014). Among the microorganisms investigated, particular attention has been given to Gram-positive and Gram-negative bacteria, specially *Staphylococcus aureus* and *Escherichia coli.*

As presented in a review by Alves *et al.* (2015), there is great scope for the application of PDI. Work has already investigated the use of the photodynamic oxidative stress for the elimination of insect pests, like mosquitoes vectors of the pathogens responsible for diseases like malaria (*Anopheles*), yellow fever (*Culex,Aedes*) dengue fever (*Aedes*) and encephalitis (*Aedes, Culex, Anopheles*) (Dondji *et al.*, 2005; Wohllebe *et al.*, 2009; Lucantoni *et al.*, 2011; El-Tayeb *et al.*, 2013).

The eradication of foodborne pathogenic microorganisms can also be achieved by PDI. Research has already shown its effectiveness against some filamentous fungi Penicillium spp., *Aspergillus* spp (Luksiene *et al.*, 2007) and some bacteria as *Salmonella enterica, Bacillus cereus and, Listeria monocytogenes* (Luksiene *et al.,* 2009; Buchovec *et al.*, 2009; Buchovec *et al.*, 2010). In this work, the focus will be on the photodynamic inactivation of bacterial cells.

Table 1.3 – Microorganisms investigated through the photoinactivation processes.

Microorganism		Name	References
Fungi	**Filamentous**	*Aspergillus niger*	Luksiene *et al.*, 2007; Preuβ *et al.*, 2014.
		Cladosporium cladosporioides	Preuβ *et al.*, 2014.
		Penicillium purpugenum	Luksiene *et al.*, 2007; Preuβ *et al.*, 2014.
	Yeast	*Saccharomyces cerevisiae*	Strakbovskaya *et al.*, 1999.
		Candida albicans	Bertoloni *et al.* 1982; Demidova and Hamblin, 2005; Funes *et al.*, 2009; Alvarez *et al.*, 2014.
Bacteria	**Gram-positive**	*Bacillus subtilis*	Silva *et al.*, 2012; Parakh *et al.*, 2013.
		Bacillus cereus	Luksiene *et al.,* 2009; Oliveira *et al.*, 2009; Silva *et al.*, 2012.
		Sarcina lutea	Nisnevitch *et al.*,2009.
		Staphylococcus aureus	Bertoloni *et al.* 1982; Usacheva *et al.*, 2003; Bozja *et al.*, 2003; Demidova and Hamblin, 2005; Magaraggia *et al.*, 2006; Nisnevitch *et al.*, 2009; Schastak *et al.*, 2010; Naik *et al.*, 2011; Vilela *et al.*, 2012; Rossi *et al.*, 2012; Rolim *et al.*, 2012; Nakonieczno and Grinholc, 2012; Alves *et al.*, 2013; Arenas *et al.*, 2013; Parakh *et al.*, 2013; Dastgheyb

			et al., 2013; Kossakowska *et al.*, 2013; Hanakova *et al.*, 2014; Johnson *et al.*, 2014.
		Staphylococcus epidermidis	Nisnevitch *et al.*,2009; Hegge *et al.*, 2012; Dastgheyb *et al.*,2013; Mamone *et al.*, 2014.
		Staphylococcus warneri	Alves *et al.*,2013
		Enterococcus hirae	Ergaieg and Seux, 2009.
		Enterococcus faecalis	Bertoloni *et al.* 1982; Usacheva *et al.*, 2003; Orlandi *et al.*, 2013.
		Enterococcus seriolicida	Merchat *et al.*, 1996.
Bacteria	**Gram-positive**	*Listeria monocytogenes*	Buchovec *et al.*, 2010.
		Streptococcus pneumonia	Usacheva *et al.*, 2003.
		Streptococcus mutans	Maisch *et al.*, 2009.
		Streptococcus sobrinus	Luthi *et al.*, 2009.
		Micrococcus sp.	Gomes *et al.*, 2013.
		Actinomyces naeslundii	Cieplik *et al.*, 2013.
		Peptostreptococcus micros	Lauro *et al.*, 2002.

Bacteria	**Gram-negative**	*Escherichia coli*	Merchat *et al.*, 1996; Valduga *et al.,* 1999; Bozja *et al.*, 2003; Usacheva *et al.*, 2003; Lazzeri *et al.*, 2004; Demidova and Hamblin, 2005; Magaraggia *et al.*, 2006; Banfi *et al.,* 2006; Caminos *et al.*, 2006; Caminos *et al.*, 2008; Ergaieg *et al.*, 2008; Ergaieg and Seux, 2009; Ragas *et al.,* 2010; Rossoni *et al.,* 2010; Komagoe *et al.,* 2011; Vilela *et al.*, 2012; Parakh *et al.*, 2013; Nakonechny *et al* 2013; Dastgheyb *et al.*, 2013; Orlandi *et al.*, 2013; Alves *et al.,* 2013; Johnson *et al.*, 2014
		Vibrio fischeri	Alves *et al.*, 2011.
		Shigella flexneri	Nisnevitch *et al.*, 2009.
		Salmonella spp.	Buchovec *et al.*, 2009; Nisnevitch *et al.*,2009; Ishikawa *et al.*, 2009.
		Pseudomonas aeruginosa	Usacheva *et al.*, 2003; Philippova *et al.*, 2003; Tegos *et al.*, 2006; Nisnevitch *et al.*,2009, Schastak *et al.*,2010; Giulinani *et al.*, 2010; Sabbahi *et al.,* 2013; Parakh *et al.,* 2013.
		Klebsiella pneumoniae	Bertoloni *et al.* 1982; Nisnevitch *et al.*,2009, Rossoni *et al.,* 2010.
		Desulfovibrio sp.	Street and Gibbs, 2010.
		Vibrium anguilarum	Merchat *et al.*, 1996.
		Enterobacter cloacae	Rossoni *et al.,* 2010; Junqueira *et al.,* 2010.

		Hemophilus influenza	Usacheva *et al.*, 2003
Bacteria	**Gram-negative**	*Aggregatibacter actinomycete mcomitans*	Maisch *et al.*, 2009
		Prevotella intermedia	Lauro *et al.*, 2002
		Fusobacterium nucleatum	Lauro *et al.*, 2002
		Actinobacillus actinomycetemcomitans	Lauro *et al.*, 2002
		Yersinia pseudotuberculosis	Walther *et al.*, 2009
Protozoa		*Acanthamoeba spp.*	Ferro *et al.*, 2006
		Colpoda inflata	Kassab *et al.*,2002
Viruses		*Hepatitis A virus*	Casteel *et al.*,2004
		Influenza Virus	Perlin *et al.*, 1987
		Herpes Virus	Perlin *et al.*, 1987; Smetana *et al.*, 1998.

Since the findings of Bertoloni *et al.* in 1982, several other studies which investigated the effect of PDI on bacteria have shown that Gram-positive bacteria are more sensitive to this treatment than Gram-negative bacteria (Figure 1.11).

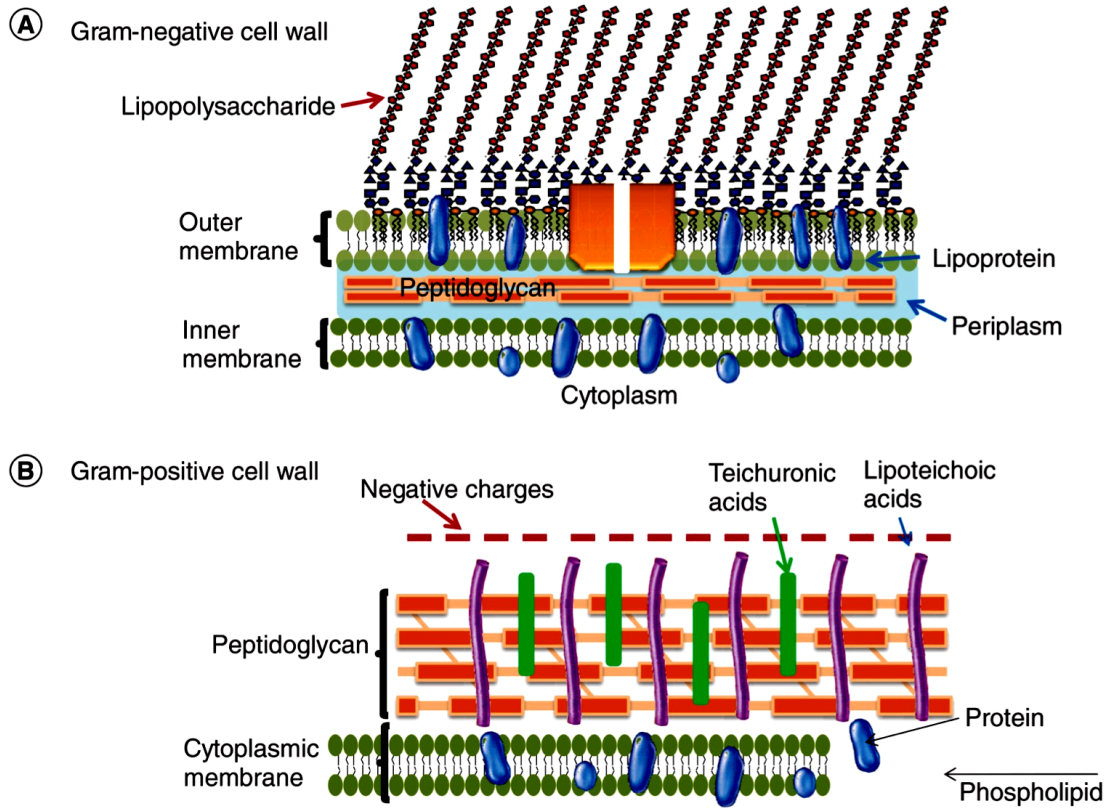

Figure 1.11 - Schematic representation of the different cellular envelopes of Gram-negative bacteria (A) and Gram-positive bacteria (B) (Yin *et al.*, 2016).

This resistance is related to the presence of a lipopolysaccharide (LPS) outer membrane in the cell wall of Gram-negative bacteria, which offers a barrier to exogenous antimicrobial agents. This outer membrane is formed by a complex mix of a phospholipidic bilayer intercalated by lipoproteins and β-barrel proteins and covered by lipopolysaccharides in the outer leaflet (2–7 nm) (Vollmer and Seligman, 2010).

The LPS acts like a physical and/or chemical barrier through which singlet oxygen and/or oxyradicals must pass to be able to interact with vital cell components, increasing its protection. In addition to that, the fact that $^1O_2$ is extremely short lived makes the process more difficult (Ergaieg and Seux, 2009; Dai *et al.,* 2012).

This outer membrane is absent in Gram-positive bacteria, which have a cell wall composed only of multiple peptidoglycan layers intercalated by lipoteichoic and teichoic

acids, offering a degree of porosity to bacterial cell, allowing an easier penetration of the photosensitiser (Silhavy *et al.,* 2010, Alves *et al.,* 2014).

In order to overcome the resistance created by the LPS membrane of Gram-negative bacteria different types of photosensitisers have been investigated. Studies have shown that certain types of photosensitisers, like cationic porphyrins, phthalocyanines and chlorines and thiazine dyes, are able to pass through the LPS and interact with the DNA and the cytoplasmic membrane, causing its damage and consequently, cell death (Figure 1.12) (Durantini, 2006; Jori and Coppellotti, 2007; komagoe *et al.*, 2011).

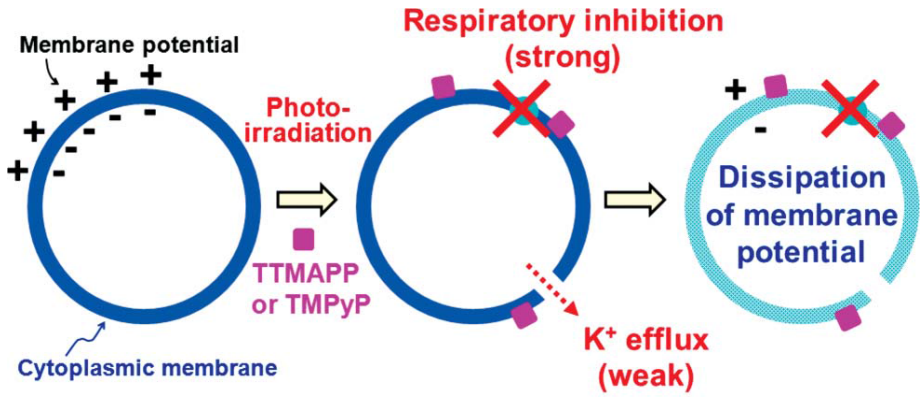

Figure 1.12 - Example of a photosensitiser mechanism of action on the cytoplasmic membrane of *S. aureus* cells (Komagoe *et al.*, 2011).

Different types of cellular damage can be caused by the reactive oxygen species depending on the various interaction modes that can occur between the cell and the PS (Komagoe *et al.*, 2011; Alves *et al* 2013, Pereira *et al.*, 2014).

1.3.2.1 Effect of photosensitisers on bacterial cells

The effect of the photosensitiser on the cell depends mainly on its interaction with it. Three possibilities may be considered: the photosensitiser does not bind to the cell, meaning that the ROS effect will be restricted to the cell wall; the photosensitiser binds to the cells, outside the cell wall, restricting the region where the ROS damage can be caused; or it is actively transported or translocated through the cell wall, being able to interact with the organelles and release ROS internally (Alves *et al.*, 2014).

The photosensitiser binding and uptake into cells is affected by factors related to its structure, its degree of hydrophobicity, the number of positive charges and the spatial distribution of substituents, which seem to play important roles in the photosensitiser/cell

interaction. In addition, the bacterial Gram-type also affects the photosensitiser binding, due to the different constitution of the bacterial cell wall (Alves *et al.,* 2013; Preuss *et al.,* 2013). As various vital cellular components can be destroyed by ROS, the mode of action for each of them will be explained separately.

Cytoplasmic membrane

One of the targets of PDI is the plasma membrane, since ROS can cause its damage, through oxidation. The damage caused is irreversible and leads to the leakage of the intracellular content, like ATP and K^+ ions, causing the inactivation of enzymes and transport systems. Due to the fact that the charge and morphology of bacterial outer membrane can differ significantly from one to the other, each bacterium exhibits a different susceptibility to PDI (Hamblin and Hasam, 2004; Kuznetsova and Kaliya, 2013).

As shown in Figure 1.4, Gram-negative bacteria have two membrane bilayers, the asymmetric outer membrane, which is composed manly by lipopolysaccharides (LPS) in the outer leaflet and by phospholipids in the inner leaflet, and the inner bilayer, composed by phospholipids (Vollmer and Seligman, 2010).

The spatial conformation of the LPS, containing salt bridges due to the presence of Mg^{2+} and Ca^{2+} ions, makes them very compact and therefore an impermeable barrier to photosensitisers. However, photosensitisers that are positively charged are able to trespass this barrier through the generation of electrostatic forces between the cationic photosensitiser and the constituents of the Gram-negative cell wall. These forces will then promote the destabilisation of the wall native organization and allow the photosensitiser to bind and penetrate into the cell (Jori, 2006; Domingues *et al.*, 2009).

Studies have suggested that porphyrins can attach to the outer surface of the Gram-negative cells cytoplasmic membrane or can pass through their outer membrane (Pudziuvyte *et al.*, 2009; Kamagoe *et al.*, 2011). In addition to that, the photosensitiser relative position and orientation in relation to the membrane-water interface (degree of hydrophobicity) interferes in its binding capacity (Cordeiro *et al.,* 2012).

Gram-positive bacteria have a distinct cell wall and for that reason their interaction with a photosensitiser occurs in a different way. The absence of the LPS outer membrane and the presence of a porous peptidoglycan cell wall facilitates the entry of the photosensitiser to the cytoplasm. The photosensitiser can also bind to the

phosphatidylglycerols present in the membrane, leading to damages and rearrangements of these molecules (Epand and Epand, 2009).

Proteins

Since prokaryotic bacterial cells do not have intracellular membrane-organelles, the proteins present in their cytoplasm are vital, being responsible for the production of energy, lipid biosynthesis, and protein secretion and transportation (Almeida *et al.*, 2015). These molecules are considered one of the major cellular targets of photodynamic oxidation due to the fact that they are abundant in the cellular cytoplasm. Singlet oxygen can interact with protein side-chains by both physical quenching and chemical reaction (Davies, 2003).

Photo-oxidation of proteins can lead to damage such as the increase in the susceptibility to unfolding and to conformational changes; the formation of high-molecular-mass aggregates (dimers and higher species) and fragmentation (Pattison *et al.*, 2012).

Nucleic acids

PDI can also induce DNA damage and it can occur through different pathways. The reaction can happen by the direct contact between the excited photosensitiser and the DNA molecule; it can be mediated by reactive oxygen species (ROS); or it can involve other secondary intermediates (i.e. decomposition products of the excited molecules or lipid peroxidation products) (Epe, 2011).

The direct contact can happen through the photosensitiser intercalation between the GC base pairs or through its interaction with the AT base pairs in the DNA minor groove (Kovaleva *et al.*, 2012). Research has also shown that PDI can induce DNA strand breaks even if the photosensitiser is not bound to the DNA (Boye and Moan, 1980; Fiel *et al.*, 1981).

RNA can also be affected by PDI. It can be directly degraded by the reactive oxygen species generated in the process, or its production can be affected by damage caused to the transcription machinery proteins bound to the DNA (Salmon-Divon *et al.*, 2004).

1.4 Photodynamic inactivation for water disinfection

Starting around the 1970's, interest in the application of PDI for water disinfection grew (Gerba *et al*, 1977; Archer and Rosenthal, 1977; Archer and Juven, 1977). The reasons behind this increased interest are varied, with the formation of disinfection by-products

and the high costs involved in the currently used disinfection techniques, being the main ones (Bonnett *at al.,*2006; Carvalho *et al.*, 2007; Rossi *et al.,* 2012).

When the first researchers considered the use of PDI for the disinfection of water, their aim was to disinfect wastewater using the photosensitiser methylene blue. In their work, Gerba *et al.* (1977) investigated the use of sensitisers for the removal of coliforms and poliovirus from water. They discovered that parameters like temperature, pH, and dye concentration influenced the effectiveness of the process; however, they believed that wastewater organics did not interfere with the process. They also found solar energy to be a good alternative to the use of artificial light.

In the same year, researchers from Israel (Acher and Rosenthal, 1977) were also investigating the use of methylene blue and rose Bengal for the disinfection of the sewage from circulated oxidation ponds of Haifa, Tel Aviv and Nazareth areas. The samples were irradiated using solar light and a mercury lamp, and the most probable number (MPN) method was used for cell enumeration. Their work showed that methylene blue was more efficient than rose bengal, and that solar light gave a better response in the removal of faecal coliforms then the artificial one. Following this work, Arher's group also investigated the inactivation of an *E.coli* strain isolated from sewage, which was added to sewage and potable water for experiments under solar light. Using rose bengal and methylene blue, up to 8-log reduction in the bacterial numbers was achieved (Acher and Juven, 1977).

Later on, Cooper and Goswami, 2002, investigated the use of methylene blue and rose bengal, for simultaneous photosensitised disinfection and detoxification of water. Their laboratory scale reactor used petri dishes containing water with added aromatic hydrocarbons (benzene and toluene) and *E. coli,* as model contaminants. The light source was solar light. They observed a 3-log reduction in the number of cells after 30 minutes of irradiation; however, the sunlight alone also led to inactivation (95%).

While these experiments focused on the use of methylene blue and rose bengal, later experiments started to explore the use of porphyrins in the photodynamic disinfection of water, since studies were demonstrating their efficacy when used in photodynamic inactivation of infectious microorganisms, in the clinical area (Bertolini, 1982; Jori and Spikes, 1984, Villaneuva, 1993).

In their work, Jemli *et al.* (2002) compared the efficacy of the cationic porphyrin TMPyP with rose Bengal and methylene blue. Their aim was to disinfect wastewater for

agricultural use using sunlight. They achieved good reduction in the number of faecal coliforms, with the porphyrin being more efficient than the other two photosensitisers. Magaraggia *et al.* (2006) also used porphyrins in their experiments, in order to investigate their efficacy against *E. coli*, *S. aureus* and *Saprolegnia* spp in a phosphate buffer saline, and in a pilot aquaculture plant containing *Saprolegnia*-infected rainbow trout. They found the porphyrin to be effective in deactivating the bacteria in all situations, and concluded that the system promotes low environmental impact.

An investigation of PDI for the inactivation of recombinant bioluminescent *E. coli* was performed by Alves *et al.,* 2008. In their work, they evaluated a new approach, bacterial luminesce method, to monitor the bacterial response to the treatment, in order to accelerate the development of photodynamic antimicrobial therapy in drinking and residual water treatment. Three different cationic porphyrins where used in the experiment, which were irradiated by a white light (380-700nm). With the study, they demonstrated that it is possible to rapidly photoinactivate bioluminescent *E. coli* with cationic *meso*-substituted porphyrins, and that, the photoinactivation pattern obtained with the bioluminescence method was similar to the one shown by the plating technique for the *E. coli* strain treated with the Tri-Py+-Me-PF.

Recently, Bartolomeu *et al.* (2017) investigated the efficacy of PDI for wastewater treatment. Their experiments involved three different set ups, one testing filtered wastewater with added *E. coli*; pure wastewater, without filtration; and phosphate buffered saline (PBS) solution with added *E. coli.* The photosensitiser used was the cationic porphyrin Tetra-Py+-Me and the system was irradiated by an artificial white lamp (380-700nm). They observed total inactivation of *E. coli* (~5-log), after 30 minutes of irradiation (7.2 J/cm^2), for both, wastewater and PBS systems. For the pure wastewater, 90 minutes were necessary to inactivate *Enterococci* and 120 minutes for *E. coli.* These results show the suitability of the system as an alternative for wastewater disinfection. Also, it highlights that a secondarily treated wastewater is as susceptible to PDI as PBS, showing that PBS is a good alternative from preliminary experiments regarding the use of PDI for water disinfection.

Even though the use of photosensiters in solution had and have shown good results in deactivating microorganisms, these conditions are not ideal when considering the application of PDI for water disinfection. With the photosensitiser free in solution, its release in the environment after the treatment would be inevitable, which could cause harmful effects to other living beings. The photosensitiser removal would then be

required when considering the method for practical applications in a water treatment system, which would be laborious and not cost effective (Valkov *et al.,* 2014).

However, as the photosensitiser does not have to go through or bind to the cytoplasmic membrane, to be able to effectively inactive the bacterial cell (Dahl *et al.*, 1987), photosensitiser immobilisation would be an interesting approach to address this problem, as the photosensitiser would still be effective for microbial inactivation, it would not leach into the water, and its reuse would be possible, thereby making the system cost-effective and environmental friendly (Alves *et al.*, 2008; Spagnul *et al.,* 2015).

A number of research groups have investigated the application of immobilised photosensitisers for antimicrobial purposes where they incorporated the photosensitisers to a polymeric support (Spagnul *et al.,* 2015). However, only a few of them investigated their use for water disinfection. Table 1.4 summarises the photosensitiser that have been used immobilised to a solid matrix for water disinfection purposes.

Table 1.4 – Immobilised photosensitisers applied for water disinfection

Photosensitiser	**Solid matrix**	**Bacteria**	**Reference**
tetra tertiary butyl zinc phthalocyanine (TBZnPc) and zinc phthalocyanine tetrasulfonic acid (ZnPcTS)	Silicate	*E. coli*	Artarsky *et al.*, 2006
5,10,15,20-Tetrakis(p hydroxyphenyl)porphyrin (1, p-THPP), 5,10,15,20-tetrakis(p-aminophenyl)porphyrin (2, p-TAPP) and Zinc(II) phthalocyanine tetrasulfonic acid tetrasodium salt	Chitosan membrane	*E. coli*	Bonnet *et al.*, 2006
Ru(II) phenantroline complexes Ru(II) bipyridyl complex	Porous silicone cylinders, cationic nylon, cellulose and poly(vinylidene difluoride) membranes	*E. coli and* *E. faecalis*	Jímenez-Heranzez *et al.*, 2006
tris(4,7-diphenyl-1,10-phenanthroline)ruthenium(II) dichloride and	Porous silicone	*E. faecalis*	Manjon *et al.*, 2009

tetrasodium tris(1,10-phenanthrolinyl-4,7-bis(benzenesulfonate))ruthenate(II)			
tris(4,4′-diphenyl-2,2′-bipyridine)ruthenium(II) and tris(4,7-diphenyl-1,10-phenanthroline)ruthenium(II)	Porous silicone	*E. faecalis*	Manjon *et al.*, 2010
[5-(pentafluorophenyl)-10,15,20-tris(4-pyridyl)porphyrin, 5-(pentafluorophenyl)-10,15,20-tris(1-methylpyridinium-4-yl)porphyrin tri-iodide and 5-(pentafluorophenyl)-10,15,20-triphenylporphyrin	Magnetic silica nanoparticles	*E. coli, E. faecalis and T4-like Phage*	Carvalho *et al.*, 2010
[5-(pentafluorophenyl)-10,15,20-tris(1-methylpyridinium-4-yl)porphyrin tri-iodide]	Magnetic silica nanoparticles	*Allivibrio fischeri*	Alves *et al.*, 2014
Rose bengal and methylene blue	Polystyrene flims	*E. coli and S. aureus*	Valokonv *et al.*, 2014
Tris(4,7-diphenyl-1,10-phenanthroline)ruthenium(II) dichloride and 1-(4-Methyl)-piperazinylfullerene	Porous silicone	*E. faecalis*	Manjon *et al.*, 2014
9,14-dicyanobenzo[b]triphenylene-3-carboxylic acid (DBTP-COOH)and 9,10-Anthraquinone 2-carboxylic acid	Silica	*E. coli*	Benabbou *et al.*, 2011
5-(N-tetradecylpyridinium-4-yl)-10,15,20-tris(N-methylpyridinium-4-yl)porphine tetrachloride	Silica microparticles	*E. coli and S. aureus*	Magaraggia *et al.*, 2013
Methylene blue and Rose bengal	Polystyrene films	*E. coli and S. aureus*	Nakonechny *et al.*, 2013
Ru(II) phenantroline complex-C60 fullerene	Porous silicone	*E. faecalis*	Manjon, *et al.*, 2014
metallophthalocyanines	Polystyrene electrospun nanofibers	*E. coli*	Osifeko, and Nyokong, 2014

Jimenez-Hernandez *et al.* (2006) performed experiments with two Ru(II) derived complexes immobilised onto porous silicone and different membranes, in a home-made microreactor system irradiated by a Xenon lamp. The bacteria, *E. coli* and *E. faecalis,* were suspended (10^3 CFU/ml) 9.5ml of MilliQ, which was passing through the reactor (15ml/h). They observed up to 90% of bacterial inactivation, showing the effectiveness of the material in producing reactive oxygen species.

Another group that used immobilised photosensitiser in a laboratory scale photoreactor was Bonnet *et al.* (2006). They immobilised two different porphyrins to a chitosan membrane (poly(D-glucosamine)) which was used to inactivate *E. coli* in a saline suspension. The lamp used was a halogen lamp and one static and one circulating photoreactor (Figure 1.13) were used.

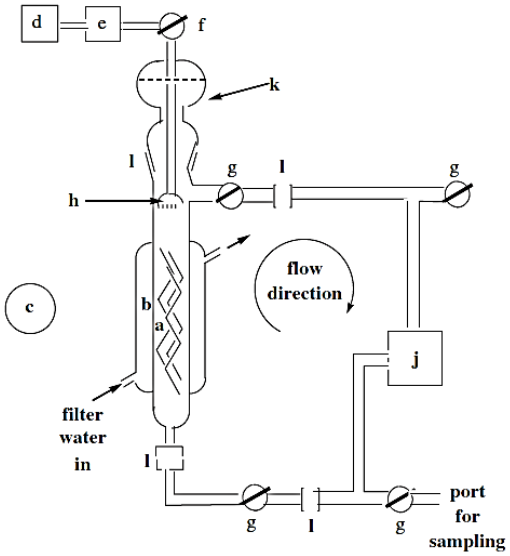

Figure 1.13 - Circulating water photoreactor system used by Bonnet *et al.,* 2006. a—membrane; b—water jacket, continuous flow, infra-red filter; c—light source; d—air pump; e—bacterial air filter; f—3-way tap/pressure release; g—2-way taps; h—frit for aeration; j—peristaltic pump; k—reservoir.

An interesting immobilisation approach was taken by Carvalho *et al.* (2010). They immobilised three porphyrins on magnetic nanoparticles, which would facilitate its recovery in a wastewater treatment plant just by applying a magnetic field. While two of the magnetic silica nanoparticles where aggregating in water, the one with a cationic porphyrin showed to be stable. The antimicrobial studies showed that the novel cationic nanomagnet-porphyrin hybrids are efficient for the photoinactivation of bacteria and phages, requiring a maximum light dose of 43.2 J/cm^2 for their inactivation.

Recent work, by Osifeko and Nyokong (2014) used metallophthalocyanines embedded in polystyrene electrospun nanofibers. The experiments were performed in quartz cuvettes containing 1ml of *E. coli* suspension in PBS. The nanofibers showed to be effective in deactivating *E. coli*, with a 5-log reduction being observed after 30 minutes (60mJ*/*cm^2).

Overall, the PDI process is a promising ecologically-friendly alternative for water disinfection since it requires visible light, which can ideally be sunlight, as the energy source, and uses oxygen dissolved in water as the oxidising agent. Also, the fact that developing tropical countries, where surface water contamination is a common problem, have intense sunlight incidence available, makes it even more attractive (Jiménez-Hernández *et al*, 2006, Ergaieg *et al.*, 2008).

The potential for the development of PDI for the disinfection of water coupled with an interest in the development of an alternative approach for the disinfection of water led to this study. Studies in this area to date are limited presenting opportunities for research on a number of aspects, which will be explored in this thesis, including investigations on experimental systems used, a broader range of bacteria and the consideration of a practical application of the technology.

1.5 Aim and objectives of the project

The aim of the project was to investigate the application of photodynamic inactivation for the disinfection of water. The objectives were:

- To design an efficient experimental system for antibacterial photodynamic inactivation;
- To characterise and evaluate TMPyP as photosensitiser for antibacterial photodynamic activation;
- To determine the response of a range of microorganisms to TMPyP at different concentrations;
- To evaluate the role of bacterial cell characteristics in the response to the treatment;
- To immobilise the porphyrin to a solid matrix for water disinfection at laboratory scale.

2. Materials and Methods

2.1 Materials

2.1.1 Photosensitiser

The porphyrin 5,10,15,20-Tetrakis(N-methyl-4-pyridyl)-21,23H-porphyrin tetratosylate (TMPyP or T_4MPyP) was purchased from Porphyrin Systems Lübeck, Germany. TMPyP is a water-soluble tetracationic porphyrin, with N-methylated pyridine substituents which are nearly perpendicular to the plane of the porphyrin. Its chemical structure showing its characteristic tetrapyrrole ring is presented in Figure 2.1 and its properties are shown in Table 2.1.

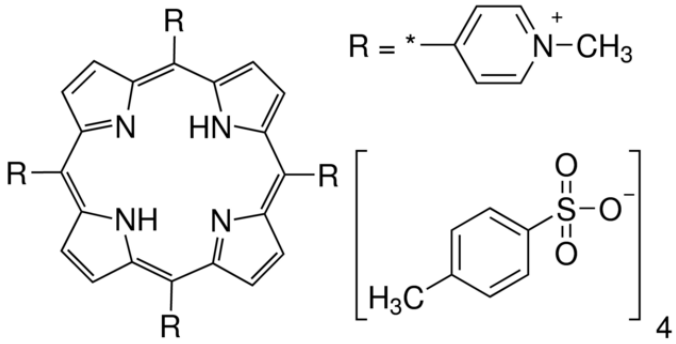

Figure 2.1 – Chemical structure of the porphyrin TMPyP.

Table 2.1 - Properties of the porphyrin TMPyP.

Molecular weight (g/mol)	1363.63
λmax abs (nm)	422
Purity	98%
Solubility	Water soluble

2.1.2 Bacteria

The bacteria used in this study are listed in Table 2.2.

Table 2.2 - Bacterial strains used in the study.

Strain	Source	Growth temperature
Escherichia coli DSM 498	DSMZ*	30 ºC
Escherichia coli DSM 1103	DSMZ*	35 ºC
Shigella sonnei DSM 5570	DSMZ*	35 ºC
Salmonella enterica DSM 17058	DSMZ*	35 ºC
Pseudomonas putida DSM 6125	DSMZ*	30 ºC
Pseudomonas fluorescens DSM 50090	DSMZ*	30 ºC
Pseudomonas aeruginosa PAO1	DSMZ*	35 ºC
Enterobacter aerogenes DSM 30053	DSMZ*	35 ºC
B. subtilis DSM 10	DSMZ*	30 ºC
Staphylococcus aureus DSM 799	DSMZ*	35 ºC
Escherichia coli (T37-1)	Environmental isolate Tolka River, Dublin	30 ºC
Pseudomonas putida CP1	Research laboratory culture collection	30 ºC

*DSMZ – Deutsche Sammlung von Mikroorganismen und Zellkulturen - German Collection of Microorganisms and Cell cultures.

Bacteria were maintained on Nutrient Agar (Oxoid) at 4ºC. The cultures were preserved by growing overnight in 10ml of nutrient broth. 0.85 ml of overnight culture was mixed in 0.15 ml of 30% (v/v) sterile glycerol solution and stored in Eppendorf's at -80ºC.

2.1.3 Buffer

Phosphate buffered saline (PBS) (Fisher Chemical) was prepared by dissolving 1 tablet in 100ml of distilled water and autoclaved at 121ºC for 15 minutes.

2.1.4 Growth media

The growth media described in Table 2.3 were used in this study. All of them were prepared in accordance with the manufacturer's instructions. For nutrient broth, aliquots of 10ml were dispensed into glass universals prior to the autoclave sterilisation at 121ºC for 15 minutes.

Table 2.3. Growth media used in the different experiments.

Medium	Source	Purpose
Nutrient broth	Oxoid	Bacterial Growth
Muller-Hinton broth	Oxoid	Antibiotic response
M9 – Minimal broth	Oxoid	Pigment production
Nutrient agar	Oxoid	Bacterial Growth
Muller-Hinton agar	Oxoid	Antibiotic response
MacConkey agar	Oxoid	Selective growth
Pseudomonas agar supplemented with SR103	Oxoid	Pigment production
King agar A	Sigma-Aldrich®	Pigment production
King agar B	Sigma-Aldrich®	Pigment production

2.1.5 Chemicals

All the chemicals used in this study were purchased from Sigma-Aldrich® (Gillingham, UK) and are listed in Table 2.4.

Table 2.4 – Chemicals used in this study.

Chemical	Specification
Dimethyl sulfoxide (DMSO)	≥99.9%
Acetone	≥99.9%
2-Hydroxyethyl methacrylate (HEMA)	containing ≤250 ppm monomethyl ether hydroquinone as inhibitor, 97%
Ethylene glycol dimethacrylate (EGDMA)	containing 250 ppm MEHQ as inhibitor, 99%
Methacrylic acid (MMA)	98%, containing 90-110 ppm monomethyl ether hydroquinone as inhibitor
Luperox® A98	Benzoyl peroxide reagent grade, ≥98%
Alumina	neutral activated, Brockmann activity

2.1.6 Lamps

Three different LED lamps were used (Figure 2.2).

A – *Monochromatic 525nm LED lamp with an area of 32 cm^2, which was custom made in DCU using LEDs supplied from Roithner Lasertechnik, Vienna, Austria.*

B – *Visible light (400-700nm) LED lamp with an area of 19.6 cm^2, purchased from Maplins, Dublin.*

C – *Dichromatic (430 and 660 nm) LED lamp with an area of 730 cm^2, purchased from LED Supplies (UK) Limited, London, UK.*

Figure 2.2 – Lamps used for the PDI experiments. (A) Monochromatic 525nm LED lamp (B) Visible light (400 -700 nm) LED (C) Dichromatic (460 and 630 nm) LED lamp.

2.2 Methods

2.2.1 Experimental System

PDI experiments were performed with the bacteria listed in Table 2.2. The medium used for the experiments was PBS and the photosensitiser used was the cationic porphyrin TMPyP. Two types of vessels were used: 96-well plates and glass petri dishes, which were irradiated using all 3 lamps in different experimental runs (see item 2.1.6).

2.2.1.1 Medium

The medium used on this study was PBS, since it helps to maintain a pH and osmotic balance throughout the experiment. The amount of dissolved oxygen in the solution was measured with a dissolved oxygen meter (HANNA 9146 – HANNA® Instruments, UK) and was found to be close to saturation.

The pH in the different porphyrin solutions (3.65, 5 and 10μM) was neutral (7), as indicated by measurements made with a universal indicator paper (Lennox, Dublin, Ireland).

2.2.1.2 Porphyrin

The photosensitiser used in this study was the porphyrin TMPyP (see Fig. 2.1) and it was investigated at different concentrations for its capacity of photoreacting with bacteria in an aqueous medium. Its photochemical and photophysical characteristics and its capacity to generate reactive oxygen species were investigated using the following methods.

Extinction coefficient calculation

The extinction coefficient, or molar absorptivity, defines how strongly a substance absorbs light at a given wavelength. According to Beer's Law, the molar absorptivity of a compound is constant, and the absorbance is proportional to its concentration, when it is dissolved in a certain solvent and measured at a specific wavelength. For this reason, molar absorptivity is known as molar extinction coefficient (ε) and can be calculated as follows (Weast *et al.,* 1975).

$$\varepsilon = \frac{A_\lambda}{c.L}$$

Where, A_λ is the compound absorbance at a specific wavelength, *c* is the compound concentration (mol/L) and *L* is the light path length, in centimetres (always adjusted to 1cm in laboratory spectrophotometers).

Ultraviolet-visible spectroscopy

UV-visible spectroscopy was used to characterise and define TMPyP Soret and Q bands. The ultraviolet-visible (UV-vis) spectrum of the porphyrin TMPyP in aqueous solution was obtained using (UV-3100PC - VWR, Ireland) 1 nm resolution over a 350-700 nm wavelength range. All spectra were obtained in PBS (which was used as the blank).

Reactive oxygen species (ROS) production

The production of ROS by different concentrations of TMPyP was investigated using the molecular probe CM-H_2DCFDA (5-(and-6)-chloromethyl-2',7'-dichlorodihydrofluorescein diacetate, acetyl ester) (Invitrogen™, ThermoFisher, Dublin) following the methodology described by Hanakova *et al.* (2012). After incubation with TMPyP at different concentrations (3.65, 5 and 10μM) and irradiation for 30 minutes, the suspensions were treated with 10μmol/l CM-H_2DCFDA for 30 min at 37 ◦C in darkness. The fluorescence of CM-DCF (oxidised form) (excitation 495 nm and emission 530 nm) was recorded by the 96-well microplate reader (Tecan Infinite F200, Switzerland). Negative controls were

performed with the cells without porphyrin and a positive control was performed with hydrogen peroxide (0.03% v/v).

Near-infrared spectroscopy - singlet oxygen generation

Photosensitised $^1O_2$ generation by TMPyP, in air equilibrated PBS and D_2O, was monitored directly by near-infrared emission spectroscopy (NIR), through the emission of $^1O_2$ at *ca.* 1270 nm (Kearns, 1971). NIR emission spectra were recorded using an Andor iDus InGaAs detector coupled with a Shamrock 163 spectrograph with excitation using a 4 mW 405 nm diode laser (Thorlabs LDM 405). The singlet oxygen quantum yield of TMPyP was then determined by comparing the wavelength integrated intensity of its emission spectrum to a reference one (Montalti *et al.,* 2006). The standard reference used was the compound ruthenium trisbipyridyl chloride $[Ru(bpy)_3]Cl_2$ (Gutiérrez *et al.*, 2003). The equations for the calculation of Φ are shown below:

$$\Phi_{TMPyP} = \Phi_R \frac{I_{TMPyP}}{I_R} . \frac{A_R}{A_{TMPyP}}$$

Where, Φ_{TMPyP} is the quantum yield of TMPyP, Φ_R is the standard known quantum yield, I_{TMPyP} is the integrated emission intensity of TMPyP, I_R is the standard integrated emission intensity, and A is each compound absorbance at the excitation wavelength. I was then calculated as follows:

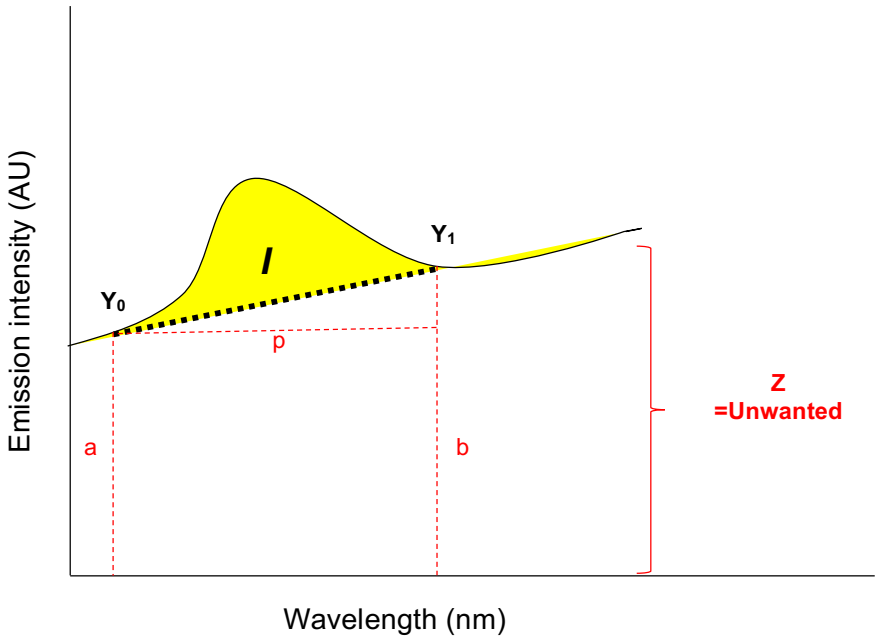

Figure 2.3 – Schematic representation of the graph for the integrated emission calculation.

$$I = (\sum y_0 : y_1) - z$$

Where *I* is the integrated emission intensity, y_0 is the wavelength value at the start of the curve, y_1 is the wavelength value at the end of the curve and *z* is the unwanted area under the curve (trapezoid) (Figure 2.3). The trapezoid (z) area was calculated as follows:

$$Z = p\left(\frac{a+b}{2}\right)$$

Evaluation of TMPyP mutagenicity– Ames test

The microplate format mutagenicity assay (AMES-MOD ISO™ kit, EBPI Inc. Canada), was used to test the genotoxicity of the porphyrin TMPyP at different concentrations. The test was performed according to the manufactures instructions, briefly described as follows. The lyophilised bacteria S*almonella typhimurium* TA-100 was grown overnight at 37ºC in nutrient broth, after that, its OD was adjusted to 0.05 at 600nm. In a 24-well plate, 1.6ml of each TMPyP aqueous solution (2.5 µM, 5 µM and 10 µM) was mixed with

200µl the exposure solution and to 200µl of the bacterial suspension, in triplicate. For the positive control of mutagenicity, sodium azide (NaN_3) was used and the positive control wells were performed in duplicate. Sterile DI water was used as the negative control and was also performed in duplicate. The plates were then incubated at 37ºC for 100 minutes. After that, the 1.6ml from each well was transferred to different vessels containing 8.7ml of bromocresol reversion media and mixed. Each mixture was then plated into half of a 96-well plate (48 wells) for a total of 144 replicates. The 96-well plates were then incubated for 72 hours at 37ºC. Within two days, cells which have undergone the reversion to *His* will grow into colonies. Metabolism by the bacterial colonies reduces the pH of the medium, changing the colour of that well from purple to yellow. This colour change was detected visually and the plates were scored based on that. The number of wells containing revertant colonies were counted for each sample and compared to the positive control (yellow coloured wells). Average score for negative or background control is ≥ 0 and ≤ 15 revertant wells per 48-well section. Average score for positive (standard mutagen) controls is ≥ 25 revertant wells per 48-well section on day 2.

2.2.1.3 Vessels

Two types of vessels were used to perform the PDI experiments – 96-well plates and glass Petri dishes.

96-well plates

96-well plates (Greiner bio-one, Cruinn, Dublin) were used to perform preliminary experiments. The plate set up is described in Fig. 2.4. The 24 central wells were used (Figure 2.4) since on those wells there was a higher light incidence (monochromatic and multichromatic lamp). 100µl of PBS was added to each of the 24 wells. To the 3 first wells, from the first column, were added as well: 80µl of PBS and 20 µl of a 200µM TMPyP stock solution, achieving a concentration of 20µM TMPyP/well. With the help of a multi-channel pipette, 100µl were taken from those 3 first wells and transferred to the 3 next ones (left to right), in a process of serial dilutions, achieving always half of the concentration of the previous wells. This procedure was repeated 4 times. After that, 5µl of the bacterial suspension was added to each well to give a final concentration of 10^5 CFU/ml. Positive controls (control 1), were the bacterium added to 100 µl of PBS (no porphyrin); and negative controls (control 2), were just PBS was added to the wells, with the aim of verifying its sterility, were also performed. A dark control was performed by keeping a plate, with the same set up as the on explained above, in the dark. And a light

control was also performed by keeping a plate with similar set up (excluding the porphyrin), under the lamp. The experiments were performed in triplicate.

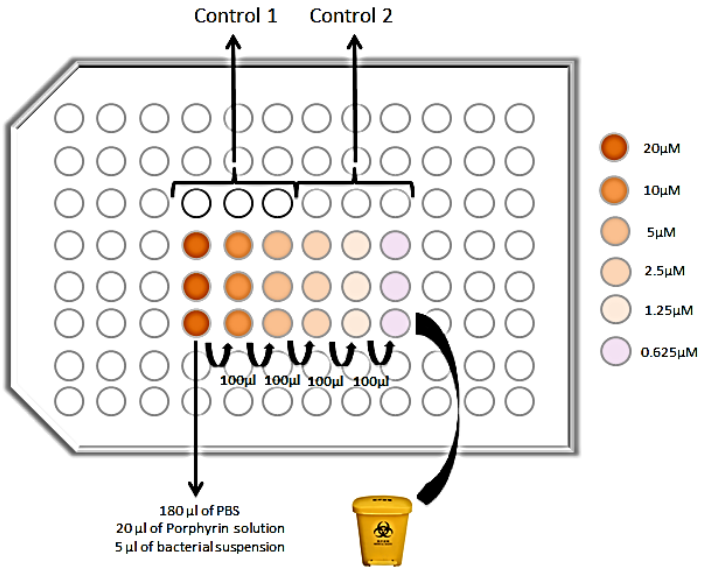

Figure 2.4 – Representation of the 96-well plate with the treatments distribution in the central area.

Samples were taken before light exposure - T_0. The plate was then placed under the lamp device (only one light source over the plate) for different time intervals. After each specific time of exposure, samples were taken to evaluate the number of cells using the drop plate technique. Only the monochromatic and multichromatic lamps were used with this vessel.

Glass petri dishes

Glass Petri dishes (60x15 mm) (DURAN®, VWR, Ireland) were used to perform the experiments with larger volumes. The final volume used was 10 ml which included the particular concentration of porphyrin (3.65, 5 or 10µM) in PBS and the inoculum (0.1ml). After setting up the plates, samples were taken before the light exposure (T_0). The plate was then placed under the lamp (only one light source over the plate) for different time intervals. All the three lamps were used with the glass Petri dishes. In all cases the inoculum size used was 10^5 CFU/ml.

2.2.1.4 Light dose calculation

A monochromatic 525nm LED lamp, a visible light (400-700 nm) LED lamp and a dichromatic LED lamp (Figure 2.3) were used. The set up for the monochromatic and

multichromatic lamps are shown in figure 2.5, and the set up for the dichromatic lamp is illustrated in Figure 2.6. The fluence rate of each lamp was measured by a radiometer (Delta Ohm HD 2101.2) equipped with an irradiance probe (LP 471 RAD).

In the case of the monochromatic 525 nm and the visible LEDs the distance between the plates and the lamps was 3 cm, delivering an average fluence rate of 1.01 mW/cm^2 for the monochromatic lamp and 0.97mW/cm^2 for the multichromatic lamp (Fig. 2.5).

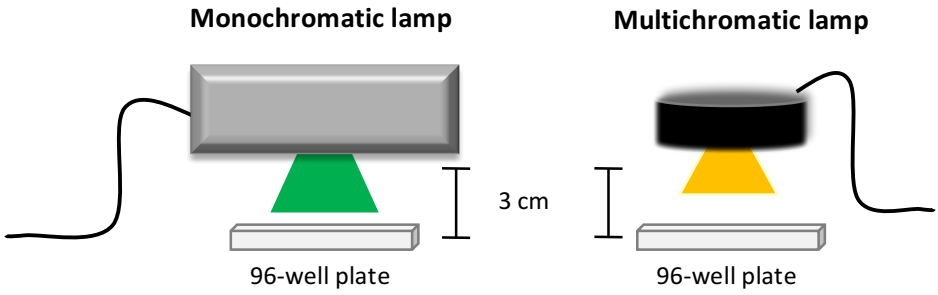

Figure 2.5 – Representation of the light incidence, from the monochromatic 525nm LED lamp and the visible (λ ≥400nm) LED lamp over the 96-well plates.

In the case of the dichromatic LED source (430 and 660nm), the distance between it and the samples was 25 cm, giving an average fluence rate of 21.93 mW/cm^2 (Fig. 2.6).

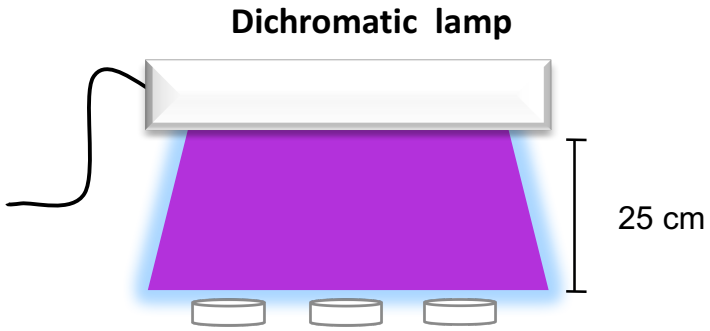

Figure 2.6 – Representation of the light incidence, from the dichromatic (430 and 660nm) lamp over the petri dishes.

The light dose (Q), energy density, was calculated according the following equation (En-Sheng *et al.*, 2012):

$$Light\ dose\ \left(\frac{J}{cm^2}\right) = lamp\ fluence\ rate\ \left(\frac{W}{cm^2}\right).\Delta t\ (s)$$

2.2.2 Inoculum preparation

Bacteria were grown aerobically overnight in 10 ml of nutrient broth at 150 rpm and at the temperature specified in Table 2.2 for each strain. Overnight cultures were washed twice (4000rpm for 20 minutes) and re-suspended in 10ml of PBS. The optical density was adjusted to give the desired number of cells.

Cocultures of *E. coli* T37-1 and *P. aeruginosa* PAO1 were investigated and were prepared in two different ways, growing together and growing separately. For the bacteria grown separately, each strain was grown as described above. After that, 50µl of each bacterial suspension was added to the petri dish containing PBS with TMPyP at a concentration of 3.65µM, for irradiation. For the bacteria grown together, 50µl of each bacterial suspension (prepared as described above) was added to a universal containing 10ml of nutrient broth. The co-culture was then incubated at 30º and 150 rpm overnight, and washed following the same steps described previously.

2.2.3 Methods used to monitor the response of the bacteria to PDI.

The response of the bacteria to PDI was monitored using culturable techniques including the streak plate method, the drop plate method and the plate count method.

Streak plate technique

The streak plate technique was used to qualitatively identify the presence and the absence of bacterial growth in the 96-well plates. A loopful was taken from each well, with each different treatment and streaked onto a nutrient agar plate. The absence or presence of growth were expressed with a (+) or (-) signal, respectively.

Drop plate technique

The drop plate technique was performed according to Herigstad *et al.* (2001) with a modification in the sample size. For this method, drops of the sample (5µl) were dispensed on the agar plate in triplicate. When dry, the plates were incubated at 30º C for 24h and the colonies within the drops were counted. Only drops with 3 – 30 colonies were counted. The average count of triplicates (N) was used to calculate the number of bacteria as follows:

$$\frac{N}{5.10^{-3}} = number\ of\ \frac{CFU}{ml}$$

Pour plate technique

The pour plate technique was used by preparing serial dilutions of the sample in tubes containing 9 ml of PBS, and plating onto nutrient agar plates. The plates were incubated at 30ºC or 35ºC, depending on the strain, for 24h. The total number of colonies were counted on plates with colonies in the range of 30-300. The average count of triplicates (N) was used to calculate the number of bacteria as follows:

$$N\ x\ dilution\ factor = \ number\ of\ \frac{CFU}{ml}$$

The numbers were expressed using logarithmic notation, where the value presented is the base 10 logarithm of the concentration (CFU/ml). It was calculated as follows:

$$\log_{10}(\ Nx\ dilution\ factor) \ = \ \log\frac{CFU}{ml}$$

Inactivation rate

A simple linear regression was used to calculate the rate of inactivation of each bacterium. The following equation, suggested by the work of Ergaieg and Seux (2009), was used:

$$\log_{10}(N(t)) = \ -kt + \ \log_{10}(N(0))$$

Where k is the photoinactivation rate constant (min^{-1}), $N_{(0)}$ and $N_{(t)}$ are the bacterial concentrations expressed in log units before and after exposure to the lamps at a given time t (min). All the data were analysed in Excel.

2.2.4 Antibiotic profile of the bacteria

The antibiotic profile of the bacteria was determined by the Kirby-Bauer disc diffusion method and the minimum inhibitory concentration (MIC) of tetracycline and ampicillin was also determined.

Kirby-Bauer disc diffusion method

The antimicrobial susceptibility test was performed following the Kirby-Bauer disc diffusion method (Bauer *et al.*, 1966). Each bacterium was grown overnight in nutrient broth and its OD was adjusted to give a concentration of 10^8 CFU/ml (0.09 for *E. coli* DSM 1103 and *S. aureus* DSM799 and 0.02 for the remaining bacteria). The bacterial suspension was them spread onto the surface of a Muller-Hinton agar plate (triplicates)

with a cotton swab. After the inoculum had dried the antibiotic discs (6mm) (Table 2.5) were placed on the agar surface with the help of a disc dispenser (Oxoid™). The plates were incubated overnight and the diameter of the zones of inhibition (halos) was measured as shown in Figure 2.7.

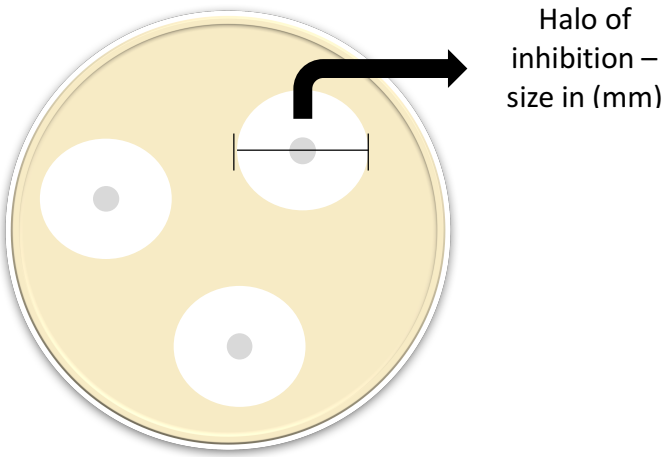

Figure 2.7 – Halo of inhibition from the Kirby-Bauer disc diffusion method.

Table 2.5 – Antibiotic discs used for the antimicrobial susceptibility test.

Antibiotic	**Amount per disc**
Imipenem	10µg
Ampicillin	10µg
Ciprofloxacin	10µg
Cefotaxime	30µg
Tetracycline	30µg
Erythromycin	30µg
Vancomycin	30µg

Minimum Inhibitory Concentration

The 12 bacterial strains were challenged against two antibiotics, Tetracycline and Ampicillin. The standard 96-well plate method, described by Andrews (2001), was used. After the plate set up (Fig. 2.8), where two-fold dilutions (antibiotic stock solution in water) were carried out starting from an initial concentration of 5000µM down to 0.78µM, and 5µl of bacterial suspension was added to each well, the plates were incubated at 30ºC or 35º C for 17-20h.The absorbance from each well was measured using a plate reader at 660 nm (Tecan*i*-control – Infinite 200). A positive control was carried out with bacterial cells without the addition of antibiotic and a negative control as carried out with the media without bacterial cells.

The MIC of the cocultures (*E. coli* T37-1 with *P. aeruginosa* PAO1, and *E. coli* T37-1 with *P. fluorescens* DSM 50090), grown together and grown separately, was also assessed and their inoculum was prepared as explained in item 2.2.2. The antibiotic used was ampicillin, with the concentrations varying from 5000µM down to 0.78µM. The streak plate technique, where a loopful taken from each well was taken and plated in McConkey agar and King A agar, was used to identify the presence and absence of growth of each bacterium.

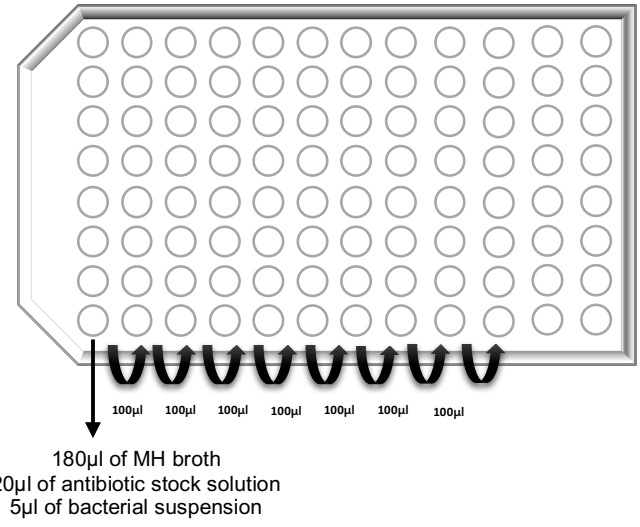

Figure 2.8 - 96 well-plate set up for MIC determination. Two-fold dilutions were carried out in series, from the left to the right.

2.2.5 Pigment production measurement

Pigment production by *Pseudomonas* strains was evaluated by spectrophotometric analysis. *Pseudomonas* strains were grown in LB (supplemented with 10 mM glucose);

M9 (supplemented with 10 mM glucose); nutrient broth; King A and King B media. Following growth, the organisms grown on agar, King A and King B media, were resuspended in PBS. The resuspended cultures and the cultures grown in broths were then centrifuged (13,000 rpm for 10 min). The supernatants were spectrophotometrically analysed (VWR UV 3100 PC Spectrophotometer). The spectra were registered in the wavelength range from 300 to 800 nm and were compared to spectra of pigments already reported in the literature. The spectrum for pyomelanin was reported by Kurian *et al.* (2014), those for phenazine-1-carboxylic acid (PCA) and pyocyanin by Mavrodi *et al.* (2013) and that for pyoverdine by Braud *et al.* (2009). A peak at 310 nm is ascribed to pyocianin, a peak at 364 nm is ascribed to phenazine and peak at 400 nm is ascribed to pyoverdine presence in the media (Orlandi *et al.,* 2015).

2.2.6 Bacterial cell aggregation measurement

Settling method

To study cell aggregation, the bacterial cells were diluted to 10^8 cells/ml in PBS. Optical density was determined in 1 ml plastic cuvettes (SARSTEDT) using a Spectrophotometer (VWR UV- 300PC) at 600 nm. The bacteria were allowed to aggregate and settle for 60 min at room temperature in plastic cuvettes under static conditions while monitoring the decrease in optical density (OD) every 15 min. Settling as a consequence of aggregation was quantified as a percentage reduction in OD after 60 min.

$$\% \, aggregation = \frac{OD0\,\mathrm{min} - OD60min}{OD0min} \, X \, 100$$

Where OD_{0min} is the initial OD at the start of an experiment and OD_{60min} is the OD after 60 min. All measurements were done at 600 nm using PBS without bacteria as blank (Das *et al.,* 2013).

Microscopic method

Overnight cultures of bacterial cells were stained with the dye SYTO9 (Invitrogen™, ThermoFisher, Dublin) and mounted in cavity glass slides using 1.2% agarose gel (Sigma-Aldrich®, Gillingham, UK). The slides were observed using a confocal laser scanning microscope (CLSM) (Leica SP8, Leica, Germany). SYTO 9 was excited by a white light laser at 485 nm and the fluorescence emission was detected at 498 nm. Planktonic and aggregated bacterial cells fluoresced green, all the images were obtained

using 100x lens magnification using oil immersion. Z-stacks were used to capture images of the aggregates.

2.2.7 Porphyrin immobilisation

To investigate the performance of immobilised porphyrin, TMPyP was immobilised in two different matrices, glass beads and a polymer.

Glass bead coating

Glass beads measuring 5mm (diameter) (Merck, Germany) were used as a support to immobilise the porphyrin TMPyP. 20 glass beads were placed in a glass Petri dish (60x15mm) and soaked in a 10μM stock solution of TMPyP in DI water (Fig. 2.9). The beads were kept soaking overnight at room temperature and placed in an oven at 60ºC for 30 minutes to evaporate the remaining water. The beads were then used for PDI experiments. The porphyrin concentration in the beads was calculated based on the UV-visible absorbance spectrum (Figure 2.10) taken of the bottom of the plate where the beads were stained. The value found was ~3.04μM (calculations in Appendix I).

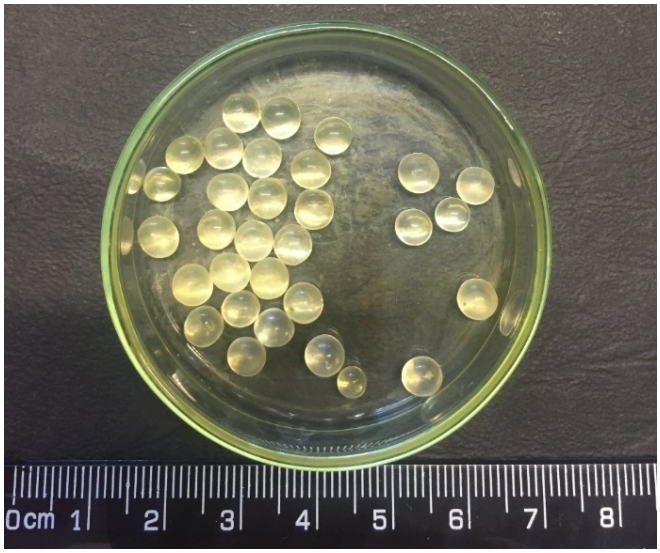

Figure 2.9 – TMPyP coated glass beads (5mm).

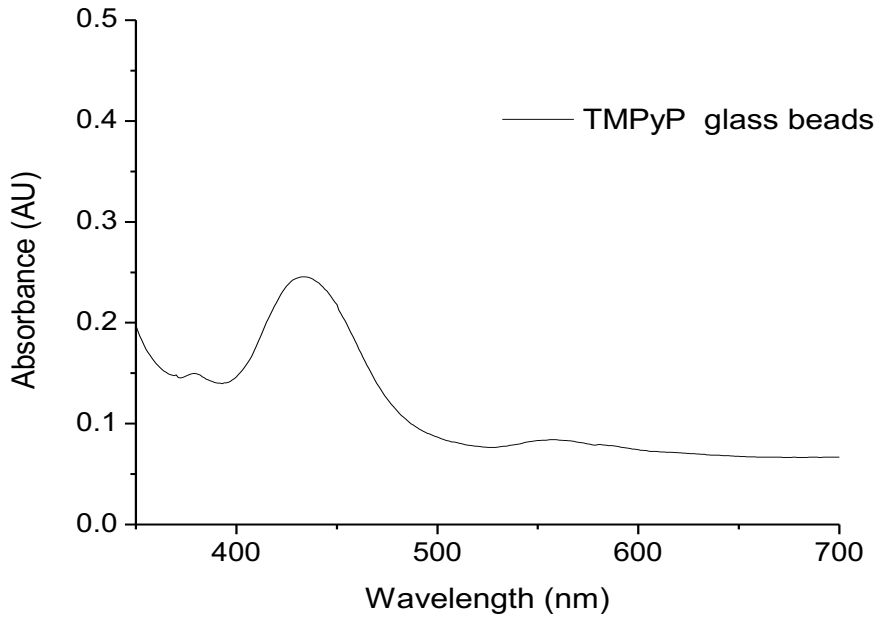

Figure 2.10 – UV-visible spectrum of the porphyrin coating the glass Petri dish.

Polymeric matrix incorporation

Hydrogels were used as the polymeric matrix for immobilisation of the porphyrin and were prepared according to a modified method described by Brady *et al.* (2007). They were produced by free radical polymerisation of HEMA (2-hydroxyethyl methacrylate, 80% w/w) with MAA (methacrylic acid, 20% w/w), using the method reported by Brady *et al.*, (2007). The cross-linking agent used was EGDMA (ethylene glycol dimethacrylate, 1% w/w), and the initiator used was BPO (benzoyl peroxide, 0.4% w/w). After removing the inhibitors from the monomers by passing them through a neutral alumina plug, 80g of HEMA and 20g of MAA were weighed and mixed in glass beakers. The initiator was then added to the monomer mixtures (it was used as received). The mixture was stirred mechanically on a magnetic plate until all the components were well dissolved. Specific amounts of TMPyP stock solution (in water) was added to the mix to get hydrogel films with a range of porphyrin concentrations (3.65 μM, 5 μM and 10 μM). 3 ml of the final solution was then added to the bottom of 60x15 mm glass Petri dishes and covered with the lid. These plates were subsequently placed in an oven at 90 °C for 2 hours to enable the polymerisation reaction. The films (Fig. 2.11) were then washed and soaked in sterile distilled water for 14 days in order to remove any remaining monomer. The hydrogel films thickness was measured with a calliper, and their average value was 0.7 ±0.002 mm. The polymer was then ready for use in the PDI experiments.

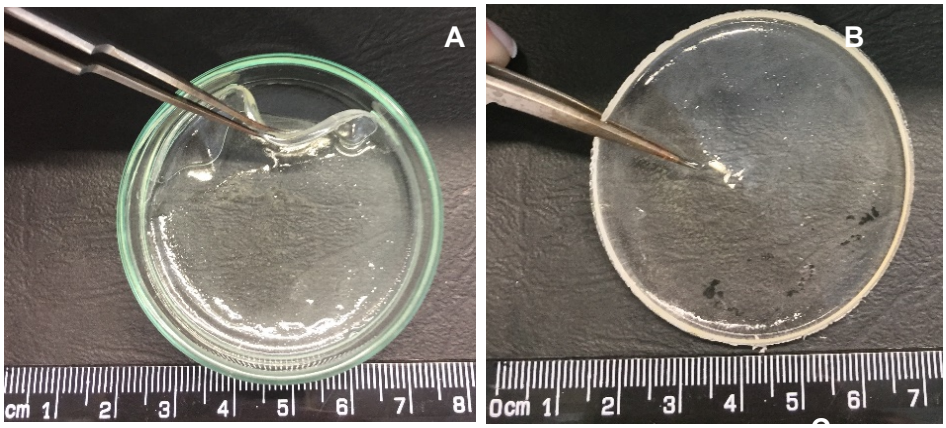

Figure 2.11 – TMPyP immobilised into a hydrogel polymeric matrix. A – hydrogel inside the Petri dish mould and B – hydrogel film.

Monitoring TMPyP leaching

To assess possible leaching of the porphyrin during irradiation from either of the two matrices employed, polymer and glass beads, and spectra were run using UV-visible spectroscopy. After different time intervals of irradiation under the dichromatic lamp, 1 ml aliquots were taken from the petri dishes and placed in plastic cuvettes to measure the optical density (300 to 700nm). The presence of a peak at 422nm indicated the presence of TMPyP in the PBS solution.

2.2.8 PDI with immobilised porphyrin

PDI with hydrogels

The hydrogels were placed in the bottom of a glass petri dish (60x15mm) and covered with 9.9ml of PBS and 100µl of bacterial suspension, to give a final concentration of 10^5 CFU/ml. The plates were then irradiated under the dichromatic lamp (λ=430 and 660nm) for different time intervals. 1ml aliquot samples were taken. The polymer without porphyrin was used as a control, and dark controls with the polymers and porphyrin were also performed. In this experiment, the bacteria tested were *E. coli* T37-1 and *P. fluorescens* DSM 50090. The pour plate technique was used to monitor cell numbers.

PDI with glass beads

Twenty glass beads (5mm) coated with TMPyP were placed in the bottom of a glass petri dish (60x15mm) and covered with 9.9ml of PBS and 100µl of bacterial suspension, to give a final concentration of 10^5 CFU/ml. The plates were then irradiated under the

dichromatic lamp (λ= 430 and 660nm) for different time intervals. 1ml aliquot samples were taken. The beads without porphyrin were used as a control, and dark controls with the beads and porphyrin were also performed. In this experiment, the bacteria tested were *E. coli* T37-1 and *P. fluorescens* DSM 50090. The pour plate technique was used to monitor the cell numbers.

2.2.9 Data Analysis

All data related to cell enumeration were statistically analysed in Microsoft Excel 2016. All the UV-visible absorbance spectra and fluorescence spectra were normalised in Origin8 SR0, 2007.

3. Results

3 Results

The study investigated the response of bacteria to PDI with a view to using the technology for the disinfection of water. The findings of the study are presented in three sections. In the first section 3.1, the development of the laboratory scale experimental system used is described. Following the development of the experimental system, the use of the system to investigate the response of a range of Gram-positive and Gram-negative bacteria to PDI is presented in Section 3.2. The final section of results, Section 3.3, focuses on factors influencing the response of *E. coli* and *Pseudomonas* species to PDI. The response of these bacteria when grown in cocultures and also when the porphyrin is immobilised, important factor for the practical application of the technology, were considered.

3.1 Development of the experimental system

In developing the lab-scale experimental system, consideration was given to the porphyrin to be used, the medium, the vessel, the lamps and the bacteria to be investigated.

The photosensitiser used was the porphyrin TMPyP and the medium was PBS, and the results are described in the following section. Three different multi-LED lamps were used – a monochromatic lamp with emission at 525nm; a visible light with emission between 400-700nm and a dichromatic lamp with emission at 430 and 660 nm. Preliminary screening was carried out in 96-well plates, where a volume of 100µl was irradiated, and later experiments were carried out in Petri dishes, where 10ml aliquots were phototreated.

3.1.1 The porphyrin TMPyP

The porphyrin 5,10,15,20-Tetrakis(N-methyl-4-pyridyl)-21,23H-porphyrin tetratosylate (TMPyP) was the photosensitiser used in this study. Photochemical and photophysical properties of TMPyP were characterised using ultraviolet-visible (UV-vis) spectroscopy, fluorescence spectrometry, and near-infrared spectroscopy.

The UV-vis spectroscopic analysis is important since it provides information regarding the position of the Soret and Q-bands in TMPyP (Pasternack *et al.*, 1972), which are key features of a photosensitiser when considering its application for PDI. It is also useful for the calculation of the compound extinction coefficient, which tells how much light can be absorbed by it in determined solution, in this case, PBS.

Fluorescence spectrometry was used to measure the fluorescence emitted by the ROS probe CM-H_2DCFDA (excitation 495 nm and emission 530 nm). Near-infrared spectroscopy is a useful tool to measure the production of singlet oxygen through its phosphoresce at *ca*.1270nm.

3.1.1.1 UV-visible spectroscopy

UV-visible spectroscopy was used to characterise the electronic absorptions spectrum of the porphyrin TMPyP when in PBS solution. Its spectrum can be found in Figure 3.1, where the presence of its two distinct regions, typical of porphyrins, are evident. At the wavelength 422nm is the peak corresponding to the Soret band (λmax), and the four less intense Q-bands correspond to the three smaller peaks at ca. 520 nm, 554 nm, 585 nm, and 641 nm (Figure 1.7 insert).

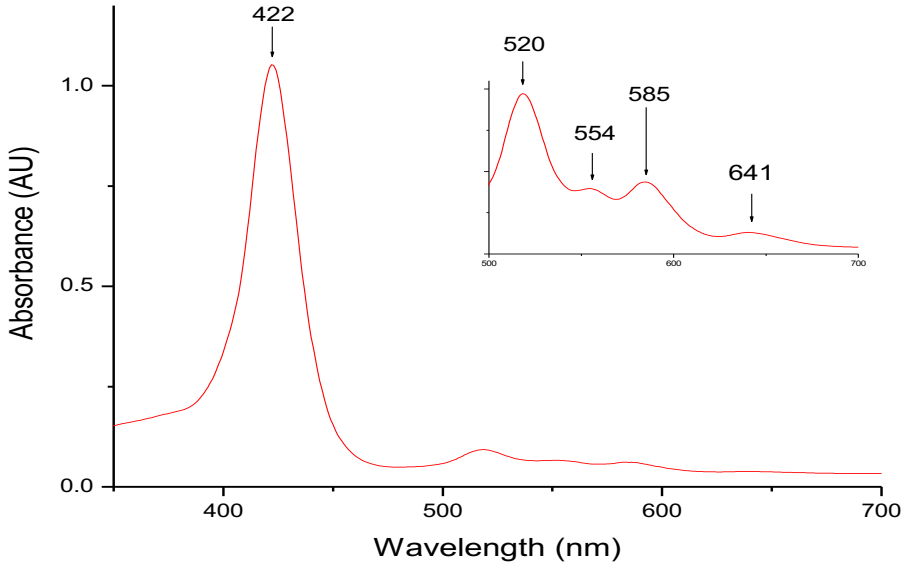

Figure 3.1 – UV-visible spectrum of the wavelength absorbance for the porphyrin TMPyP in PBS. Insert shows the four Q-bands.

3.1.1.2 Extinction coefficient calculation

In order to calculate the extinction coefficient (ε) of TMPyP in PBS, the absorbance of known concentrations of TMPyP (2.5, 3.65, 5, 7 and 10 μM) in PBS solution was measured by UV-vis spectrophotometry at 422nm, and the following calibration curve (Figure 3.2) was obtained.

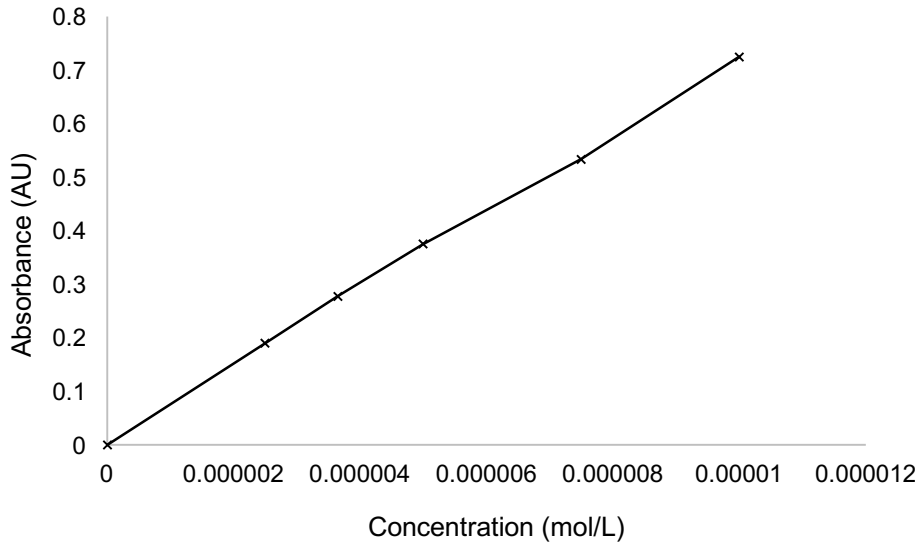

Figure 3.2 – Calibration curve of TMPyP absorbance versus its concentration at 422nm (y=71541x+0.0087, with R^2 = 0.9989).

Based on the calibration curve, the extinction coefficient could be calculated, using the equation given in item 2.2.1.2, and was found to be ε = 76,000 $M^{-1}.cm^{-1}$ (calculations in Appendix I).

3.1.1.3 Reactive oxygen species (ROS) production

The ROS production by the porphyrin TMPyP in PBS solution, at three different concentrations (3.65, 5 and 10 μM) was measured by the fluorescence emission of the probe oxidised product of the probe CM-H_2DCFDA. The product CM-DCF emits fluorescence at 530nm when excited at 495nm. The relative fluorescence units for each concentration and the controls are shown in Figure 3.3. As can be observed, with the increase in TMPyP concentration there is a slight increase in the fluorescence emission, indicating an increase in ROS production. When comparing the values to the positive control, hydrogen peroxide (H_2O_2 – 0.03% v/v), and the negative control, PBS, it is evident that the porphyrin is effective in producing ROS.

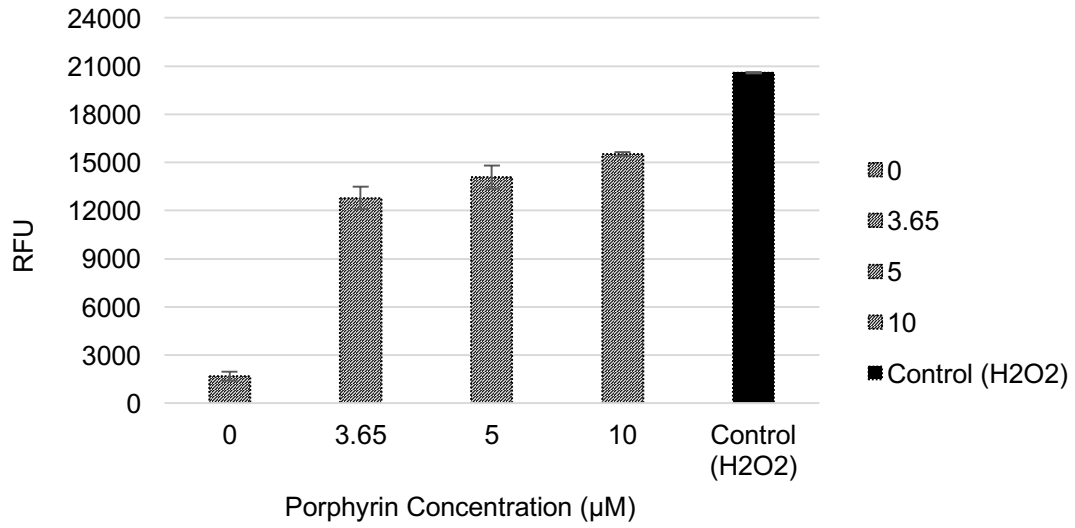

Figure 3.3. ROS production by the porphyrin TMPyP at the concentrations 0, 3.65, 5 and 10μM. Hydrogen peroxide (H_2O_2) was used as a positive control.

3.1.1.4 NIR-spectroscopy

The singlet oxygen generation by the porphyrin TMPyP was calculated indirectly by measuring the production of singlet oxygen through its phosphoresce at *ca*.1270nm using NIR spectroscopy. The NIR emission spectra for TMPyP and ruthenium trisbipyridyl (standard reference compound) in D_2O PBS solution are shown in Figure 3.4.

The singlet oxygen quantum yield of TMPyP was determined by comparing the wavelength integrated intensity of its emission spectrum to a reference one as explained in item 2.2.1.2 of the Materials and Methods section. The reference standard used was the compound ruthenium trisbipyridyl chloride $[Ru(bipy)_3]Cl_2$, which has a reported quantum yield of Φ_R=0.22. The value found for TMPyP quantum yield was Φ_{TMPyP} = 0.74 (calculations in Appendix I).

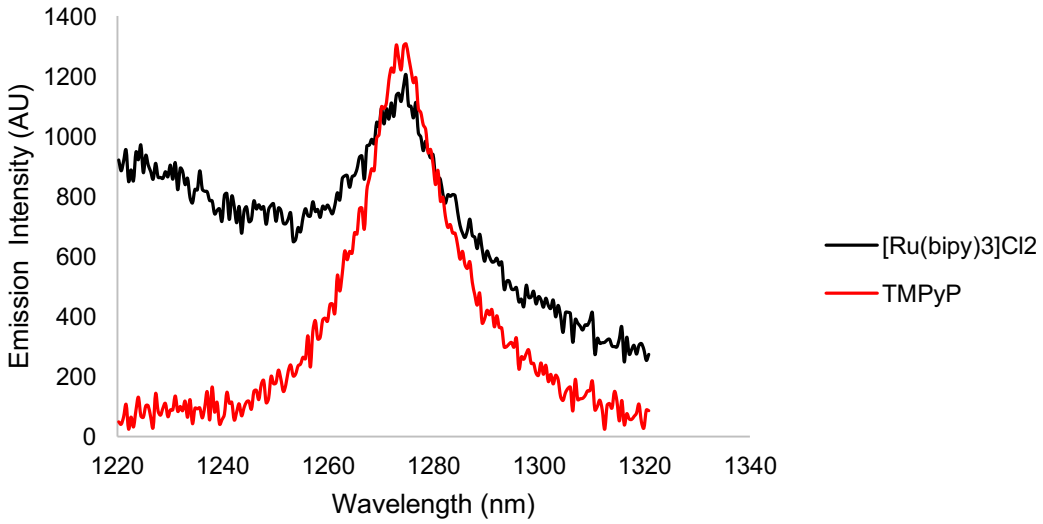

Figure 3.4 - NIR emission of $^1O_2$ generated by TMPyP in air equilibrated PBS (D_2O); excitation at 405 nm (4 mW). The reversibility was monitored by integration of the area of the emission band at ca.1270 nm over four cycles.

3.1.1.5 Evaluation of TMPyP mutagenicity – Ames test

Since the aim of this project is to evaluate the applicability of porphyrin in a polishing step to deliver safe drinking water, the risk of consumption of porphyrin must be considered as well as its effects. For this reason, the mutagenic potential of TMPyP at different concentrations was evaluated using the Ames test (AMES-MOD ISO™).

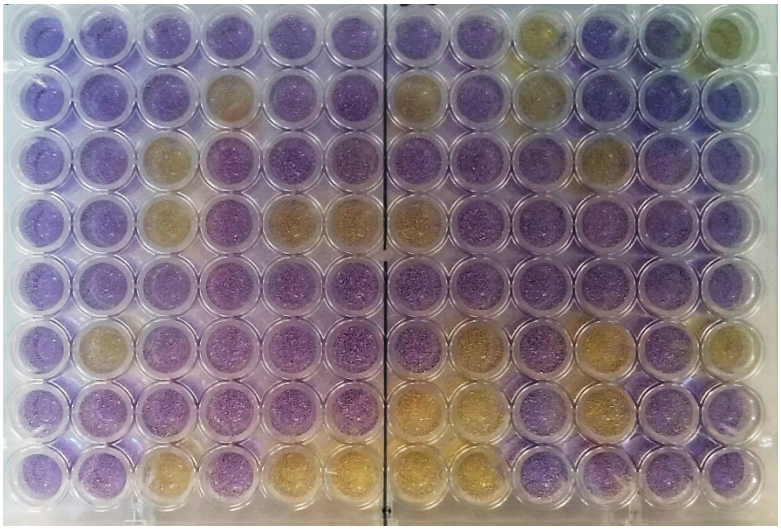

Figure 3.5– 96-well plate showing the revertant (yellow) and non-revertant (purple) wells observed in AMES-MOD ISO™ test.

A compound is considered mutagenic if the average score for positive results (yellow wells) (Figure 3.5) is greater than 25 revertant wells per 48-well. The expected value for the negative control is ≤15 revertant wells which was observed in this case. The expected value for a known mutagen, such as the positive control sodium azide (NaN_3), is ≥25 revertant wells. As can be seen in Table 3.1, the average number of positive wells for the test performed with AMES-MOD ISO™ was ≤20, indicating that none of the concentrations here investigated can cause mutagenicity.

Table 3.1 – Average number of revertant wells per sample analysed.

Sample	**Average number of revertant wells**
TMPyP at 2.5μM	11 ± 3.5
TMPyP at 5μM	14 ± 5
TMPyP at 10μM	20 ± 2
Sodium Azide (positive control)	32 ± 2.8
DI water (negative control)	10 ± 0.5

3.1.2 Medium

The medium used was PBS. In all experiments, the level of dissolved oxygen in the medium was > 90% ensuring an adequate supply of oxygen for the PDI reaction. The pH of the medium was 7 and was not altered following the addition of a range of concentrations of the porphyrin investigated (3.65μM, 5μM and 10 μM).

3.1.3 The experimental vessel

Experiments in 96-well-plates

Experiments were first performed in 96-well plates. In order to optimise the concentration of porphyrin and the time of exposure, the response of *E. coli* T37-1 and *P. putida* DSM 6125 to a range of concentrations of TMPyP (0.625 μM – 20 μM) over a three-hour time period, was investigated. The streak plate method was used as an initial rapid screening approach and the presence or absence of growth was recorded for both the monochromatic lamp (Table 3.2) and the multichromatic lamp (Table 3.3).

Table 3.2 – The response of *E. coli* T37-1 and *P. putida* DSM 6125 to TMPyP (0, 0.625, 1.25, 2.5, 5, 10 and 20 μM) under the irradiation of the monochromatic lamp (λ=525nm).

TMPyP	**Light control**		**0.625 μM**		**1.25 μM**		**2.5 μM**		**5 μM**		**10 μM**		**20 μM**	
Time	1	2	1	2	1	2	1	2	1	2	1	2	1	2
0 minutes	+	+	+	+	+	+	+	+	+	+	+	+	+	+
30 minutes	+	+	+	+	+	+	+	+	+	+	-	+	-	+
60 minutes	+	+	+	+	+	+	+	+	-	+	-	+	-	+
90 minutes	+	+	+	+	+	+	+	+	-	+	-	-	-	-
120 minutes	+	+	+	+	+	+	+	+	-	-	-	-	-	-
150 minutes	+	+	+	+	+	+	+	+	-	-	-	-	-	-
180 minutes	+	+	+	+	+	+	+	+	-	-	-	-	-	-
Dark Control	+	+	+	+	+	+	+	+	+	+	+	+	+	+

(+) = presence of growth; (-) = absence of growth / 1= *E. coli* T37-1, and 2 = *P. putida* DSM 6125.

Table 3.3 – The response of *E. coli* T37-1 and *P. putida* DSM 6125 to TMPyP (0, 0.625, 1.25, 2.5, 5, 10 and 20 μM) under the irradiation of the multichromatic lamp (λ≥400nm).

TMPyP	**Light control**		**0.625 μM**		**1.25 μM**		**2.5 μM**		**5 μM**		**10 μM**		**20 μM**	
Time	1	2	1	2	1	2	1	2	1	2	1	2	1	2
0 minutes	+	+	+	+	+	+	+	+	+	+	+	+	+	+
30 minutes	+	+	+	+	+	+	+	+	+	+	+	+	+	+
60 minutes	+	+	+	+	+	+	+	+	+	+	+	-	-	-
90 minutes	+	+	+	+	+	+	+	+	-	+	-	-	-	-
120 minutes	+	+	+	+	+	+	+	+	-	-	-	-	-	-
150 minutes	+	+	+	+	+	+	+	+	-	-	-	-	-	-
180 minutes	+	+	+	+	+	+	+	+	-	-	-	-	-	-
Dark Control	+	+	+	+	+	+	+	+	+	+	+	+	+	+

(+) = presence of growth; (-) = absence of growth / 1= *E. coli* T37-1, and 2 = *P. putida* DSM 6125.

The two bacteria investigated responded similarly to the two lamps when the porphyrin was used at the lower concentrations, 0.625μM, 1.25μM and 2.5μM, which were not effective in deactivating any of the bacteria under the conditions evaluated and were not considered for further investigations. TMPyP concentrations ranging from 5 μM - 20 μM were effective in killing the bacteria, with the monochromatic lamp showing to be more effective than the multichromatic one, depending on the time of exposure.

In the case of 5 μM TMPyP, *E. coli* was inactivated after 60 minutes of exposure to the monochromatic lamp and 90 minutes with the multichromatic one. Interestingly, *P. putida* required 2 hours of exposure to be inactivated by the two lamps. At the concentration of 10 μM, *E. coli* reduced the time of response to 30 minutes, for both lamps, while *P. putida* had also a 30 minutes reduction for the monochromatic lamp and the multichromatic one.

At the highest concentration tested, 20 μM, a 30 minutes irradiation period with the monochromatic lamp was required to inactivate *E. coli* and 90 minutes for *P. putida*. When using the multichromatic lamp, a similar time period (dose), 60 minutes, was necessary to deactivate both bacteria. Bacterial numbers were not affected by the treatment with the light only (light control) or by the porphyrin only (dark control).

The drop plate technique was used to quantify the response of bacteria to the treatment in 96 well plates. As in the previous experiments *E. coli* T37-1 and *P. putida* DSM 6125 had distinct responses to the treatment. Two further strains from each genus, *E. coli* DSM 498 and *P. putida* CP1 were also investigated.

The responses *of E. coli* DSM 498, *E. coli* T37-1, *P. putida* DSM 6125 and *P. putida* CP1 in the presence of the porphyrin TMPyP (10μM and 20 μM) and following exposure to the multi-LED monochromatic lamp is described in Figs. 3.6 and 3.7. In all cases the initial cell number was 10^5 CFU/ml and the experiments were carried out in 96-well plates as described in Section 2.2.4.1. Samples were taken after every 10 minutes for 60 minutes and surviving cell numbers were determined using the drop plate method. There was no change in the number of cells for either the dark or the light controls. In addition, lower concentrations tested in this system did not inhibit the bacterial growth.

When the numbers of bacteria were monitored with time, the bacteria showed a two-stage pattern in response to the treatment – an initial rapid decrease of approximately 3-log in the numbers of cells followed by a slower rate of cell death. As had been noted previously, the *E. coli* strains were more sensitive to the treatment than the *Pseudomonads*. The response of *E. coli* T37-1 was similar for both 10μM and 20μM TMPyP. The initial rapid response phase for *E. coli* DSM 498 was also similar for both

concentrations of TMPyP, however the remaining cells were killed more rapidly with the higher concentration of TMPyP. The *Pseudomonas* species showed a lag in response to the treatments. The lag time was greatest, up to 40 minutes, for *P. putida* CP1 when 10μM TMPyP was used. The lag for *P. putida* DSM 6125 was shorter, at 20 minutes, for the same concentration of TMPyP. The lag was reduced to 10 minutes for both *Pseudomonas* strains when 20μM TMPyP was used.

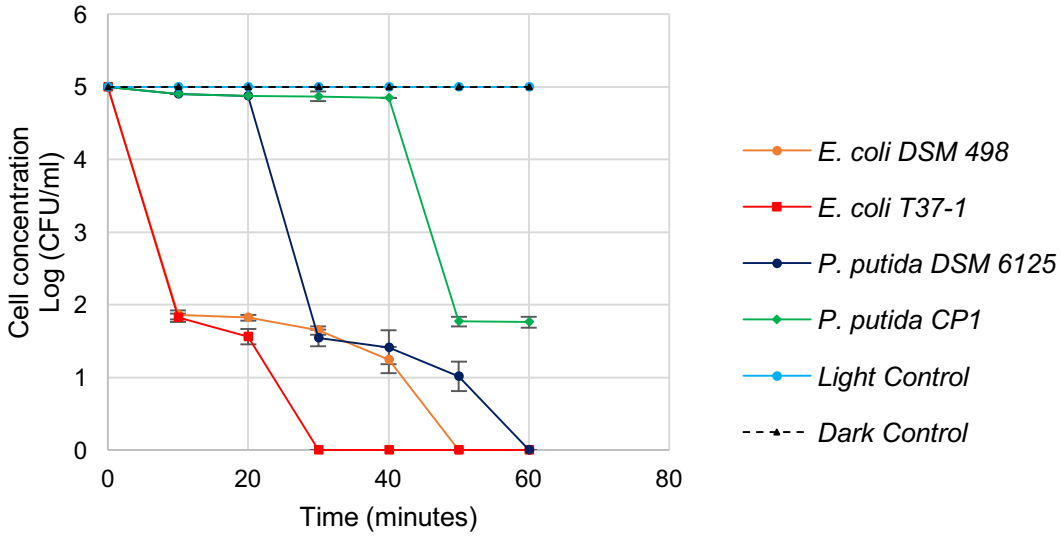

Figure 3.6. Logarithmic reduction in the number of bacteria treated with porphyrin TMPyP (10μM solution) following 60 minutes of exposure to the monochromatic lamp (λ=525nm).

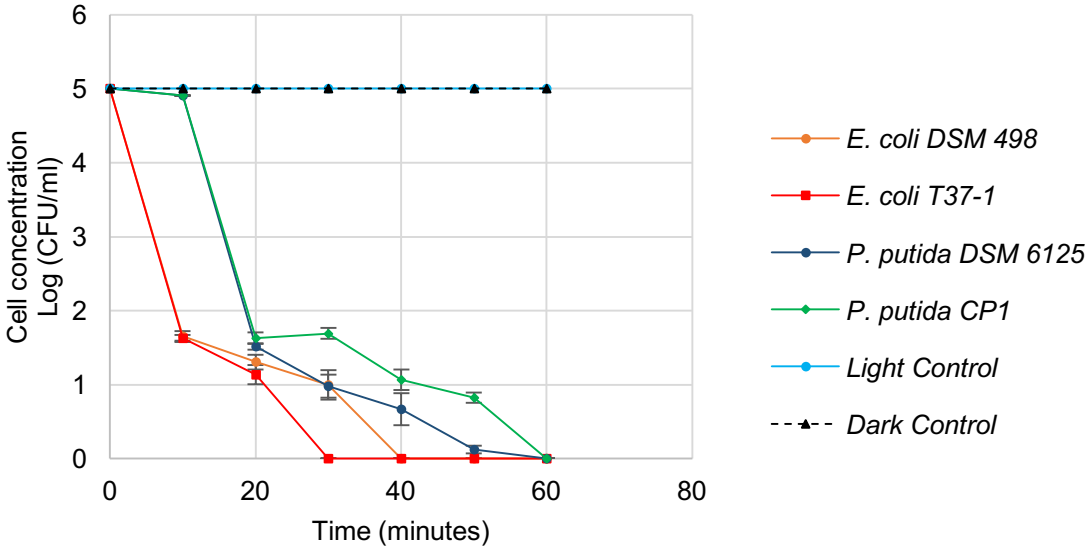

Figure 3.7. Logarithmic reduction in the number of bacteria treated with porphyrin TMPyP (20μM solution) following 60 minutes of exposure to the monochromatic lamp (λ=525nm).

The times and dosage necessary for a 3-log reduction in the number of cells and for total deactivation (5-log reduction) for all four organisms are summarised in Table 3.4. The greater resistance of the *Pseudomonas* species is reflected in the higher dosage required for inactivation.

Table 3.4. Length of time/dosage necessary for a 3-log reduction and total deactivation of bacteria under exposure to the monochromatic multi-LED lamp (λ=525nm).

Bacteria	**3-log reduction**		**5-log reduction (Total deactivation)**	
	10μM	**20 μM**	**10 μM**	**20 μM**
***E. coli* T37-1**	10 minutes/ 0.606 J/cm^2	10 minutes/ 0.606 J/cm^2	30 minutes/ 1.818 J/cm^2	30 minutes/ 1.818 J/cm^2
***E. coli* DSM 498**	10 minutes/ 0.606 J/cm^2	10 minutes/ 0.606 J/cm^2	50 minutes / 3.03 J/cm^2	40 minutes / 2.424 J/cm^2
***P. putida* CP1**	50 minutes / 3.03 J/cm^2	20 minutes / 1.212 J/cm^2	no data	60 minutes / 3.636 J/cm^2
***P. putida* DSM 6125**	30 minutes/ 1.818 J/cm^2	20 minutes / 1.212 J/cm^2	60 minutes / 3.636 J/cm^2	60 minutes / 3.636 J/cm^2

3.2 Investigating the response of Gram-negative and Gram-positive bacteria to PDI

Having investigated at the response of Gram-negative bacteria towards PDI, it was of interest to also look at the response of Gram-positive bacteria. Eight different bacteria were investigated – Gram-negative *E. coli* T37-1, *E. coli* DSM 498, *E. coli* DSM 1103, *P. putida* CP1, *P. putida* DSM 6125, *P. fluorescens* DSM 50090 and Gram-positive *B. subtilis DSM* 10, *S. aureus* DSM 799. In all cases the initial inoculum size was 10^5 CFU/ml and the TMPyP concentration used was 3.65μM. In order to increase the working volume, it was decided to use glass Petri dishes (60x15 mm). The larger volume also enabled the response of the organism to be monitored using the plate count technique. Initially, the lamps used were the monochromatic (λ=525nm) and multichromatic (λ≥400nm) ones. As they have a small size, only one Petri dish could fit under the light source (see Figure 2.5), which made the experiment laborious. For that reason, later on the experiments were performed with the dichromatic lamp (λ= 430 and 660nm), a bigger and more powerful lamp which facilitated the experiment performance (see Figure 2.6).

Monochromatic lamp (λ=525nm)

The results obtained for the 8 different microorganisms treated under the monochromatic lamp, are described in Fig. 3.8. All the organisms were exposed to 3 hours of light irradiation, corresponding to a dosage of 10.9 J/cm^2. Each bar represents the log of the cell concentration of each microorganism for the 3 different treatments. For all the experiments, dark controls, where the same conditions of the experiment were kept but with no light exposure, and light controls, were the plate with microorganisms was exposed to the light but without addition of sensitizer, were performed, with no microbial inactivation.

The *E. coli* strains and *S. aureus DSM799* were the microorganisms most sensitive to the treatment. *E. coli* T37-1 and *E. coli* DSM 1103 presented almost total deactivation, 5-log reduction after the 3 hours and *S. aureus* DSM 799 was completely inactivated. As already shown in the experiments in 96-well plates, Pseudomonads were more resistant to the treatment, the two *Pseudomonas putida* strains suffered a reduction of 2-log and *P. fluorescens* was not affected by the treatment. The spore former *B. subtilis* did not show any reduction in the cell concentration when exposed to this light dosage.

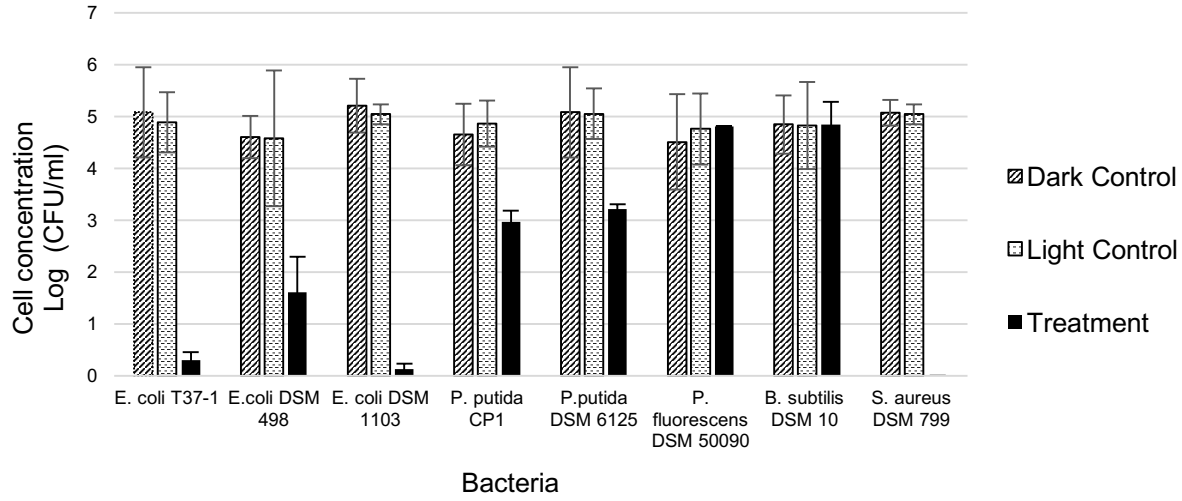

Figure 3.8– Cell concentration, in logarithmic scale, of 8 bacteria after 180 minutes of exposure to the monochromatic lamp (λ=525nm).

Multichromatic lamp (λ>400nm)

The same experiments performed with the monochromatic lamp were repeated using the multichromatic lamp. Figure 3.9 shows the results for the 8 microorganisms treated with the porphyrin TMPyP at a concentration of 3.65μM. All the organisms were exposed to 3 hours of light irradiation, corresponding to a dosage of 10.47 J/cm^2, very similar to the one provided by the multichromatic lamp. Dark and light controls were also performed, with no change in the number of cells before and after the treatment.

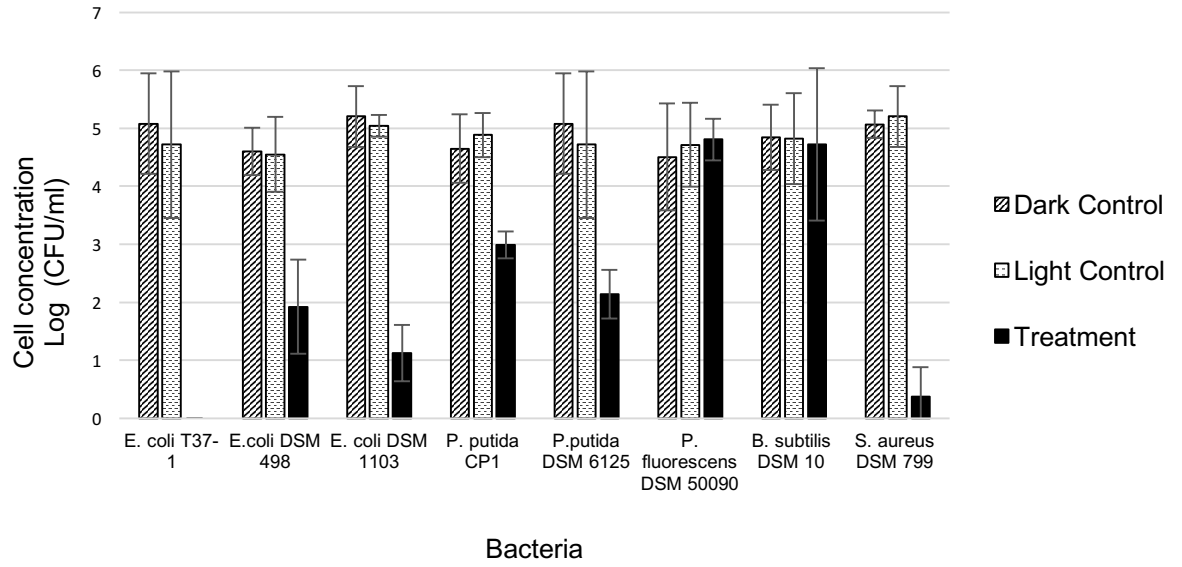

Figure 3.9 – Cell concentration, in logarithmic scale, of 8 bacteria after 180 minutes of exposure to the multichromatic lamp (λ≥400nm).

The treatment with the multichromatic lamp showed a similar response to the one with the monochromatic lamp. The *E. coli* strains and *S. aureus* were most vulnerable to the treatment. *S. aureus and E. coli* T37-1 were totally deactivated, followed by a 4-log reduction of *E. coli* DSM 1103. *E. coli* DSM 498 had a decrease of approximately 3.5-log in the number of cells. *P. putida* CP1 and *P. putida* DSM 6125 presented a 2 and 3-log reduction, respectively. Again, *P. fluorescens* and *B. subtilis* DSM 10 did not respond to the conditions employed in this experiment.

Dichromatic lamp (λ= 430 and 660nm)

The monochromatic and multichromatic lamps were small and limited the scale of the experiments. It was then decided to use a larger lamp system – a Dichromatic lamp (λ= 430 and 660nm). Using this lamp (see Figure 2.6) allowed up to 12 Petri dishes to be used in the experiments, thus facilitating multiple treatments and replication. The wavelengths of the lamp were chosen to suit the porphyrin being investigated. The lamp was more powerful than the earlier lamps. The light dose provided by the dichromatic lamp, after 60 minutes of irradiation, was 78.94 J/cm^2, almost seven times higher than that provided by the smaller lamps.

In total twelve bacteria were investigated. They included the eight bacteria investigated with the smaller lamps – Gram-negative *E. coli* T37-1, *E. coli* DSM 498, *E. coli* DSM 1103, *P. putida* CP1, *P. putida* DSM 6125, P. fluorescens DSM 50090 and Gram-positive *B. subtilis* DSM 10, *S. aureus* DSM 799 and four additional pathogenic strains - *S. sonnei* DSM 5570, *S. enterica* DSM 17058, *E. aerogenes* DSM 30053 and *P. aeruginosa* PAO1. In all cases the initial inoculum size was 10^5 CFU/ml and the TMPyP concentrations used were 3.65μM, 5 μM and 10 μM. The response of the bacteria over time was monitored using the plate count technique. Dose response curves were plotted and the results were expressed in terms of log reduction, light dose and the rate of cell inactivation /minute. The findings are grouped for the Gram-negative bacteria and the Gram-positive bacteria as follows.

3.2.1 Gram-negative bacteria

The results for the Gram-negative bacteria studied are initially presented for members of the family *Enterobacteriaceae* and then members of the family *Pseudomonaceae.*

Members of the family Enterobacteriaceae

The responses of *E. coli* T37-1, *E. coli* DSM 498, *E. coli* DSM 1103, *S. sonnei* DSM 5570, *S. enterica* DSM 17058, *E. aerogenes* DSM 30053, all members of the Family *Enterobacteriaceae,* following exposure to TMPyP at the concentrations of 3.65μM, 5 μM and 10 μM are described in Fig. 3.10. The rate of inactivation of the organisms and the dose required for total deactivation or a 5-log reduction in the number of cells is described in Table 3.5.

When the porphyrin concentration was 3.65μM (Fig. 3.10a), *E. coli* T37-1, *E. coli* DSM 498 and *E. coli* DSM 1103 showed a total deactivation after being exposed to a light dose of 39.47 J/cm^2. *S. enterica* DSM 17058 and *S. sonnei* DSM 5570 *required* a dose of 59.21 J/cm^2 for a 5-log reduction. *E. aerogenes* showed to be the most resistant bacteria among the family, requiring 75 minutes (98.68 J/cm^2) of light irradiation for total death of the cells. As can be observed, a slight increase in the concentration of TMPyP, from 3.65 μM to 5 μM (Fig. 3.10b), influenced the PDI efficiency for some of the bacterial strains. *E. coli* DSM 1103, *S. sonnei DSM 5570, E. aerogenes DSM 30053* required 15 minutes less of exposure to the lamp to be completely inactivated. When the concentration of porphyrin was increased to 10μM (Fig. 3.10c) the time/dose necessary for eliminating the bacteria present in the glass Petri dishes, did not suffer a major reduction when compared to the previous concentrations used. Only *E. aerogenes* DSM 30053 had the dose necessary for its inactivation from 78.94 J/cm^2 to 59.21 J/cm^2.

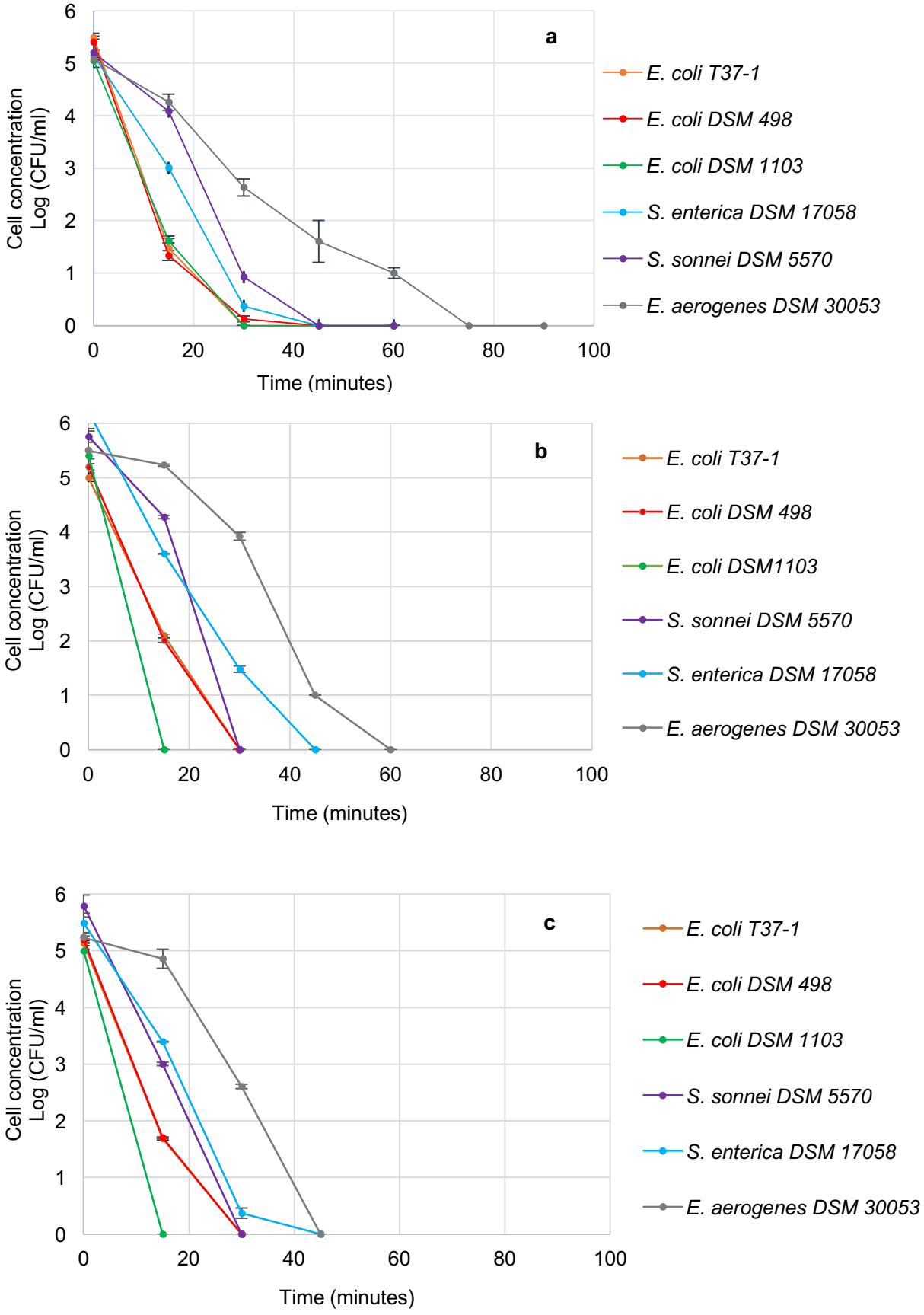

Figure 3.10 – Logarithmic reduction in the number of 5 *Enterobacteriaceae* bacteria following exposure to the Dichromatic lamp with TMPyP at 3.65 (a) 5 (b) and 10μM (c)

Table 3.5. Length of time/dosage necessary for a 5-log reduction and total deactivation of bacteria from *Enterobacteriaceae* family, under exposure to the Dichromatic lamp (430 and 660 nm) with TMPyP at 3.65μM.

Bacteria	**5-log reduction (Total deactivation)**					
	3.65 μM		**5 μM**		**10 μM**	
	Time/dose	**Rate**	**Time/dose**	**Rate**	**Time/dose**	**Rate**
***E. coli* T37-1**	30 minutes/ 39.47 J/cm^2	0.1218 min^{-1}	30 minutes/ 39.47 J/cm^2	0.1668 min^{-1}	30 minutes/ 39.47 J/cm^2	0.1711 min^{-1}
***E. coli* DSM 498**	30 minutes / 39.47 J/cm^2	0.120158 min^{-1}	30 minutes / 39.47 J/cm^2	0.1731 min^{-1}	30 minutes / 39.47 J/cm^2	0.1731 min^{-1}
***E. coli* DSM 1103**	30 minutes / 39.47 J/cm^2	0.168264 min^{-1}	15 minutes / 19.73 J/cm^2	0.3332 min^{-1}	15 minutes / 19.73 J/cm^2	0.3345 min^{-1}
***S. enterica* DSM 17058**	45 minutes / 59.21 J/cm^2	0.114196 min^{-1}	45 minutes / 59.21 J/cm^2	0.1380 min^{-1}	45 minutes / 59.21 J/cm^2	0.122 min^{-1}
S. sonnei DSM 5570	45 minutes / 59.21 J/cm^2	0.115444 min^{-1}	30 minutes/ 39.47 J/cm^2	0.1918 min^{-1}	30 minutes / 39.47 J/cm^2	0.1931 min^{-1}
E. aerogenes DSM 30053	75 minutes / 98.68 J/cm^2	0.067738 min^{-1}	60 minutes / 78.94 J/cm^2	0.0916 min^{-1}	45 minutes / 59.21 J/cm^2	0.1163 min^{-1}

Members of the family Pseudomonaceae

The response of four *Pseudomonas*, *P. putida* CP1, *P. putida* DSM 6125, *P. fluorescens* DSM 50090, *and P. aeruginosa* PAO1 to various concentrations of TMPyP (3.65μM, 5 μM and 10 μM) are described in Fig. 3.11.

When treated with TMPyP at 3.65μM (Fig. 3.11a), the response of *P. putida* CP1 and *P. putida* DSM 6125 was similar and quickest. *P. aeruginosa* PA01 had a similar initial response to *P. putida* CP1 and *P. putida* DSM 6125 but took longer for total inactivation. The response of *P. fluorescens* DSM 50090 was the slowest. The organism showed an initial lag of 15 minutes before inactivation and took 90 minutes for total inactivation. The rate of deactivation and the dose required are summarised in Table 3.6. A different length of exposure time was required by each of the bacteria, in order to achieve a total deactivation. *P. putida* CP1 and *P. putida* DSM 6125 responded very similarly to the treatment, being totally inactivated after 60 minutes (78.94 J/cm^2). PAO1 required 75 minutes (98.68 J/cm^2) and *P. fluorescens* DSM 50090 required 90 minutes (118.42 J/cm^2) for total death.

Under a concentration of 5 μM (Fig. 3.11b), *P. putida* CP1 and *P. putida* DSM 6125 had the time/dose necessary for a 5-log reduction in the number of cells reduced by half, while *P. fluorescens* DSM50090 required 15 minutes less of light exposure to achieve total inactivation of its cells. For the bacterium *P. aeruginosa* PAO1 a reduction of 30 minutes in the time of exposure to the phototreatement was achieved. When the concentration of porphyrin was increased to 10μM (Fig. 3.11c), only *P. fluorescens* DSM 50090 responded different to the treatment, having the time for inactivation reduced by 30 minutes when compared to the slowest concentration.

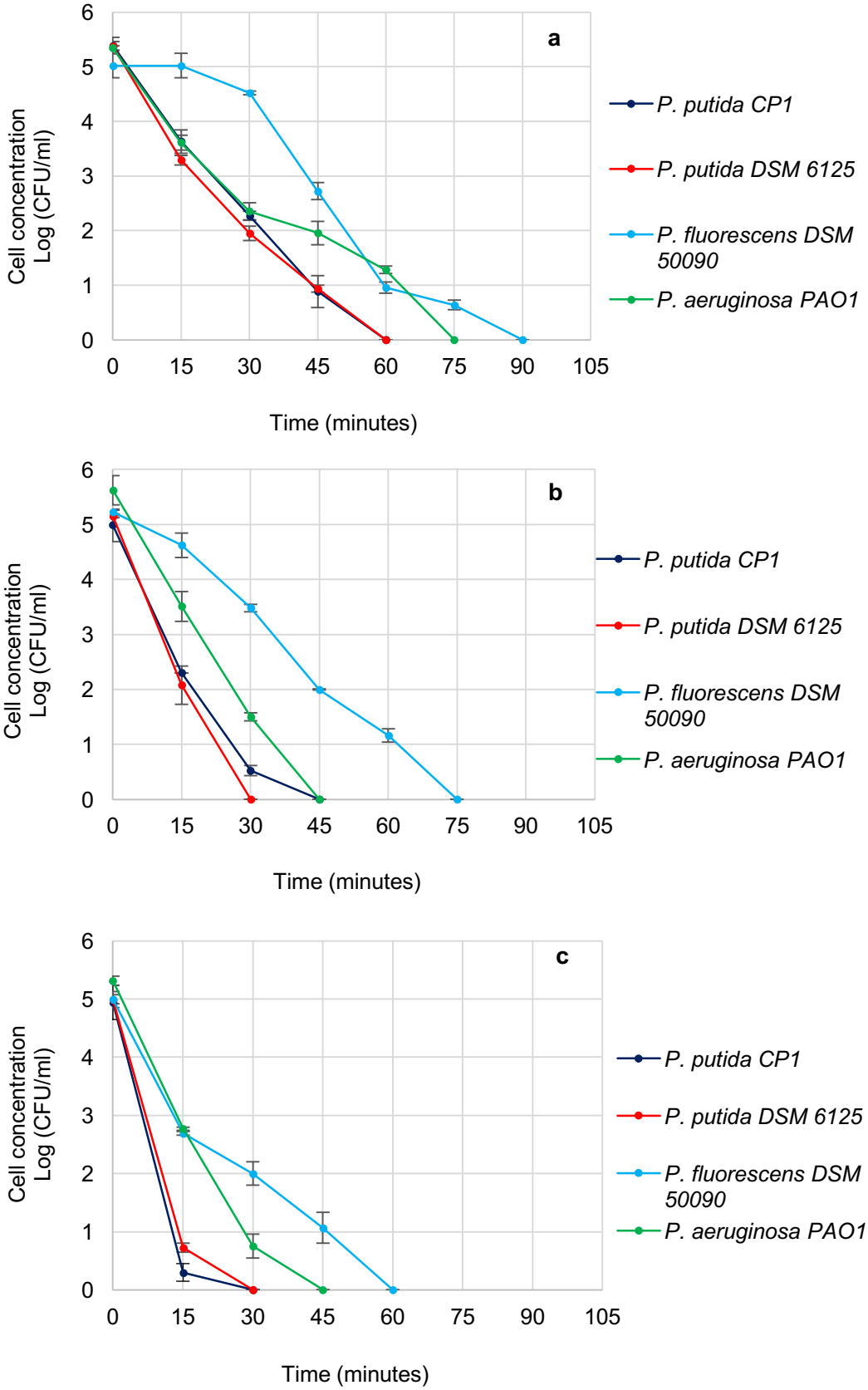

Figure 3.11 – Logarithmic reduction in the cell concentration of *Pseudomonas* spp. bacteria after exposure to the Dichromatic lamp with TMPyP at 3.65μM (a), 5μM (b) and 10μM (c).

Table 3.6. Length of time/dosage necessary for a 5-log reduction and total deactivation of *Pseudomonads,* under exposure to the Dichromatic lamp (430 and 660 nm) with TMPyP at 3.65μM.

Bacteria	**5-log reduction (Total deactivation)**					
	3.65 μM		**5 μM**		**10 μM**	
	Time/dose	Rate	Time/dose	Rate	Time/dose	Rate
***P. putida* CP1**	60 minutes/ 78.94 J/cm^2	0.08979 min^{-1}	30 minutes/ 39.47 J/cm^2	0.1107 min^{-1}	30 minutes/ 39.47 J/cm^2	0.1647 min^{-1}
***P. putida* DSM 6125**	60 minutes / 78.94 J/cm^2	0.089579 min^{-1}	30 minutes / 39.47 J/cm^2	0.1714 min^{-1}	30 minutes/ 39.47 J/cm^2	0.1663 min^{-1}
***P. fluorescens* DSM 50090**	90 minutes / 118.42 J/cm^2	0.055776 min^{-1}	75 minutes / 98.68 J/cm^2	0.069648 min^{-1}	60 minutes / 78.94 J/cm^2	0.1081 min^{-1}
***P. aeruginosa* PAO1**	75 minutes / 98.68 J/cm^2	0.071241 min^{-1}	45 minutes / 59.21 J/cm^2	0.124961 min^{-1}	45 minutes / 59.21 J/cm^2	0.1180 min^{-1}

3.2.2 Gram-positive Bacteria

The response of two Gram-positive bacteria was investigated – the spore forming bacterium *B. subtilis* DSM 10 and the pathogenic organism *S. aureus* DSM 799. The deactivation curve for both bacteria is described in Fig. 3.12. Unlike when the monochromatic and multichromatic lamps were used and no deactivation was observed, *B. subtilis* was deactivated using the dichromatic lamp. For the concentration of 3.65μM (Fig. 3.12a) a total deactivation and a 5-log reduction in the number of cells was achieved at 90 minutes and a light dose of 118.42 J/cm^2. The pathogenic organism *S. aureus DSM 799* was readily deactivated with a 5-log reduction in the number of cells in 45 minutes and a light dose of 59.21 J/cm^2, as can be seen. The increase in the concentration of TMPyP, from 3.65 μM to 5 μM (Fig. 3.12b), influenced the PDI efficiency only for *S. aureus* DSM 799, which took 30 minutes less to be inactivated. When the concentration of porphyrin was increased to 10μM (Fig. 3.12c), the time/dose necessary for eliminating the bacteria *B. subtilis* DSM 10 was reduced from 90 to 60 minutes.

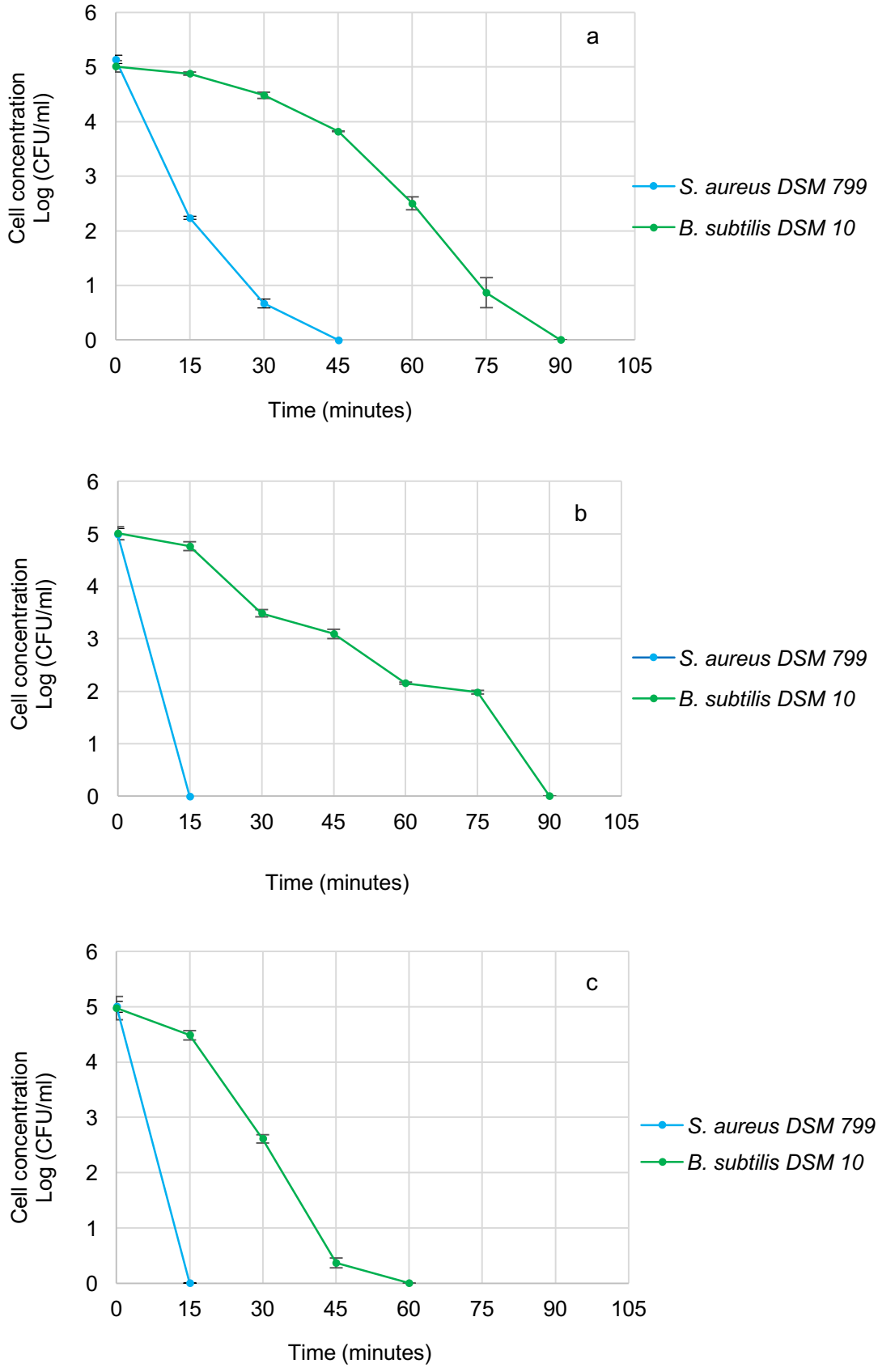

Figure 3.12 – Logarithmic reduction in the cell concentration of *B. subtilis* DSM 10 and *S. aureus* DSM 799 bacteria after exposure to the dichromatic lamp with TMPyP at 3.65μM (a), 5μM (b) and 10μM (c).

Table 3.7. Length of time/dosage necessary for a 5-log reduction and total deactivation of Gram-positive bacteria, under exposure to the Dichromatic lamp (430 and 660 nm) with TMPyP at 3.65μM.

Bacteria	**5-log reduction (Total deactivation)**					
	3.65 μM		**5 μM**		**10 μM**	
	Time/dose	Rate	Time/dose	Rate	Time/dose	Rate
***S. aureus* DSM 799**	45 minutes / 59.21 J/cm^2	0.1141 min^{-1}	15 minutes / 19.73 J/cm^2	0.3329 min^{-1}	15 minutes / 19.73 J/cm^2	0.3321 min^{-1}
***B. subtilis* DSM 10**	90 minutes / 118.42 J/cm^2	0.0556 min^{-1}	90 minutes / 118.42 J/cm^2	0.0556 min^{-1}	60 minutes / 78.94 J/cm^2	0.0829 min^{-1}

3.2.3 Antibiotic profile of the bacteria

The antibiotic profile of the bacteria was determined against seven commonly used antibiotics using the Kirby-Bauer disc diffusion method. The antibiotics investigated were imipenem (10µg), ampicillin (10µg), ciprofloxacin (10µg), cefotaxime (30µg), tetracycline (30µg), erytromycin (30µg) and vancomycin (30µg). The minimum inhibition concentration of two of the antibiotics, tetracycline and ampicillin, was also determined.

3.2.3.1 Kirby-Bauer disc diffusion method

The bacteria were grown in the presence of imipenem (10µg), ampicillin (10µg), ciprofloxacin (10µg), cefotaxime (30µg), tetracycline (30µg), erytromycin (30µg) and vancomycin (30µg). Inhibition of growth was observed as a zone of inhibition surrounding the antibiotic disc. The results are described in Table 3.8. All the bacteria studied showed susceptibility to the antibiotics imipinem, ciprofloxacin, and tetracycline and all but two of the *E. coli* strains showed resistance to vancomycin. In the case of the other three antibiotics, ampicillin, erythromycin and cefotaxime, any resistance was confined to strains of *Pseudomonas* and in the case of ampicillin, *E. aerogenes DSM 30053* also showed resistance.

Table 3.8 – Zone of inhibition (mm) for the antibiotics disc of: imipenem (10µg); ampicillin (10µg); ciprofloxacin (10µg); cefotaxime (30µg); tetracycline (30µg); erytromycin (30µg); and vancomycin (30µg) against 12 different bacterial strains.

Microorganism	**imipenem**	**ampicillin**	**ciprofloxacin**	**cefotaxime**	**tetracycline**	**Erythromycin**	**vancomycin**
E. coli DSM 1103	45.67 ± 0.58	38 ± 0	34 ± 2	24 ± 1	29.34 ± 3	29.34 ± 0.58	17.34 ± 0.58
E. coli DSM 498	27.67 ± 0.58	19.67 ± 1.52	43.34 ± 3	34.67 ± 1.15	28.34 ± 1.52	18.34 ± 1.15	0
E. coli T 37-1	34.34 ± 0.58	19.67 ± 0.58	40 ± 2	32 ± 2	26.67 ± 2	21.34 ± 1.52	9.67 ± 0.58
P. putida CP1	33.34 ± 1.52	0	32.34 ± 0.58	16.67 ± 1.15	16.34 ± 0.58	0	0
P. putida DSM 6125	32 ± 1	0	34 ± 0	19 ± 0	17.67 ± 0.58	0	0
P. fluorescens DSM 50090	23.67 ± 1.15	0	32 ± 2	0	22.67 ±1.15	0	0
P. aeruginosa PAO1	24 ± 1	0	37.67 ± 1.15	19 ± 1	13.34 ± 2	11.34 ± 0.58	0
S. sonnei DSM 5570	25.67 ± 0.57	19 ± 1	38.34 ± 1.15	28.67 ± 1.15	8.34 ± 0.58	12.34 ± 0.58	0
S. enterica DSM 17058	30 ± 1	23.34 ± 1.52	39 ± 1	27 ± 1	23.67 ± 1.15	14.67 ± 0.58	0
E. aerogenes DSM 30053	17 ± 0	0	37 ± 0	18.67 ± 1.52	21.67 ± 1.52	15 ± 0	0
S. aureus DSM 799	40.34 ± 1.15	34 ± 0.58	29.67 ± 0.58	20 ± 1	23 ± 1	15.67 ± 0.58	0
B. subtilis DSM 10	20.34 ± 0.58	30.34 ± 1.52	48 ± 0	10.67 ± 0.58	31.34 ±1.52	11 ± 0	0

3.2.3.2 Minimum Inhibitory Concentration

The MIC (Minimum Inhibitory concentration) method (plate set up shown in Figure 2.8) was used to evaluate the response of the bacterial strains to different concentrations of the antibiotics tetracycline and ampicillin. The results are described in Table 3.9.

The majority of the microorganisms were more susceptible to tetracycline than to ampicillin. In the case of the *Pseudomonad* species, *E. aerogenes DSM 30053* and *B. subtilis DSM 10* which showed greater resistance to PDI, a significantly higher MIC value for ampicillin was obtained than that for the other organisms.

Table 3.9 – Minimum Inhibitory Concentration of the antibiotics Tetracycline and Ampicillin against 12 different bacterial strains.

Microorganism	***MIC for tetracycline***	***MIC for ampicillin***
E. coli T 37-1	*0.78 µg/ml ± 0.007*	*3.12 µg/ml ± 0.002*
E. coli DSM 498	*0.78 µg/ml ± 0.005*	*3.9 µg/ml ± 0.02*
E. coli DSM 1103	*1.56 µg/ml ± 0.003*	*0.78 µg/ml ± 0.001*
S. aureus DSM 799	*1.56 µg/ml ± 0.003*	*0.78 µg/ml ± 0.001*
S. sonnei DSM 5570	*50 µg/ml ± 0.003*	*12.5 µg/ml ± 0.001*
S. enterica DSM 17058	*1.56 µg/ml ± 0.002*	*12.5 µg/ml ± 0.004*
P. putida CP1	*0.78 µg/ml ± 0.004*	*250 µg/ml ± 0.002*
P. putida DSM 6125	*0.78 µg/ml ± 0.004*	*125 µg/ml ± 0.001*
P. aeruginosa PAO1	*25 µg/ml ± 0.001*	*1250 µg/ml ± 0.003*
E. aerogenes DSM 30053	*3.12 µg/ml ± 0.004*	*250 µg/ml ± 0.001*
P. fluorescens DSM 50090	*3.12 µg/ml ± 0.002*	*2500 µg/ml ± 0.003*
B. subtilis DSM 10	*0.78 µg/ml ± 0.01*	*2500 µg/ml ± 0.001*

3.3 A study of factors influencing the response of *E. coli* and *Pseudomonas* species to PDI

Among the twelve bacterial strains investigated with PDI, the *Pseudomonad* group (*P. putida* CP1*, P. putida* DSM 6225, *P. fluorescens* and *P. aeruginosa* PAO1) showed resistance to PDI, while *E. coli* was more sensitive to the treatment. Interestingly, a different behaviour was also observed among the four *Pseudomonas* strains, with the *P. putida* strains inactivated in a shorter time (60 minutes) than *P. aeruginosa* (75 minutes), followed by *P. fluorescens* (90 minutes). For this reason, further studies investigating the *Pseudomonas* cells and their behaviour, compared or in conjunction with *E. coli*, were carried out. The response of the organisms when grown in co-culture and when the porphyrin was immobilised was also investigated.

3.3.1 Pigment production measurement

Pigment production is associated with *Pseudomonas* species and has been linked with resistance to environmental stress. As the bacterial pigmentation production changes depending on the medium composition, among other factors, the ability of *P. aeruginosa PAO1, P. fluorescens* DSM 50090*, P putida* CP1*,* and *P. putida* DSM 6125 to produce pigments was evaluated by growing them on media as described in section 2.2.5.

LB and M9 were chosen because they have been shown to induce phenazine and pyoverdine production in *Pseudomonas* strains (Mavrodi *et al.,* 2001, Orlandi et al 2015). King A induces the production of pyocinin, while King B induces the production of pyoverdine (fluorescein) (King *et al.,* 1954).

The UV-Visible spectra of the supernatant of the four different *Pseudomonas* strains, *P. aeruginosa PAO1, P. fluorescens* DSM 50090*, P. putida* CP1 and *P. putida* DSM 6125*,* grown in different media, are shown in Figures 3.13 to 3.17. A peak at 310 nm is ascribable to pyocyanin, a peak at 364 nm is ascribable to phenazine and a peak at 400 nm is ascribable to pyoverdine (Orlandi *et al.*, 2015). Figure 3.13 shows the spectra for the supernatant when the *Pseudomonas* where grown in LB. The peak at 364nm shows the production of phenazine by *P. aeruginosa* and the peak at 400 nm is characteristic of pyoverdine.

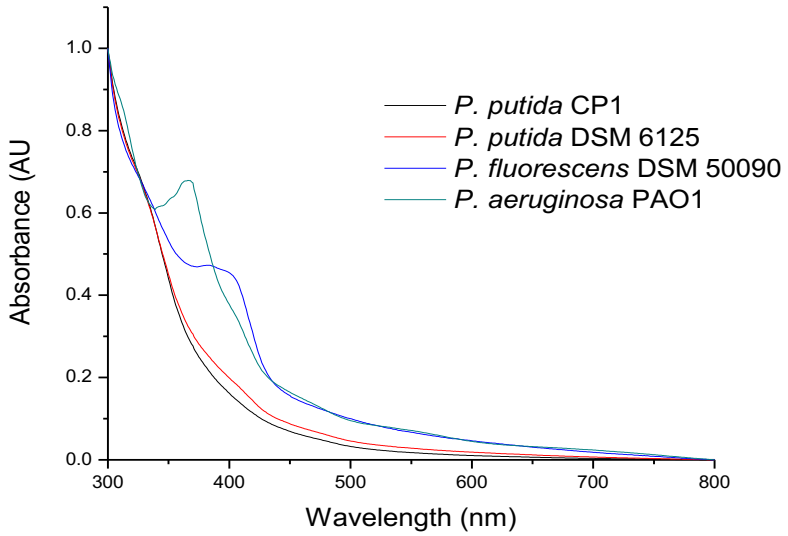

Figure 3.13 - UV–Visible spectra of the supernatant of the four different *Pseudomonas* strains grown in Luria-Bertani (LB) medium.

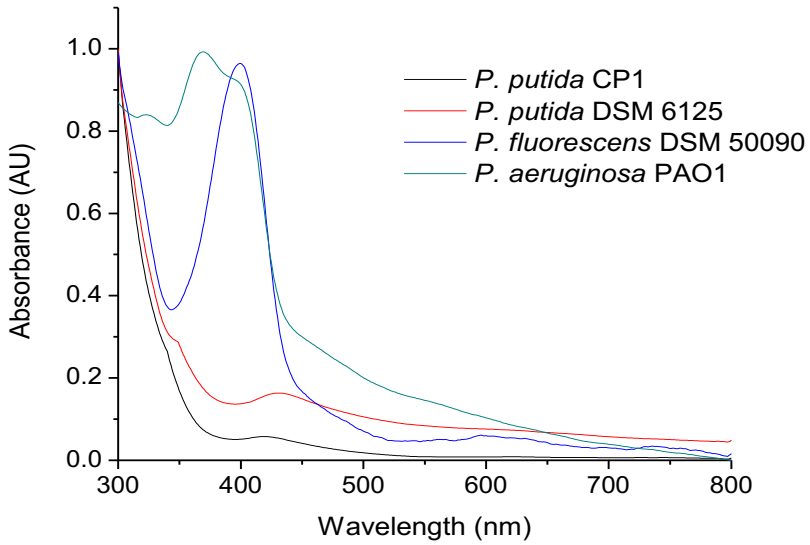

Figure 3.14 - UV–Visible spectra of the supernatant of the four different *Pseudomonas* strains grown in M9 medium.

When grown in M9, *P. fluorescens* (400nm) produces pyoverdine and *P. aeruginosa* produces two pigments, phenazine (364 nm) and pyoverdine (400nm) (Figure 3.14).

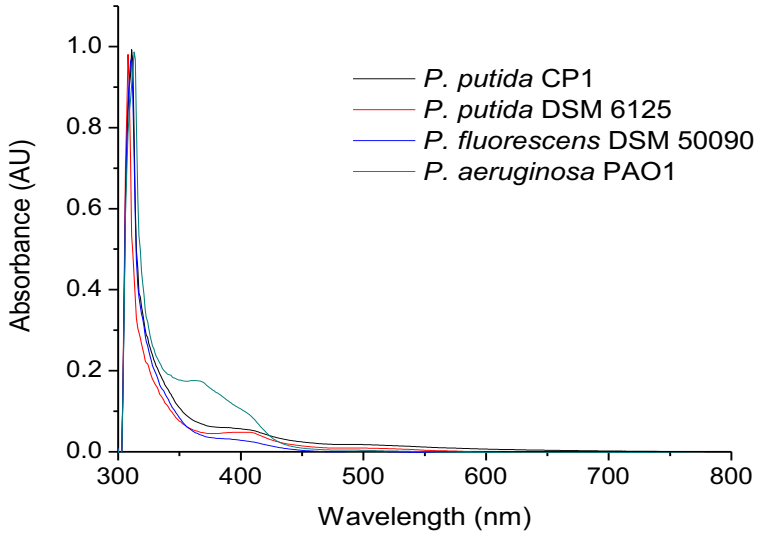

Figure 3.15 - UV–Visible spectra of the supernatant of the four different Pseudomonas strains grown in King A medium.

The four *Pseudomonas* supernatant absorption spectra (Figures 3.15 and 3.16), show characteristic peaks indicating pigment production in the media King A and King B, respectively. For King A, a peak at 310nm can be observed for the al the bacteria indicating the production of pyocyanin, and a small peak at 364nm indicates the production of phenazine by *P. aeruginosa.* For King B media, the peak at 400nm is ascribable to pyoverdine, also called fluorescein in the past (Montie, 1998) and all four strains released this pigment under these growth conditions.

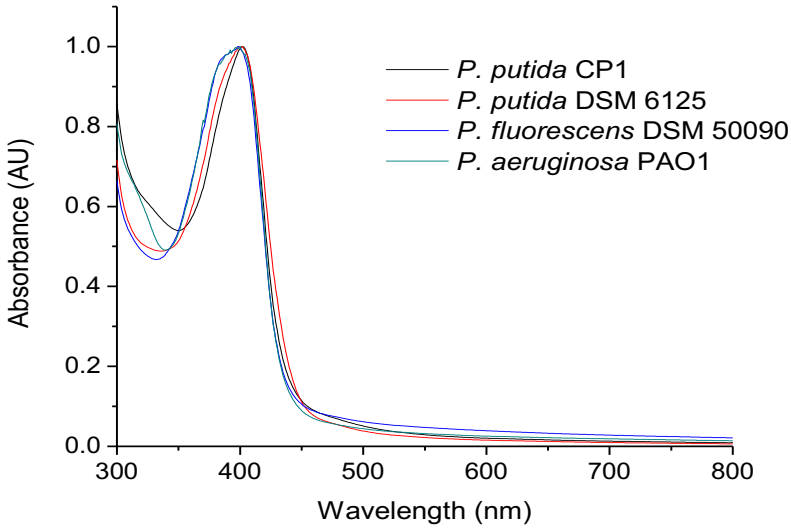

Figure 3.16 - UV–Visible spectra of the supernatant of the four different *Pseudomonas* strains grown in King B medium.

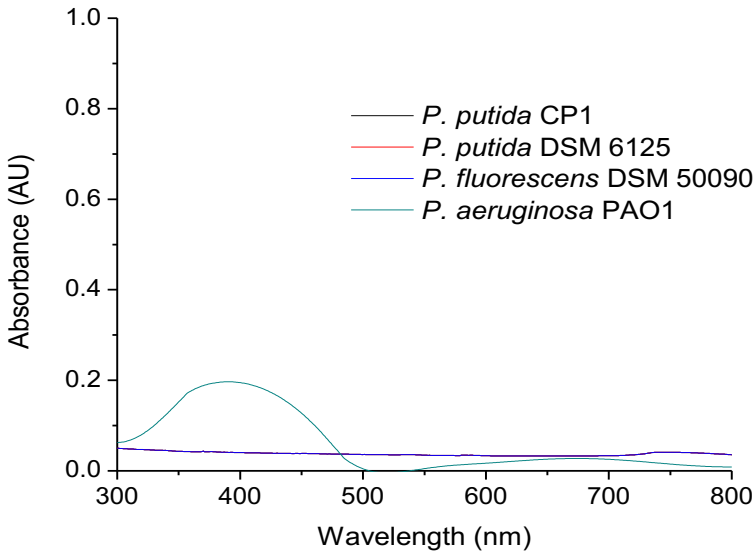

Figure 3.17 - UV–Visible spectra of the supernatant of the four different *Pseudomonas* strains grown in nutrient broth.

As can be seen in Figure 3.17, only *P. aeruginosa* PAO1 produces pigment when grown in nutrient broth, with a small peak indicating the production of pyoverdine (400nm). The production of other pigments is not evident in this medium.

3.3.2 Aggregation and settling of bacterial cells

A visual inspection of the two strains of *Pseudomonas*, *P. fluorescens* DSM50090 and *P. aeruginosa PAO1,* showed that they aggregated when grown in nutrient broth for use in the PDI investigations. Their response to PDI was shown to be significantly slower than the other bacteria, including the other strains of pseudomonas *P. putida* CP1 and *P. putida* DSM 6125. Aggregation of all four strains of Pseudomonas was measured as described in 2.2.6 and compared with a strain of *E. coli*.

Aggregation when measured as a percentage reduction in optical density due to settling, was greatest for *P. fluorescens* DSM50090 (40 %) followed by *P. aeruginosa* PAO1 (19.8 %) and significantly greater than the other organisms (Figure 3.18).

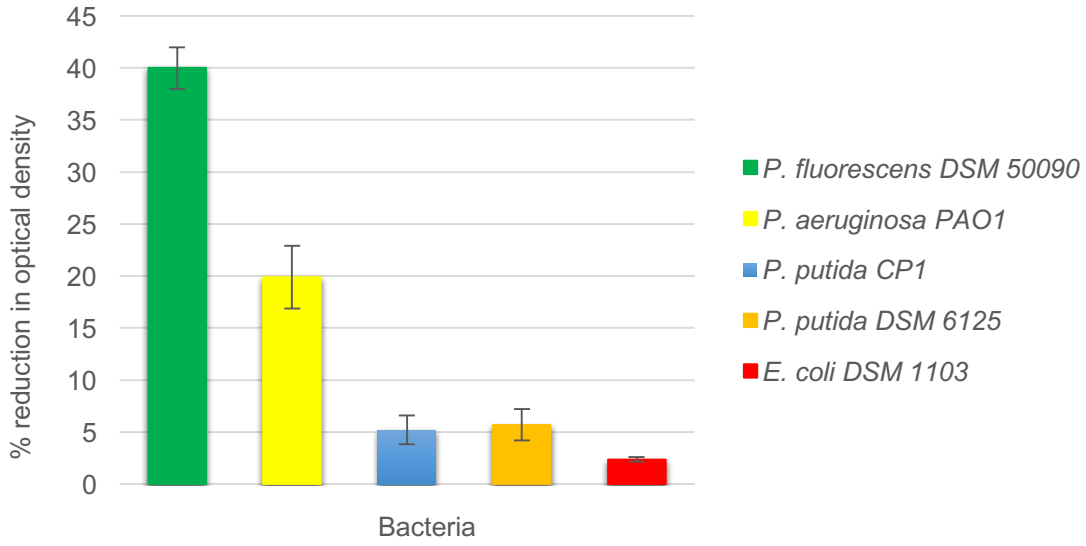

Figure 3.18 – Percentage reduction in optical density after 60 min due to aggregation/settling of bacterial cells.

A closer look at *Pseudomonad* species using confocal microscopy showed that when stained with the green fluorescent dye, SYTO 9, *P. putida* CP1 and *P. putida* DSM 6125 cells are found in their planktonic form, when grown overnight in nutrient broth (Figure 3.19). When grown under the same conditions, *P. fluorescens* DSM 50090 and *P. aeruginosa* PAO1 were found as aggregates, as can be observed on the Z-stack micrographs (Fig. 3.20).

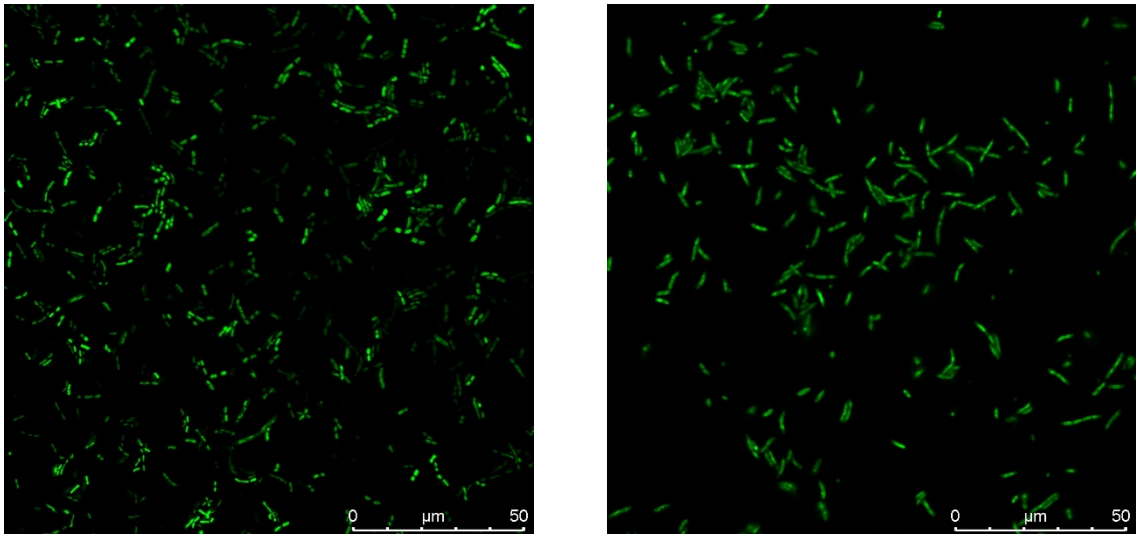

Figure 3.19 - CLSM micrographs (x100) of *P. putida* CP1 (left) and *P. putida* DSM 6125 (right) planktonic cells after overnight growth in nutrient broth.

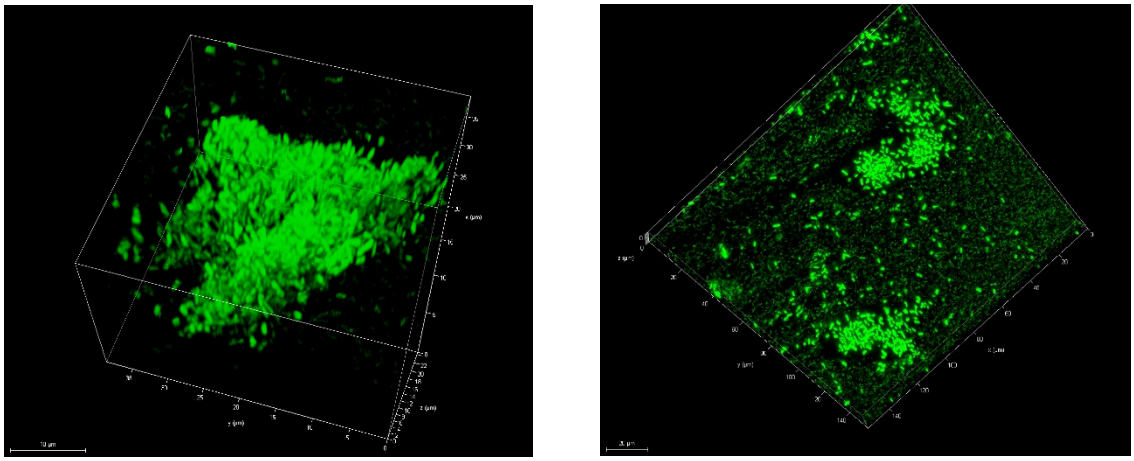

Figure 3.20 - CLSM micrographs (Z-stack – 100x) of *P. fluorescens* DSM 50090 (left) and *P. aeruginosa* PAO1 (right) agglomerates after overnight growth in nutrient broth.

3.3.3 Studies with cocultures

It was of interest to study the response of bacteria to PDI in mixed culture thus mimicking the conditions more usually encountered in the natural environment.

The effect of PDI on a coculture of the bacteria *E. coli*T-37 and *P. aeruginosa* PAO1 was evaluated. *E. coli*T-37, an environmental isolate, had been shown to be sensitive to PDI while *P. aeruginosa* PAO1, a pathogenic organism and widely distributed in the environment was shown to be more resistant. The response of the bacteria was monitored using the plate count method. The numbers of *E. coli* were distinguished from *P. aeruginosa* PAO1 by using a differential medium, MacConkey agar, where *E. coli* colonies appear pink due to lactose fermentation (MacConkey, 1905).

PDI with cocultures

The responses of *E. coli* T-37 and *P. aeruginosa* PAO1 to PDI were studied following the growth of the cultures together and separately as described in Section 2.2.2. The resulting deactivation curves are presented in Figure 3.21 and 3.22, respectively.

In both cases, *Pseudomonas* cells were shown to be more resistant than *E. coli* cells. When the bacteria were grown together (Fig. 3.21), they were more resilient to PDI than when grown separately (Fig. 3.22).

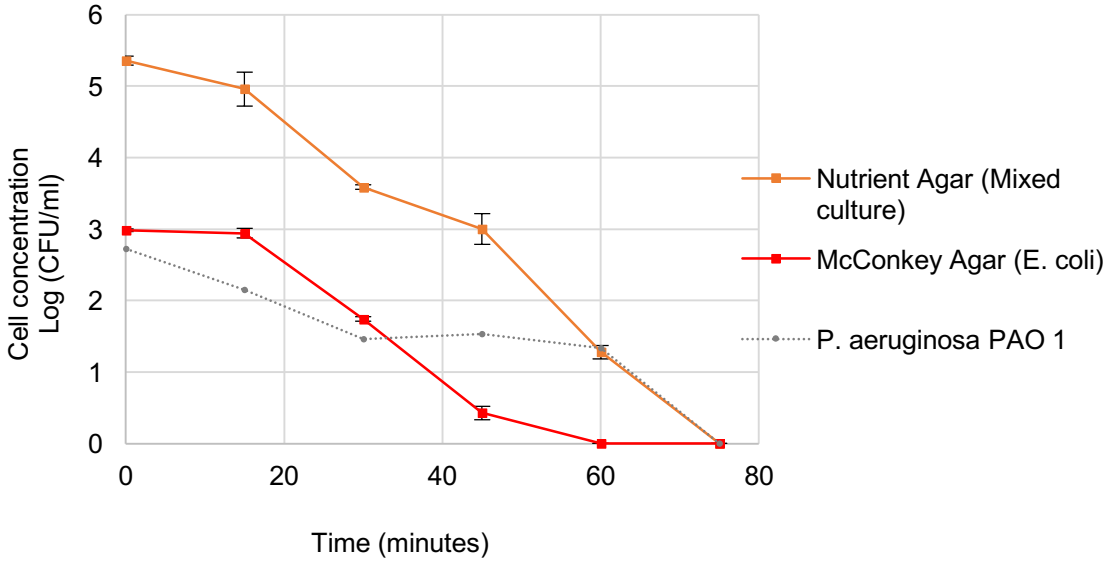

Figure 3.21 - Logarithmic reduction in the cell concentration of a coculture (grown together) of *E. coli*T37-1 and *P. aeruginosa* PAO1 after exposure to the dichromatic lamp with TMPyP at 3.65μM. The orange line shows the numbers for the total counts and the red line shows the numbers for *E. coli*T37-1 only. The dotted line shows the possible numbers *P. aeruginosa* PAO1, obtained by subtracting the total count in NA by the McConkey agar counts.

When comparing the results with the ones of each bacterium treated alone (3.65 μM), the time required to deactivate *Pseudomonas* was extended, since the initial inoculum size was reduced from 10^5 to ~10^3 CFU/ml. For the *Enterobacteriaceae* double the time was required to completely inactivate the bacterial cells (60 minutes - 78.94 J/cm^2).

For the coculture grown separately, but phototreated together, *E. coli* required 15 minutes more to be inactivated than when in pure culture. While PAO1 responded similarly to when grown together with *E. coli.*

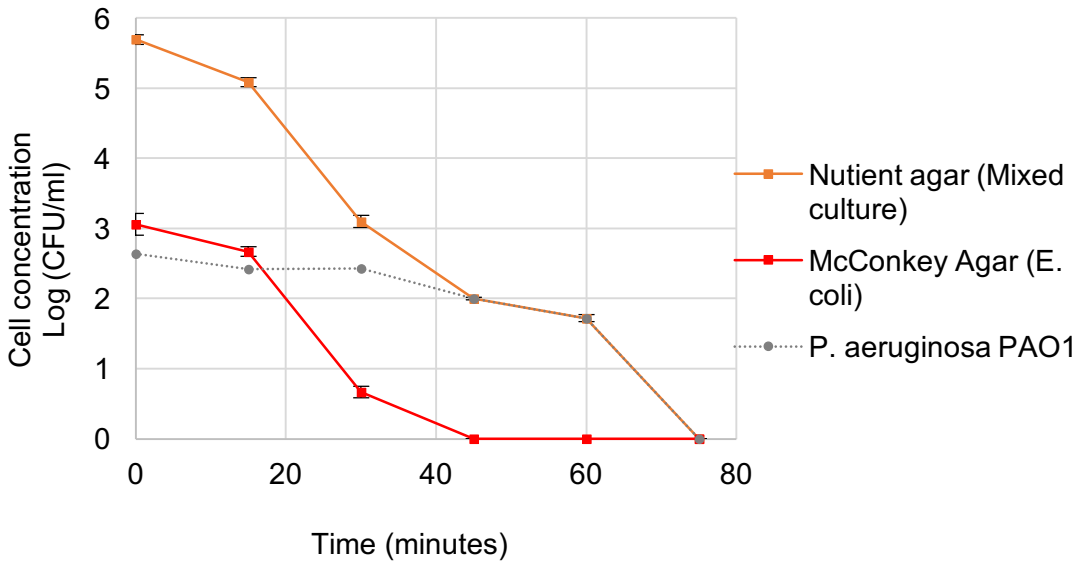

Figure 3.22 - Logarithmic reduction in the cell concentration of a co-culture (grown separately) of *E. coli*T37-1 and *P. aeruginosa* PAO1 after exposure to the Dichromatic lamp with TMPyP at 3.65µM. The orange line shows the numbers for the total counts and the red line shows the numbers for *E. coli*T37-1 only. The dotted line shows the possible numbers *P. aeruginosa* PAO1, obtained by subtracting the total count in NA by the McConkey agar counts.

Confocal microscopy was used to analyse the coculture, and as can be observed in Figure 3.23 agglomerates are formed when the two bacteria were cultivated together.

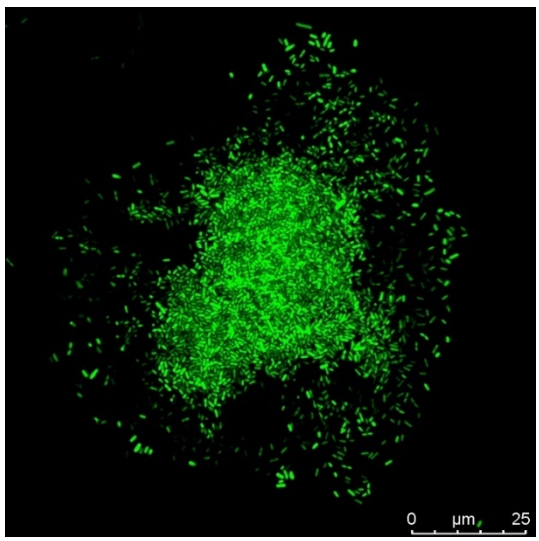

Figure 3.23. CLSM micrographs (x100) of the co-culture of *P. aeruginosa PAO1* and *E. coliT37-1* after growing together overnight in nutrient broth and stained with SYTO9.

MIC of cocultures

E. coli T37-1 and *P. aeruginosa* PAO1, when treated as cocultures, responded differently to the treatment when compared with the pure cultures treated with the same concentration of porphyrin (3.65μM). For this reason, it was of interest to investigate the response of the cocultures to antibiotics. The MIC of the cocultures with the antibiotic ampicillin was investigated. This antibiotic was chosen due to the prior MIC results (Table 3.6) with the pure cultures, where a significant difference in the antibiotic concentration needed to inhibit the growth of the two bacteria was found.

The MIC values were obtained using the method described in item 2.2.4. The streak plate technique, using the differential media MacConkey agar and King A agar, was applied to identify the presence or absence of growth of each bacterium.

As can be observed in Table 3.9, the MIC concentration for the coculture of *E. coli* and *P. aeruginosa*, when grown together, was 2500μg/ml, and 1250μg/ml when grown separately. For the coculture of *E. coli* and *P. fluorescens*, the values found were 5000 μg/ml for the bacteria grown together and 2500μg/ml for when they were grown separately.

When comparing these results with the ones found for the *Pseudomonads* pure cultures, when grown together, the cocultures required double the ampicillin concentration for growth inhibition. It is also clear, from these results that *E. coli* had its inhibitory concentration increased, to a value between 19.5 and 9.7μg/ml, when cultivated associated with *Pseudomonas.*

Table 3.9 – Evaluation of the presence or absence of growth of cocultures (*E. coli* T37-1 and *P. aeruginosa* PAO1 and *E. coli* T37-1 and *P. fluorescens* DSM 50090*)*, after MIC with ampicillin, in McCokey agar (*E. coli* T37-1) and King A agar (*Pseudomonas*) media.

Concentration (µg/ml)			**10,000**	**5,000**	**2,500**	**1,250**	**625**	**312.5**	**156.2**	**78.1**	**39.06**	**19.53**	**9.76**	**4.88**	**2.44**	**1.22**	**0.61**
McConkey agar	**A**	***GT***	-	-	-	-	-	-	-	-	-	-	+	+	+	+	+
		GS	-	-	-	-	-	-	-	-	-	-	+	+	+	+	+
	B	***GT***	-	-	-	-	-	-	-	-	-	+	+	+	+	+	+
		GS	-	-	-	-	-	-	-	-	-	+	+	+	+	+	+
King A agar	**A**	***GT***	-	-	-	+	+	+	+	+	+	+	+	+	+	+	+
		GS	-	-	-	-	+	+	+	+	+	+	+	+	+	+	+
	B	***GT***	-	-	-	+	+	+	+	+	+	+	+	+	+	+	+
		GS	-	-	+	+	+	+	+	+	+	+	+	+	+	+	+

GT = grown together; ***GS***= grown separately; (+) = presence of growth; (-) = absence of growth. **A** = *E. coli* T37-1 and *P. aeruginosa* PAO, and **B**= *E. coli* T37-1 and *P. fluorescens* DSM 50090.

3.3.4 PDI with the immobilised porphyrin

For practical application of the technology, immobilisation of the porphyrin was investigated. Following successful immobilisation, the response of *E. coli* T37-1 and *P. fluorescens* DSM 50090 to PDI using the immobilised porphyrin was investigated.

The porphyrin was immobilised to two solid matrices, hydrogels (HEMA/MAA, 80:20) and glass beads (5mm), as described in Section 2.2.7.

The hydrogels with different concentrations of TMPyP (3.65, 5 and 10μM) and the glass beads with the porphyrin at 3.04μM, were tested under the dichromatic lamp. Any leaching of the porphyrin from the matrices was also investigated.

3.3.4.1 PDI with Glass beads

When PDI was carried out using porphyrin (3.04μM) adsorbed onto glass beads (Figure 3.24), *E. coli* was more susceptible to the treatment than *P. fluorescens,* in accordance with the results reported from the previous experiments. The *Enterobacteriaceae* required 45 minutes (59.21 J/cm^2) of irradiation to be completely deactivated, while the *Pseudomonad* took 105 minutes (138.1 J/cm^2). When comparing these results to the ones of the porphyrin in solution (3.65μM), an increase of 15 minutes in the time of irradiations was necessary for total removal of the bacteria. The results with the rates are summarised in Table 3.10.

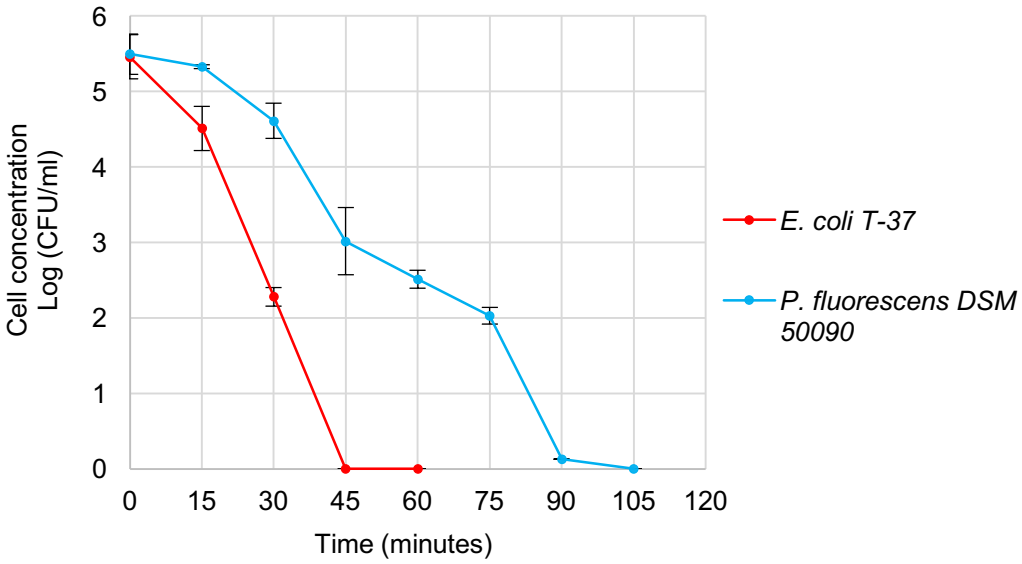

Figure 3.24 - Logarithmic reduction in the cell concentration of *E. coli* T37-1 and *P. fluorescens* DSM50090 after exposure to the dichromatic lamp with the TMPyP glass beads.

Table 3.10. Length of time/dose necessary for a 5-log reduction and total deactivation of *E. coli T37*-1 and *P. fluorescens DSM 50090,* under exposure to the dichromatic lamp (430 and 660 nm) with TMPyP coated glass beads.

Bacteria	**Total Inactivation (5-log reduction)**	
	Time / dose	**Rate**
E. coli T37-1	45 minutes / 59.21 J/cm^2	0.1212 min^{-1}
P. fluorescens DSM 50090	105 minutes / 138.11 J/cm^2	0.0523 min^{-1}

3.3.4.2 PDI with hydrogels

As shown in Figures 3.25 and 3.26, similarly to the experiments performed with TMPyP in suspension, *E. coli* was more sensitive to the treatment with the hydrogels than *P. fluorescens*. A clear lag is observed in the response for both bacteria. The response of *E. coli* T37-1 was similar when the concentrations of TMPyP in the hydrogels were 3.65μM and 5μM, requiring 150 minutes of irradiation for a 5-log reduction in the number of cells. A quicker response, half hour less, was required to completely deactivate the bacterium when the porphyrin concentration was increased to 10 μM.

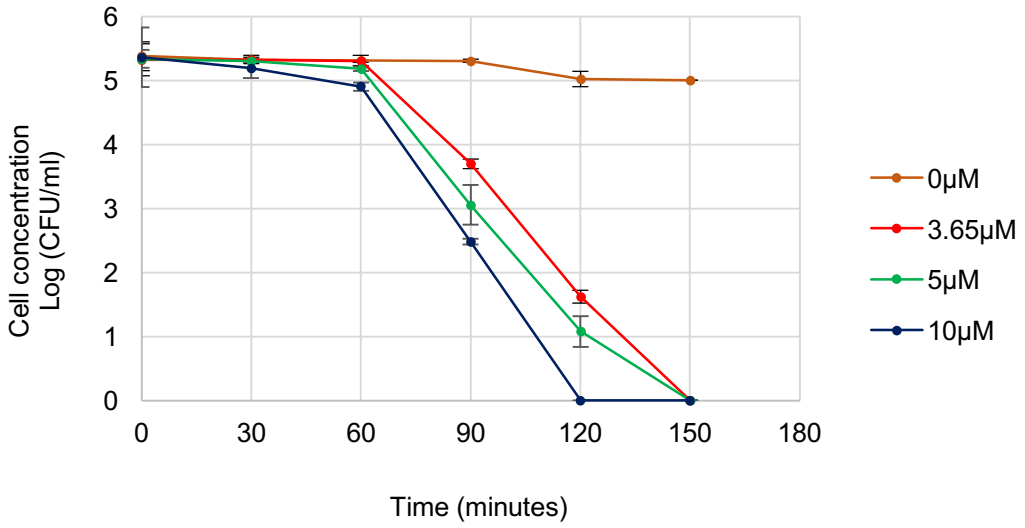

Figure 3.25 - Logarithmic reduction in the cell concentration of *E. coli* T37-1 after exposure to the Dichromatic lamp with the polymer immobilised TMPyP at the concentrations of 3.65, 5 and 10μM.

For *P. fluorescens* (Fig. 3.27), the lowest concentration of TMPyP immobilised to the hydrogel, 3.65μM did not deactivate *P. fluorescence* completely, with only a 3.5-log reduction being achieved in the time here studied. A 5-log reduction was observed when the concentration of porphyrin in the polymer was 5 and 10 μM, with 180 minutes of irradiation being required for the first one, and 150 minutes for the second.

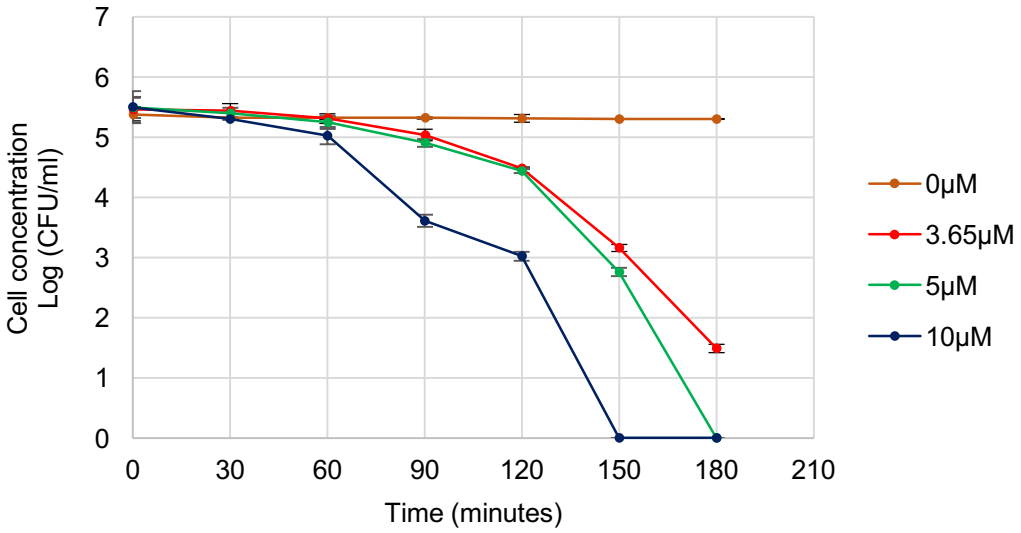

Figure 3.26 - Logarithmic reduction in the cell concentration of *P. fluorescens* DSM50090 after exposure to the Dichromatic lamp with the polymer immobilised TMPyP at the concentrations of 3.65, 5 and 10μM.

When comparing the times (doses) required for bacterial deactivation in the two different systems, suspension and inert, a considerable increase in the irradiation period was observed. In the case of *E. coli,* for the concentrations 3.65 and 5 μM, 120 minutes (157.88 J/cm^2) more of light exposure was necessary to deactivate the same bacterial number (5-log). While for the 10 μM concentration, additional 90 minutes of irradiation (118.42 J/cm^2) were necessary to eliminate all the bacteria from the solution.

When looking at P. fluorescens, even with a long irradiation time (180 minutes – 236.8 J/cm^2), the immobilised porphyrin at the lowest concentration only deactivated 3.5-log of the bacteria present in the suspension. 90 minutes (118 J/cm^2) were necessary for a 5-log reduction with the same concentrations in suspension. For the 5 μM concentration, 105 minutes (138.1 J/cm^2) more of light exposure were necessary for total deactivation and for 10 μM, the time of irradiation had to be 2.5 times longer (90 minutes - 118.42 J/cm^2).

Table 3.11. Length of time/dose necessary for a 5-log reduction and total deactivation of *E. coli T37*-1 and *P. fluorescens DSM 50090,* under exposure to the Dichromatic lamp (430 and 660 nm) with TMPyP incorporated to hydrogels at 3.65, 5 and 10μM.

Bacteria	**5-log reduction (Total deactivation)**					
	3.65 μM		**5 μM**		**10 μM**	
	Time/dose	Rate	Time/dose	Rate	Time/dose	Rate
***E. coli* T37-1**	150 minutes / 197.3 J/cm^2	0.03548 min^{-1}	150 minutes / 197.3 J/cm^2	0.3557 min^{-1}	120 minutes / 157.84 J/cm^2	0.04468 min^{-1}
***P. fluorescens* DSM 50090**	N/A	0.022 min^{-1}	180 minutes / 236.76 J/cm^2	0.03050 min^{-1}	150 minutes / 197.3 J/cm^2	0.0366 min^{-1}

3.3.4.3 TMPyP leaching in the medium

The leaching of TMPyP in the PBS solution was investigated by UV-vis spectroscopy. No leaching was observed for any of the hydrogels, as can be seen in Figure 3.27, where the UV-vis spectra from the hydrogel with the highest concentration of porphyrin (10μM) is shown. However, the glass beads leached porphyrin as shown of Figure 3.28. At the beginning of the treatment, no considerable leaching was observed, but after 60 minutes and 120 minutes of phototreatment, the leaching is evident by the peaks at 422 nm characteristics of TMPyP Soret band.

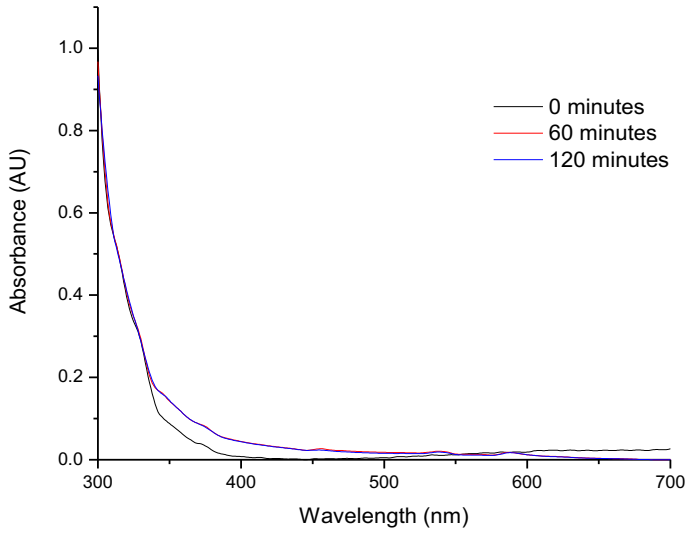

Figure 3.27 – UV-vis spectra of the PBS suspension during PDI with the hydrogel at 10μM.

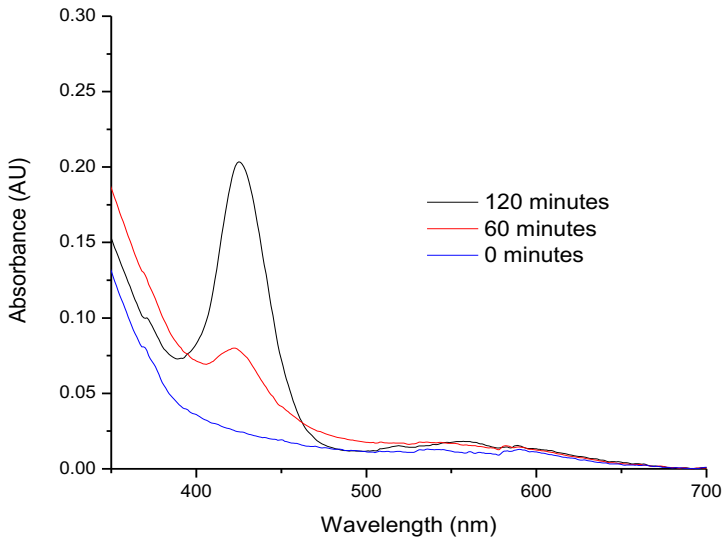

Figure 3.28 – UV-vis spectra of the PBS suspension during PDI with the glass beads.

To calculate the amount of TMPyP that leached from the glass beads into PBS, the Beer-law was used. After 60 minutes of phototreatment, TMPyP concentration in the solution was 1μM, and after 120 minutes, the concentration was 2.62 μM.

4. Discussion

4.1 Development of the experimental system

The experimental system used in PDI studies is very important as it influences any results obtained. An accurate description of the experimental system is also necessary when comparing results between different research groups and laboratories. At the recent 17th Congress of the European Society for Photobiology in Pisa, Italy in September 2017, Mark Wainwright pointed out that it would be useful to standardise experimental systems in order to better compare the findings at international level. When designing the experimental system, the parameters that need to be considered include the photosensitiser used, the lamp, the medium, the vessels, the bacterial inoculum size and time of light exposure. The importance of considering these parameters has also been highlighted by Jori (2006).

The photosensitiser

The photosensitiser plays a key role in the PDI process, since the effectiveness of the treatment is directly linked to its ability to generate reactive oxygen species. The capacity of the photosensitiser to bind to bacterial cells, increases the efficacy of the process. By inserting positively charged substituents in the peripheral positions of the tetrapyrrole macrocycle, porphyrins can be transformed into cationic entities (Alves *et al.*, 2009). This affects the hydrophobicity of the molecule and as a consequence the kinetics of activity and binding capacity to bacteria and its phototoxicity (Tavares *et al.*, 2011, Alves *et al.*, 2014).

The porphyrin used in this study was the tetracationic porphyrin 5,10,15,20-Tetrakis(N-methyl-4-pyridyl)-21,23H-porphyrin tetratosylate (TMPyP). TMPyP application in PDI has already been reported by other authors (Nitzan and Ashkenazi, 2000; Ergaieg and Seux, 2009; Komagoe *et al.*, 2011; Preuβ *et al.*, 2012; Orlandi *et al.*, 2015). It was chosen for use in this study for a number of reasons. It is positively charged, making it water soluble and more prone to be effective in deactivating bacteria, it induces changes in membrane permeability and inhibits respiration in Gram-positive and Gram-negative bacteria (Komagoe *et al.*, 2011).

The characterisation of TMPyP in terms of its photophysical and photochemical properties is very important when developing an efficient experimental system for antimicrobial photodynamic inactivation. Through UV-visible spectroscopy it was possible to identify and characterise TMPyP Soret and Q-bands when in PBS solution. As shown in Figure 3.1, the Soret band, which represented the transition from the ground state to the second excited state ($S_0 \rightarrow S_2$) (Jablonski diagram), was found to be at

422nm. The Q bands were observed at 520nm, 554nm, 585 nm and 641nm, those bands are involved in the transition of the ground state to the first excited state ($S_0 \rightarrow S_1$), which is weaker. Yang *et al.* (2002), Gulino *et al.*, (2005), Di Natale *et al.* (2000) and Paolesse & D'Amico (2007) showed that having this information helped them in the choice of the light sources to be used, since the bands represent the ideal wavelengths in which the porphyrin should be excited for an optimal production of ROS.

When the porphyrin undergoes intersystem crossing and the excited triplet state is generated, energy or electrons can be transferred to molecular oxygen, generating ROS (singlet oxygen, hydrogen peroxide, radical hydroxyl). The production of ROS can be measured directly or indirectly. A way of indirectly measuring ROS production is by using a quencher, or probe, like CM-H_2DCFDA (5-(and-6)-chloromethyl-2',7'-dichlorodihydrofluorescein diacetate, acetyl ester). When it is oxidised by the ROS generated through the porphyrin irradiation, it releases a fluorescent compound CM-DCF which is measured by a fluorimeter (excitation 495 nm and emission 530 nm). This technique was used in order to compare the amount of ROS produced by the three different concentrations (3.65, 5 and 10μM) of TMPyP that were the focus of this project. Figure 3.4 shows that there is no significant difference in the emission for the three concentrations after being irradiated for 30 minutes.

TMPyP singlet oxygen quantum yield was measured directly by NIR spectroscopy. When the porphyrin solution was excited at 405nm, the emission spectrum showed a peak at *ca.* 1270 nm, which corresponded to $^1O_2$ phosphorescence emission. A standard compound, ruthenim trisbipyridyl $[Ru(bpy)_3]Cl_2$, known as a good singlet oxygen producer (Gutiérrez *et al.,* 2003), also had its emission spectrum captured by NIR spectroscopy under the same conditions (Figure 3.5). TMPyP singlet oxygen quantum yield was then determined by comparing the wavelength integrated intensity of its emission spectrum to the reference one (Montalti *et al.,* 2006). When compared with the standard, the value found for TMPyP, Φ_R=0.74, shows that it is an efficient singlet oxygen producer, agreeing with other studies already reported in the literature (Jemli *et al.,* 2002; Ergaieg and Seux, 2009; Orlandi *et al*, 2014).

In this study, preliminary investigations showed that the lower concentrations, 0.625μM, 1.25μM and 2.5μM, of TMPyP were not effective in deactivating any of the bacteria studied. The porphyrin concentration used in the study was guided by the work of Ergaieg and Seux (2009). They found that TMPyP at a 3.65μM concentration showed to be efficient for the deactivation of the microorganisms *E. coli* DSM 1103 and *Enteroccocus hirae* DSM 3320 (5 log of CFU/ml). Concentrations of TMPyP ranging from

3.65μM - 20μM, were then investigated. However, 20μM was not found to be significantly more effective than 10μM and so the range 3.65μM - 10μM was further investigated. An increase in the porphyrin concentration, increased the effectiveness of the system to a certain extent, leading to a reduction in the time required for deactivating the bacteria treated. Komagoe *et al.* (2011), also observed in their experiments that an increase in the concentration of the cationic porphyrins TTMAPP (5,10,15,20-tetrakis{4-[*N*-(trimethyl) ammonio]phenyl}-21*H*,23*H*-porphine tetrakis(*p*-toluenesulfonate) and TMPyP (5,10,15,20-tetrakis(*N*-methylpyridinium-4-yl)-21*H*,23*H*-porphine tetrakis(*p*-toluenesulfonate) also increased the efficacy of the photodynamic process against *E. coli* and *S. aureus.* However, it was noted that at higher concentrations, an increase in concentration did not lead to an increase in cell death. This was also observed by Phillipova *et al.,* (2011) and can be explained by the fact that there is a limit in the amount of photosensitiser that can bind to the cells, so an excess of porphyrin would not improve its killing efficiency, as shown by Jemli *et al.*, (2002), Sabbahi *et al.*, (2013) and Orlandi *et al.*, (2013).

When considering the use of PDI for water disinfection, health related issues need to be considered. PDI involves the use of a photosensitiser or chemical which may have health implications. The evaluation of a compound capability of inducing mutations is an extremely important procedure when considering any safety assessment. (Pelon *et al*, 1977; Lv *et al.*, 2015; Guan *et al.*, 2017). For this reason, the mutagenicity of the TMPyP was evaluated using the Ames Test, which is a is a widely accepted bacterial reverse mutation assay. It is commonly used as a screening assay because of its ease of use, high sensitivity and reproducibility and speed in delivering results. The correlation between mutagenicity and carcinogenicity has been widely evaluated because carcinogenicity is of utmost human health concern and can result from mutagenicity (OECD, 1997; Mortelmans and Zeiger, 2000; Mestankova *et al.*, 2016).

The principle of the test is based on the detection of gene mutation caused by genetic damage produced by a chemical substance. The bacterial strains used present pre-existing mutations which leave the bacteria unable to synthesize a specific amino acid, being unable to grow and form colonies in its absence. When in contact with determined compounds, new mutations can occur at the site of these pre-existing mutations, or nearby, restoring the gene's function and allowing the cells to synthesize the amino acid and grow normally again. These strains can be of *Salmonella typhimurium* with mutation in the histidine operon, or *E. coli* WP2 with tryptophan reverse mutation (Ames *et al.*, 1973; Mortelmans and Zeiger, 2000; Mortelmans and Riccio, 2000). The Ames (AMES-MOD ISO™) test was used in this study. The strain used was the S*almonella*

typhimurium TA-100, which has the base pair substitution (G-C) type of reversion mutation. This strain is derived from the strain TA1535 and includes the plasmid pKM 101, which enhances the mutagenicity by chemicals and UV, since it increases the error-prone recombinational DNA repair pathway (Mortelmans, 1979; Mortelmans and Zeiger, 2000). The porphyrin mutagenicity was tested with TMPyP solution at the concentrations of 2.5, 5 and 10 μM, which were the concentrations of porphyrin used in this study, and no mutagenicity was detected. These results agree with previous work done by Casteel *et al.* (2004) and Grinholc *et al.* (2015) where the concentration of TMPyP tested was 100 μM and no mutagenicity was observed.

The light source

The light source is a very important consideration when planning the system design. The lamps used in studies vary with wavelengths ranging from 400 – 800 nm. This range of wavelengths is suitable for different types of photosensitisers and also simulates solar irradiation as highlighted by Rossi *et al.* (2012).

Among the lamps that have been applied in photosensitisation processes, the most common are halogen lamps (Sabbahi *et al.*, 2013; Orlandi *et al.*, 2013; Alves *et al.*, 2011; Oliveira *et al.*, 2009; Kuznetsova *et al.*, 2007; Magaraggia *et al.*, 2006 and Kassab *et al.*, 2002). LEDs were also used by some research groups (Arenas *et al.*, 2013; Parakh *et al.*, 2013 and Rossi *et al.*, 2012), as well as Xenon Lamps (Ergaieg and Seux, 2009; Ergaieg *et al.*, 2008) and Diode laser systems (Street and Gibbs, 2010).

Halogen and Xenon lamps (λ≥ 350nm) can be effective in PDI due to their high fluence rate. However, they can produce heat when used for long periods of time, which interferes in the experiments. In order to reduce the heat interference, some alternatives have been used, such as the use of an aqueous filter between the light and the photosensitiser solution (Orlandi *et al.*, 2013; Rossi *et al.*, 2012; Kuznetsova *et al.*, 2007) or the use of a water or ice bath, to keep the samples cool while immersed (Oliveira *et al.*, 2009; Alves *et al.*, 2011; Sabbahi *et al.*, 2013).

Lamps that emit at the ultraviolet range, either need to be equipped with a UV and infrared filter (Magaraggia *et al.*, 2006; Kassab *et al.*, 2002) or the vessel itself needs to remove these specific wavelengths (Rengifo-Herrera *et al.*, 2007). This is done in order to evaluate only the effect of PDI on the cells, since UV-light alone can inactivate the microorganisms (Rossi *et al.*, 2012; Graf *et al.*, 2010).

Light-emitting diodes (LED) are incoherent light sources that were developed in recent times. They have a relatively narrow emission spectrum (wavelength), are simple, cheap

and produce less heat than the other lamps commonly used in PDI. Also, LEDs are a much preferred light source, since they require low energy consumption, are safe to handle and have long life time. For these reasons, they are a great option for photodynamic studies with microbial cells (Maclean *et al.*, 2009; Ohtsuki *et al.*, 2009; Parakh *et al.*, 2013) and were chosen to perform the experiments in this study.

The monochromatic lamp (λ=525nm) was shown to be more efficient in inducing ROS generation than the multichromatic lamp (λ≥400nm). As both lamps have a very similar fluence rate, 1.01 mW/cm^2 for the monochromatic lamp and 0.97mW/cm^2 for the multichromatic one, this was probably due to the fact that TMPyP has a Q band around 520 nm (see Figure 3.1). The presence of a Q band at 520nm in TMPyP may increase the number of photons that were absorbed by it during irradiation with the monochromatic lamp, resulting in the generation of a slightly higher number of singlet oxygen, responsible for killing the bacteria (Qin *et al.*, 2007).

While both the monochromatic and multichromatic lamps were very effective for use in the experimental system, they were small in size restricting the experimental design. Since TMPyP has its Sored band at 422nm and a Q- band at 641 nm, and since it is known that blue light is the most penetrating wavelength from the electromagnetic spectrum, we infer that using a lamp with mixed LEDs with emission at these wavelengths can improve the system efficiency and therefore the disinfection activity. For that reason, a dichromatic lamp, with emission at 430 and 660 nm and an area 730 cm^2 was chosen for use in the later experiments.

Medium

It was decided to use PBS as the medium in the experimental system. According to Nitzan *et al.* (1998) and Lambrechts *et al.* (2003), the consistency of the medium to be used in the experiments has a high influence on its efficiency. Orlandi *et al.*, (2012) pointed out that the amount of photosensitiser bound to cells decreases with increasing concentrations of organic compounds in the medium. This is an important consideration when choosing the media where the experiment will be performed, since they showed that the use of a rich medium impaired the photosensitiser efficiency. They did show however, that PBS promoted the PDI process. In addition, salts present in PBS provide an isotonic medium which maintains cell integrity and viability making it a very suitable medium for experimental studies.

Vessel

Among the systems investigating photosensitisers dissolved in an aqueous solution, many different vessels have been used by other researchers, for example Petri dishes, multi-well plates, cuvettes and beakers (Spesia *et al.* 2005; Ergaieg and Seux, 2009; Nakonieczna and Grinholc, 2012; Pereira *et al.*, 2012; Rolim *et al.*,2012; Nakonechny *et al.*,2013; Arenas *et al.*, 2013; Hanakova *et al.*, 2014).

Due the fact that a small system is easier to control (temperature variations, contaminations, etc.) and that more variables can be tested at the same time, leading to faster results, the multi-well microliter plates were chosen for preliminary experiments in this study.

The experiments performed in the 96-well plates were useful to give preliminary results and an idea about the effective concentrations of the porphyrin TMPyP, to be used in larger scale experiments. However, in order to increase the working volume in the experiments, 60x15 mm glass Petri dishes were used. When the glass Petri dishes were used, the working volume was 10ml. The results obtained with the larger volume gave similar results to that for the 96 well plates when similar lamps were used (light dose 10.47 J/cm^2).

4.2 Response of bacteria to PDI

Photodynamic inactivation (PDI) is a process used for cell deactivation based on the production of free radicals by a photosensitiser irradiated with light. This principle was employed in this project to inactivate Gram-negative and Gram-positive bacteria

In the beginning, PDI was only investigated and commercialised as an alternative for cancer therapy (Agostini *et al.*, 2011), however, more recently, research has focused on its application for the eradication of infectious diseases. The main reason for this is the risk presented by the spread of antibiotic resistance amongst pathogens like Gram-positive and Gram-negative bacteria (Hamblin *et al.,* 2012),

One of the main advantages of using PDI for antimicrobial applications is the fact that it does not lead to the development of resistance by the microorganisms, due to its multitarget nature where more than one vital cell component is inactivated. To confirm this assumption, Giuliani *et al.* (2010) investigated the ability of *Pseudomonas aeruginosa*, *Staphylococcus aureus*, and *Candida albicans* strains to develop resistance due to exposure to a tetracationic Zn(II) phthalocyanine derivative. Their experiments involved a multistep resistance selection with twenty daily passages, where the

pathogens were constantly in contact with the photosensitiser, in the presence and absence of light. The results showed that after 20 consecutive treatments none of the microorganisms developed any resistance, corroborating the hypothesis that PDI does not lead to the emergence of resistant strains.

Monitoring bacterial response

The inoculum size chosen for the study was 10^5 CFU/ml. This was found to be a suitable inoculum in order to monitor response of the bacteria within the timeframe of the experiments. It also allowed the identification of a 3 $\log_{10}$ reduction, which the American Society of Microbiology has suggested as a measure of microbial removal by any new technology in order to qualify it as antimicrobial or antibacterial.

Many approaches have been used by diverse research groups to monitor photoinactivation of microorganisms following light exposure. The majority of the work reported has used the plate count technique, where serial dilutions of the solution (photosensitiser + cells), after specific time intervals of photosensitisation, are cultivated on agar plates. After incubation under suitable conditions the number of colonies formed can be determined and compared with controls (Jemli *et al.*, 2002; Bozja *et al.*, 2003; Spedia *et al.*, 2005; Caminos *et al.*, 2006; Demidova and Hamblim, 2005; Bonnett *et al.*, 2006; Ferro *et al.*, 2006; Banfi *et al.*, 2006, Vilela *et al.*, 2012; Pereira *et al.*, 2012; Nakonieczna and Grinholc, 2012; Alves *et al.*, 2013; Arenas *et al.*, 2013; Nakonechny *et al.*, 2013). The membrane filtration (MF) technique has also been used, for example when analysing wastewater, for the presence of faecal coliforms (Tota-Maharaj and Meeroff, 2013).

After the photodynamic oxidative process, the bacterial cell membrane can become compromised, leading to the release of membrane components which are a good indicator of membrane integrity. Among these components we can find small ions such as potassium and phosphate, and nucleic acids. Due to the fact that these nucleotides have strong UV absorption at 260 nm, they are described as ‘‘260 nm absorbing materials’’ and their presence can be detected by UV–Vis spectrophotometry, as demonstrated by Chen and Cooper (2002). Also, the damage to the cytoplasmic membrane can be associated with its proteins, the use of a proteomic approach to investigate the effects of PDI can be very useful. Dosseli *et al.* (2012) used the well-known proteome system of *S. aureus* to investigate the action of PDI in its cytoplasmic membrane. They performed a fractionation protocol using lysostaphin to digest the bacteria cell wall as they wanted to assess the membrane-enriched protein fraction. The

protein content in the total cell lysate was then quantified using the bicinchoninic acid method.

A lipidomic study is also an alternative to evaluate the modifications that oxidative reactions can cause in cellular lipids, since it leads to changes in their structure causing loss of function. Alves *et al.* (2013) performed experiments with *E. coli* and *S. warneri,* where the lipids from these bacteria were extracted immediately after the photosensitisation process and then quantified and characterised by thin layer chromatography (TLC) combined with mass spectrometry (MS) and gas chromatography (GC).

Alves *et al.* (2008) investigated the use of a recombinant bioluminescent *E. coli* as a rapid method to access the antibacterial effect of PDI. The bioluminescence of the bacteria was recorded using a luminometer, with a decrease in bioluminescence indicating a decrease in cell viability. The method was suitable under their experimental conditions, with the photoinactivation pattern obtained with the bioluminescence method being similar to that determined by the conventional plating technique.

Microscopy is also used to evaluate the damage by the photodynamic process. Light microscope observations were performed by Kassab *et al.* (2002), using a device equipped with a fluorescence apparatus, allowing them to observe the uptake of porphyrin by the cysts of *Colpoda inflata.* Transmission electron microscopy was used by Orlandi *et al.* (2013) with the aim of investigating the changes in the bacterial cell morphology, induced by the irradiation. Scanning electron microscopy can also be used, as described by Parakh *et al.* (2013). The technique can show changes such as membrane damage and cell deformation. Another approach used to monitor the response of microbial cells involves the use of fluorescent stains and observation using fluorimetry or epifluorescence microscopy. This technique is particularly useful when real time monitoring of the cells is of interest. One such approach uses the LIVE/DEAD® Baclight™ Viability kit. This kit has two dyes which stain nucleic acids, SYTO9 (emits a green fluorescence) and propidium iodide (PI) (emits a red fluorescence). The dye SYTO9 can enter both live and dead cells, however, the PI dye can just enter those cells with damaged membrane. When inside the cell, PI competitively binds to nucleic acids over SYTO9 giving a red fluorescence (dead cells). The live cells fluorescence green, (Salmi *et al.*, 2008; Schastak *et al.*, 2010; Parakh *et al.*, 2013).

In this study, an attempt to use the LIVE/DEAD® Baclight™ Viability kit to monitor the results. However, because the porphyrin fluorescence emission was in the same wavelength range as that of propidium iodide, it interfered with the results. The porphyrin fluoresced red making it impossible to distinguish between the dead cells. The use of further dyes was then explored including 4′,6-diamidino- 2-phenylindole (DAPI), which stains the nucleic acid of all cells, and SYTOX® Green nucleic acid stain, which only penetrates bacteria with damaged membranes. However, these dyes were also not successful due to interference from the porphyrin.

Members of the Family Enterobacteriaceae

In general, the members of the Family *Enterobacteriaceae* investigated responded well to PDI. Three species of *E. coli, S. sonnei, S. enterica* and *E. aerogenes* were studied. All six bacteria investigated were successfully inactivate by PDI. E. coli was the most sensitive to the treatment, followed by *Shigella* and *S. enterica* while *E. aerogenes* was the most resistant.

The sensitivity of Gram-negative bacteria to PDI varies. The cell wall of the Gram-negative cell is thought to contribute to resistance. However, cationic porphyrins such as TMPyP have been shown to enhance the sensitivity of these bacteria (Malik *et al.*, 1992; Minnock *et al.*, 1996). These porphyrin positive charges promotes a tight electrostatic interaction with negatively charged sites in the outer surface of the Gram-negative cell membrane, making the PDI process more efficient (Merchat *et al.*, 1996; Nitzan *et al.*, 1998; Caminos *et al.*, 2008; Cordeiro *et al.*, 2012).

Enterobacteriaceae are Gram-negative nonspore-forming, mobile or immobile, aerobic or facultative anaerobic rod-like bacteria. The family is the largest and most heterogeneous family of clinically important Gram-negative bacilli and many species can be found in the human intestinal tract, as part of its microbiota. They are also present in soil, plants and water (Holt *et al.*, 1994), making their investigation with PDI very relevant.

Escherichia coli is widely used in PDI studies. The organism is a well-known Gram-negative bacterium and member of the coliforms group. It is commonly found in the digestive system of humans and animals (Ibekwe and Grieve, 2003) and has great importance due to the complexity of its cell wall, which has an outer membrane consisting of other non-lipid components, another phospholipid bilayer, lipoproteins and lipopolysaccharides (Raetz, 1978; Epand *et al.*, 2009; Alves *et al.*, 2013). *E. coli* is generally chosen as a representative biological model for Gram-negative bacteria and

its presence in food or water is used as an indicator for monitoring the presence of other harmful microorganisms (Masters *et al.*, 2011).

The three *E. coli* strains investigated showed a 5-log reduction within 30 minutes of irradiation (39.47 J/cm^2) using 3.65μM TMPyP. The efficiency of the system is demonstrated by comparing with the work of Ergaieg and Seux (2009), They used the same porphyrin (TMPyP) at a concentration of 3.65μM, they achieved a 5-log reduction in bacterial cell numbers of *E. coli* DSM 1103 and *Enteroccocus hirae* DSM 3320 but using light doses of 256.5 and 85.5 J/cm^2, respectively. Alves *et al.,* (2013), investigated the response of *E. coli* to the TMPyP derivatives, Tri-Py$^+$-Me-PF and Tetra-Py$^+$-Me, which was irradiated by 13 parallel OSRAM 18 W/21‑840 lamps with an irradiance of 4.0mW/cm^2. In their system, a 7-log reduction was observed for *E. coli* cells upon a light dose of 64.8 J/cm^2.

When the concentration of porphyrin was increased to 5 μM, the time necessary to deactivate the bacteria remained the same for *E. coli* DSM 498 and *E. coli* T37-1 however for *E. coli* DSM 1103 the time was reduced by half (19.73 J/cm^2). Alves *et al.*, (2009) also showed that an increase in the cationic porphyrin concentration, from 1μM to 5μM, increases the inactivation efficacy. While 1μM porphyrin caused a 2-log reduction in the number of *E. coli* cells, 5μM led to a 7-log reduction, with the light doses (white light) being 64.8 J/cm^2 for both experiments.

While *E. coli* is widely studied as a representative of the family *Enterobacteriaceae,* other members of the family are a particular challenge when considering water quality and in particular water for drinking. The genus *Shigella* (human-adapted *E. coli*) is a group of Gram-negative pathogens, responsible for causing the dysentery called shigellosis. They are transmitted mainly through the faecal-oral route, being considered one of the most important waterborne and foodborne pathogens worldwide. (Yang *et al.*, 2005; Holt *et al.*, 2012; Jun *et al.*, 2016). *S. sonnei* DSM 5570 was chosen for this study because it is a pathogenic strain. Thomson *et al.*, (2015) showed that *S. sonnei* has the ability to easily acquire antimicrobial resistance genes from other commensal and pathogenic bacteria.

Salmonella is a rod-shaped Gram-negative bacteria genus which is one of the leading causes of intestinal infections, as well as the etiological agent of diseases like typhoid and paratyphoid fever (Pond, 2005). They are spread via faecal–oral route, easily contaminating aquatic environments, being found in drinking and natural water sources. Due to their resistance, this bacterium can persist in wastewater effluent even after

advanced secondary treatment (i.e. coagulation, filtration and disinfection) (Maier, Pepper, & Gerba, 2000; Wéry; Traore *et al.*, 2015)

Enterobacter is a genus of rod-shaped, non-spore-forming Gram-negative with great clinical importance since they are opportunistic pathogens, especially in intensive care unities (Mezzatesta *et al.*, 2012). They are well-known for their adaptive capability, with *E. aerogenes* being able to easily acquire resistance to β-lactam antibiotics during therapy (Thiolas *et al.*, 2005). Like the other members of the *Enterobacteriaceae family*, it can be found contaminating water bodies (Camper *et al.*, 1991).

S. enterica and *S. sonnei* were slightly more resistant to PDI than *E. coli.* Both strains were completely inactivated after 45 minutes of light exposure (59.21 J/cm^2) at 3.65 μM; When the concentration of TMPyP was increased to 5μM, *S. sonnei* was inactivated in 15 minutes. When this result is compared with earlier reports in the literature, the superior efficiency of the system used in this study is again highlighted. Nisnevitch *et al.* (2009) phototreated *Shighella flexneri and Salmonella para B,* using a white light (10.6 Klux) for 1 hour*,* applying three different photosensitisers, Methylene blue (MB), Rose Bengal (RB) and Neutral Red (NR). A reduction in the number of cells was achieved (no data shown) for *S. flexneri* with only MB (310μM) and RB (11 μM). For *Salmonella* only NR was effective in a concentration of 400 μM. Photoinactivation experiments were also conducted with another *Salmonella* strain by a Japanese group (Ishikawa *et al., 2009).* S*almonella enteritidis* was illuminated under a fluence rate 0.00365w/cm^2 for 360 minutes (dose of 78.84 J/cm^2), leading to an 8-log deactivation, the photosensitisers used were eggshell pigments (porphyrins).

Interestingly, *E. aerogenes* was the *Enterobacteriaceae* more resistant to the treatment, requiring almost double (75 minutes/98.68 J/cm^2) the irradiation dose of *E. coli* for its complete deactivation when TMPyP was used at a concentration of 3.65 μM. However, an increase in the photosensitiser concentration improved the efficiency of the treatment, with the time required for its deactivation being reduced by 15 and 30 minutes for the concentrations of 5 and 10 μM respectively. These results are comparable to other reports. Rossoni *et al.* (2010) studied the effect of RB (50μM) under irradiation of a blue LED (dose of approximately 95 J/cm^2), achieving a 6-log reduction in the number off *Enterobacter cloacae* cells. Junqueira *et al.* (2010) studied this same microorganism with the dye malachite green, under irradiation of a red laser (660nm - 27 J/cm^2), reaching a 7-log reduction in the bacterial cells. Although, in this last study the photosensitiser by itself caused an almost 4-log reduction in the number of cells, indicating its toxicity against the bacterium.

S. aureus

The bacterium *Staphylococcus aureus* was used as a model of Gram-positive bacteria. It is a pathogenic microorganism frequently associated with respiratory and cutaneous infections. Studies of the organism are important because of its presence in water bodies and its resistance to traditional antibacterial treatments (i.e. methicillin resistant *Staphylococcus aureus* – MRSA) (Tolba *et al.*, 2008; Barker-Reid *et al.* 2010; Rossi *et al.* 2012; Batalha *et al.*, 2015).

The effectiveness of the inactivation of *S. aureus* DSM 799 using TMPyP under the monochromatic lamp irradiation was high (10^5 CFU/ml) and comparable to other studies using cationic porphyrins. This microorganism was shown to be vulnerable to the photodynamic process and its antibiotic-resistance spectrum did not interfere with singlet oxygen action (Tavares *et al.*, 2010; Almeida *et al.*, 2011). Rossi *et al.*, (2012), for example, achieved a 4-log reduction in the number of cells of the same bacterial strain when they used a different cationic porphyrin which was irradiated by a blue multi-LED lamp (470nm) with a total light dose of approximately 9 J/cm^2. Similarly, Komagoe *et al.* (2012) were also able to deactivate *S. aureus* in their experiments. They used two porphyrins (5 μM), TTMAPP and TMPyP, with TTMAPP being slightly more efficient than TMPyP. After 12 minutes of irradiation (18 J/cm^2) with an overhead projector equipped with a 400 W halogen lamp, a ~7-log reduction was observed in the number of cells.

As explained by Malik *et al.* (1992), the high susceptibility of Gram-positive bacteria to PDI, especially *S. aureus*, is due to their physiology, since their cytoplasmic membrane is surrounded by a porous layer of peptidoglycan and lipoteichoic acid, which allows the photosensitiser penetrate the cell.

B. subtilis

Spore forming bacteria, members of the genus Bacillus and the genus Clostridium are Gram positive, however their ability to produce endospores makes them the most resistant bacteria to environmental stress (Hill *et al.* 1996; Skanavis and Yanko, 2001). Endospores consist of a multi-layered resistant and complex coating and their central part is composed of only 20 to 30% of the water content when compared to vegetative cells. This makes them enzymatically dormant and viable for long periods of desiccation (Setlow, 2005).

The response of *Bacillus subtilis* a Gram-positive, spore-forming bacterium was investigated as a model for spore-forming bacteria (Sousa *et al.*, 1976). *B. subtilis* DSM

10 was the bacterium that showed most resistance to the treatment. A dose of 118.42 J/cm^2 was necessary to achieve a 5-log decrease in the number of viable cells. However, the higher TMPyP concentration tested reduced the time necessary for its deactivation by half an hour.

The findings were comparable to that of Parakh *et al.* (2013) who also investigated the effect of PDI on this bacterium, however with a different photosensitiser. In their work, a LED array (λ= 450 and 625) with emission at wavelengths similar to the one used in this study, was used to irradiate two Ru(II) based complexes. A light dose of 172.8 J/cm^2 (60 minutes) was necessary for a 7-log reduction in the number of cells.

Silva *et al.*, 2012, investigated the effect of photodynamic therapy on different *Bacillus sp.* endospores. They investigated the response of *B. cereus* (ATCC 14579), *B. subtilis* (ATCC 31324), *B. licheniformis* (ATCC 14580), and *B. sphaericus* (ATCC 53969) to the photosensitiser Tri-Py$^+$-Me-PF under irradiation of a white light from a fibre optic probe (400–800 nm). They found that the endospores of *B. cereus* were the most susceptible to the treatment, followed by the *B. subtilis* ones, while the other two were resistant to photoinactivation. However, only a 1-log reduction in the number of *B. subtilis* spores was observed after exposure to 60 μM of photosensitiser and 4 min of irradiation (40.56 J/cm^2). The different responses among the different spore-forming *Bacillus* strains was unexplained.

Both Gram-positive bacteria here studied presented a very distinct response to the photoinactivation process. Under all concentrations tested, *S. aureus* DSM 799 responded very similarly to the *Enterobacteriaceae* group, requiring 59.21 J/cm^2 for its total inactivation with the lowest concentration (3.65 μM) and having it reduced to 19.73 J/cm^2 at higher concentrations (5 and 10μM). The system here applied shows to be effective for the inactivation of *S. aureus*, with the results being comparable to that of other systems using positively charged porphyrins (Di Poto *et al.*, 2009; Rossi *et al.*, 2012).

Members of the Pseudomonadaceae Family

The genus *Pseudomonas* is a large and varied genus comprising several rod-shaped, Gram-negative, aerobic, mesophilic and psychrotolerant microorganisms, characterized by simple nutritional requirements (Anzai *et al.*, 2000). This group includes numerous species, such as *Pseudomonas putida* and the well-known human opportunistic pathogen, *Pseudomonas aeruginosa* (Tümmler *et al.*, 2014). *Pseudomonas aeruginosa* is commonly associated with waterborne infections, causing severe contamination in

health care environments (Cevrvia *et al.*, 2008; Mena and Gerba, 2009). Due to its environmental and health importance, they were chosen for investigation in the present work.

Among the Gram-negative bacteria, the *Pseudomonadaceae* group were most tolerant to photodynamic inactivation. While the other Gram-negative bacteria required a light dose ranging from 39.47 to 98.68 J/cm^2 for a 5-log reduction, *Pseudomonads* needed a dose ranging from 78.94 to 118.42 J/cm^2, with *P. fluorescens* and *P. aeruginosa* requiring the longest period of irradiation in order to reduce to zero the number of viable counts.

Although no research has previously investigated the response of *P. putida or P. fluorescens* to PDI, some researchers have already investigated the use of PDI for the inactivation of *P. aeruginosa.* Sabbahi *et al.* (2013), also investigated the effect of TMPyP for antimicrobial inactivation. In their experiments, a 500W halogen lamp was used as the light source (emission in the range of 500–750 nm with peak at 650 nm), and nutrient broth was the medium used. They observed that TMPyP at a concentration of 20 μM led to a reduction of 3.3 log units for *P. aeruginosa* cells, after being irradiated for 180 minutes (540 J/cm^2). In the same year, researchers from India (Parakh *et al.*, 2013) investigated the effect of Ru(bpy) complexes on different bacterial cells, *E. coli*, *P. aeruginosa, S. aureus* and *B. subtilis*. They found the *Psedomonads* to be even more resilient than the spore former *B. subtilis,* requiring a light dose 3.5 times higher (798 J/cm^2) for it to be completely inactivated (7-log reduction).

Another group that also observed the resistance of *Pseudomonas* species to PDI. Was Tegos *et al.* (2006), who investigated the photodynamic inactivation of four bacterial strains*, E. coli, S. aureus, S. pyogenes and P. aeruginosa, P. aeruginosa* was shown to be resilient to the second-generation polycationic photosensitiser conjugates used, even when treated with an increased light dose and a photosensitiser concentration ten times higher than that used for the Gram-positive bacteria.

However, again when comparing the results in this study for *P. aeruginosa*, with the ones found in the literature, using the same porphyrin, it is clear that the system used in this study was more efficient for PDI experiments.

Although the pattern of resistance was observed by different authors, the fact that *Pseudomonas aeruginosa* is a Gram-negative bacterium was the main reason attributed to its low susceptibility to the photodynamic induced oxidative stress. In 2006, Tegos and Hamblin demonstrated the role of the efflux pump MexAB-OprM in protecting *P.*

aeruginosa from phenothiazinium dyes. More recently, 2015, a group from Italy (Orlandi *et al.*, 2015) also decided to closer investigate the *Pseudomonas* behaviour to PDI, after observing in their studies, that the photoinduced antibacterial activity of two dicationic 5,15-diarylporphyrins was less effective in *P. aeruginosa* than in the other bacteria investigated (Orlandi *et al.*, 2013).

4.3 Factors governing environmental resistance

Pigments

Other researchers have also found that PDI had a low efficacy against Pseudomonads. It was noted by Philippova *et al.* (2003) and Tegos *et al* (2006) that members of this group of bacteria are particularly resistant to photodynamic induced oxidative stress These bacteria are well known for their ability to produce pigments (Cezard *et al.*, 2015), among which we can find pyoverdine (Visca *et al.*, 2007), pyocianin (Jayaselan *et al.*, 2014), pyorubin and pyomelanin (Rodriguez-Rojas *et al.*, 2009). These pigments are thought to play an important role in managing photo-oxidative stress, as pointed out by Griffiths *et al.* (1955) around 60 years ago. They showed that a carotenoid-deficient *Rhodobacter* spp was damaged by photosynthesis in an aerobic environment. Ramel *et al.*, (2012) explained that when present, carotenoid is responsible for protecting the bacterial cells by quenching singlet oxygen.

Based on that and on the ability of *P. aeruginosa* to induce an oxidative stress response, Orlandi *et al.* (2015) investigated the function of *Pseudomonad* pigments in their resistance to PDI. Their experiments showed that PDI was more efficient against non-pigment-producing cells than the ones protected by pigments, even when they were present in small amounts. According to this work, the pigments that may contribute to cell protection against PDI are pyomelanin and phenazine. The redox activity of these two pigments was also demonstrated by Reszka *et al.* (2006) and Mai-Prochnow *et al.*, (2015).

The biosynthesis of each pigment is directly influenced by the genetics of the bacterium and by its physiological and environmental state, which depends on the composition of the growth medium, the inoculum size, temperature, aeration rate, agitation speed and incubation time (Barbhaiya and Rao, 1985; El-Fouly *et al.*, 2015; Orlandi *et al.*, 2015; Wei and Aristilde, 2015).

In order to evaluate the ability of the *Pseudomonas* strains investigated in this study to produce pigments and whether or not their production was interfering with the photodynamic activation, they were cultivated in a range of growth media The only pigments produced by P. *putida* CP1 and *P. putida* DSM 6125, were pyocianin and pyoverdine, when they were grown in King A and King B media, respectively.. *P. fluorescens* DSM 50090 produced pyoverdine when grown in LB medium, M9 and King B, and pyocianin when grown in King A. *P. aeruginosa* PAO1 was the bacterium that produced the largest variety of pigments. When grown in LB it produced phenazine; in M9 it produced phenazine and pyoverdine; in King A, it produced pyocyanin and phenazine; and in King B it produced pyoverdine.

While the ability of the Pseudomonas species to produce pigments was confirmed, none produced pigments of any significance when grown in nutrient broth. The absence of pigments in the system used for the PDI investigations negated their role in the resistance of the strains to PDI.

The role of cell aggregation

Aggregation is a strategy used by some bacteria for increased protection from environmental stress (O'Toole *et al.*, 2000; Farrell and Quilty, 2002; Sanin *et al.,* 2003; Visaggio *et al.,* 2015). This protection is associated with the presence of a matrix formed by extracellular polymeric substances, which encloses the bacterial cells (Mah and O'Toole, 2001). In PDI studies with biofilms, this matrix was shown to be able to diminish the photosensitiser diffusion and hence its association with bacterial cells (Usacheva *et al.*, 2016).

In their natural environments, bacteria quite often do not occur as freely suspended cells (planktonic) but in cell aggregates that are either freely floating or attached to surfaces as biofilms (Singh *et al.*, 2000; Stoodley *et al.* 2002). Among the bacteria that are able to form aggregates, we can highlight some *Pseudomonas*, which have been studied by several research groups (Farrell and Quilty, 2002; Sanin *et al.,* 2003; Panicker *et al.*, 2006; Klebensberger *et al.*, 2006). As aggregates, bacteria have a better metabolic function, they communicate more efficiently, and they are more resistant to biocide compounds than their planktonic forms (Bossier and Verstraete, 1996; Eboigbodin *et al.,* 2005).

Based on this observation, a closer look into the bacterial cells behaviour through optical density and confocal microscopy was taken. Using optical density measurements, the

bacterial cell aggregation was expressed in percentage of optical density reduction, which happened over time (60 minutes) due to the settling of the cells. It was possible to observe that while *P. putida* CP1 and *P. putida* DSM 6215 behaved very similarly to *E. coli* (bacteria used as a control), *P. fluorescens* and *P. aeruginosa* presented a significantly higher reduction in the optical density of their suspensions, indicating their aggregation.

When the cells where then analysed by confocal microscopy, it was clear that the two *P. putida* strains were treated in the PDI experiments, in their planktonic forms, while *P. fluorescens* and *P. aeruginosa* formed aggregates when grown in nutrient broth and were treated in that form in the PDI experiments.

The resistance of bacteria in aggregates has so far been addressed mainly with regard to antibiotics and disinfectants. However, here it is clearly playing an important role in the bacterial defence against treatment with PDI. While the extracellular polymeric matrix involved in aggregate formation can create a shield against the photosensitiser, it has been shown that a depletion in the levels of oxygen, and possibly other nutrients, occurs when *P. aeruginosa* grows in aggregates. While this depletion does not interfere in their growth rate, even at considerable high cell densities (~10^{12} ml^{-1}) (Wessel *et al.*, 2014), it can possibly interfere in the photodynamic process efficiency, since the presence of molecular oxygen is of utmost importance for the formation of the reactive oxygen species.

In addition, it is important to point out the connection between cell aggregation and pigment production. Studies have shown that the Gac singling system and the cyclic diguanylate (c-di-GMP) messenger, responsible for controlling the switch between planktonic and biofilm cell growth forms, are also responsible for the production of the pigment pyoverdine (Frangipani *et al.*, 2014; Visaggio *et al.*, 2015). Visaggio's group research enhanced the hypothesis that cell aggregation is a key trigger for pyoverdine production as well as pyoverdine-controlled virulence factors in *P. aeruginosa*.

In their latest study, Orlandi *et al.* (2017) investigated the genetic features involved in the resistance of *P. aeruginosa* to PDI. They suggested that its tolerance has a multifactorial basis, which includes the pseudomonas quinolone signalling and cytoplasmic membrane transportation. A brief mention was made to the resistance presented by one of the mutants studied, which formed aggregates.

Antibiotic profile

The use of antibiotics to treat disease started in 1928, with the discovery of penicillin. Since then, many others antibiotic agents have been discovered and are now produced in large scale around the world (Nikaido, 2009). However, the widespread and many times uncontrolled, application and discharge of antibiotics has led to the development of antibiotic-resistant bacteria (ARB) and antibiotic-resistance genes (ARGs). A famous example is the methicillin-resistant *Staphylococcus aureus* (MRSA) (Zhang *et al.*, 2009; Bouki *et al.*, 2013; Stange *et al* 2016).

The genes encoding for antibiotic resistance are not only found in hospitals but also in different environmental areas around the world, like surface water (Zhang *et al.*, 2015; Stoll *et al.*, 2012), groundwater (Li *et al.*,2014), drinking water (Schwartz *et al.*, 2003; Guo *et al.*, 2014) and sediments (Rosas *et al.*, 2015). For this reason, the World Health Organization has reported a global strategy to address and control antimicrobial resistance (WHO, 2014).

Resistance in bacteria occurs by random DNA mutation or by horizontal or vertical gene transfer. These genes are normally located on mobile elements, like plasmids, integrons or transposons. The main mechanism for spreading the resistance is horizontal gene transfer, which can occur among different strains or bacterial species (Frost *et al.*, 2005) and beyond the habitat of original hosts (Moore and Lindsay, 2001, Nikaido, 2009)

Antimicrobial susceptibility tests are used to determine which specific antibiotics a particular microorganism is sensitive to, and they can guide a physician in drug choice and dosage for difficult-to-treat infections. Among them we can find disc diffusion tests, like the one described by Bauer *et al.* (1966) or broth dilution tests, as described by Ericsson and Sherris (1971).

For the disc diffusion test the results are normally interpreted by comparing the diameter of the zone with standards, and its size is related to the susceptibility of the isolate to the drug tested (Jorgensen and Ferraro, 2009). For the broth dilution tests results are commonly reported as the minimal inhibitory concentration (MIC), which is the lowest concentration of drug that inhibits the growth of the organism. Reports typically contain a quantitative result in µg/mL and a qualitative interpretation. The interpretation usually categorizes each result as susceptible (S), intermediate (I), resistant (R), sensitive-dose dependent (SD), or no interpretation (NI). A high value means that more drug is needed to affect the organism's function or replication. A low value means that less drug is needed to affect the organism's function or replication (Levinson, 2010).

When analysing the results obtained by the Kirby-Bauer disk diffusion method (see Table 3.8), the response to three of the chosen antibiotics can be highlighted, ampicillin, erythromycin and vancomycin. While the majority of the bacteria showed resistance to vancomycin, an interesting pattern of resistance among the *Pseudomonas* strains was observed for the other two antibiotics, with the resistance to ampicillin being confirmed by the MIC results (see Table 3.9).

While *E. aerogenes* is known for its resistance to antibiotics, in particular β-lactams, like ampicillin and vancomycin, the *Pseudomonas* response was rather interesting. Ampicillin is a semi-synthetic β- lactam antibiotic that deactivates bacteria by interrupting its cell wall syntheses and inducing cell lyses. It reacts with the bacteria by binding to and inactivating penicillin-binding proteins (PBP) which are located on the inner membrane of the bacterial cell wall, interfering with the cross-linkage of peptidoglycan chains responsible for the bacterial cell wall strength and rigidity (Zeng and Lin, 2013).

Lambert (2002) has pointed out that the intrinsic resistance of *P. aeruginosa* to all classes of antibiotics can be attributed mainly to the low permeability of its cell wall in combination with its ability of removing the antibiotic molecules by the action of efflux pumps. In addition to that, Molina *et al.* (2014) has also shown that *P. putida* strains were also shown to be resistant to ß-lactams, cationic peptides. It is well known that for a more effective photodynamic inactivation process, the photosensitiser has to bind and penetrate the bacterial membrane, in order to generate the reactive oxygen species closer to the vital cell components (Hamblin and Hasan, 2004). Therefore, we can assume that the low permeability of the *Pseudomonas* cells will also interfere with the PDI efficacy.

Vancomycin is another antibiotic from the β-lactam family, which acts on metabolism and growth. This antibiotic was largely used as an alternative for the treatment of multidrug resistant strains, however, resistance to this antibiotic, especially by *Enterococci* is well known and was documented by different authors (Cetinkaya *et al.*, 2000; Boneca and Chiosis, 2003).

Erythromycin is an antibiotic member of the macrolide group. It deactivates bacteria by inhibiting its protein synthesis by restricting the ribosome function (Wolfe and Hahn, 1964; Lovmar *et al.*, 2004). According to Villedieu *et al.* (2004) this antibiotic is mainly used to treat infections caused by Gram-positive bacteria and resistance to it has been reported after an increase in its use.

Bacteria that are resistant to the treatment with this antibiotic, for example streptococci, have an efflux-mediated mechanism of defence, as reported by Varaldo *et al.* (2009). Even though P. aeruginosa biolfilms have been shown to be resistant to erythromycin treatment, in a work performed by Chua *et al.* (2016), no direct connection can be made between the resistance profile found for this antibiotic and the *Pseudomonas* low susceptibility to PDI.

Similarly, the other antibiotic used for the MIC susceptibility test, tetracycline, also acts by inhibiting protein synthesis in bacteria by restricting the association of aminoacyl t-RNA with the ribosome. For that reason, these molecules have to cross one or more membrane systems (Gram-positive or Gram-negative) in order to interact with their targets (Chopra and Roberts, 2001). All the bacteria showed susceptibility to this antibiotic.

Other researchers have also connected the low susceptibility of some bacteria to PDI to its mechanisms of defence against antibiotics. In their work, Tegos and Hamblin (2006) have shown that some of the phenothiazinium photosensitisers are substrates of multidrug resistant pumps (MDRs), which are membrane-localized proteins that pump drugs out of cells. By using MDR-deficient mutants of *S. aureus* (NorA), *E. coli* (TolC) and *P. aeruginosa* (MexAB) they observed 2 to 4 logs more killing than seen with wild-type strains. In furthers studies, Tegos *et al.* (2008) have then demonstrated that antimicrobial PDI effect can be enhanced by using a combination of the photosensitiser with an efflux pump inhibitor (EPI).

4.4 Factors influencing the practical application of PDI

The response of mixed cultures

Bacteria grow in nature as mixed cultures and so it was of interest to explore the response of mixed cultures of bacteria to PDI. To better understand and control the system, it was decided to study a co-culture of two bacteria. *E. coli* which is the most widely studied bacterium in PDI investigations was chosen. It was decided to co-culture *E. coli* with a *Pseudomonas* species due to their widespread presence in nature. To challenge the system further, one of the most resistant strains P. aeruginosa was selected.

Previous work has already investigated the response of mixed cultures to PDI, but mainly applied to the disinfection of endodontic pathogens, which normally are found as mixed cultures (mixed bacterial plaque (Bergmans *et al.*, 2008; Stojicic *et al.*, 2013).

Bergmans *et al.* (2008) investigated the bactericidal effect of PDI on strains of *S. anginosus*, *E. faecalis* and a mixed culture of *E. faecalis* and *F. nucleatum,* which were inoculated in extracted teeth root canals. They found that when the bacteria appeared as individual cells they were more susceptible to PDI than when arranged in a biofilm.

Stojicic *et al.* (2013) compared the *in vitro* efficacy of conventional PDI, using the photosensitiser methylene blue, with a modified one, where methylene blue was combined with hydrogen peroxide, or ethylenediaminetetraacetic acid, or chlorhexidine, for the deactivation of *E. faecalis* and mixed bacterial plaque in suspensions and biofilms. The authors concluded that the mixed planktonic bacteria and biofilms modified where resistant to the conventional PDI when compared to the modified one.

In order to mimic the wastewater microflora, Orlandi *et al.* (2013) investigated PDI efficacy in a mixed culture of *E. coli* and *E. faecalis* with two dicationic 5,15-diarylporphyrins irradiated by artificial and solar light. 5,15-di(N-benzyl-4-pyridyl)porphyrin showed to be effective in deactivating the pure and the mixed cultures, with no significant difference in the response between then. Both were treated with the same porphyrin concentration (5μM) and the same amount of time (75 minutes – light dose 216 J/cm^2).

A clear increase in the irradiation time (light dose) necessary to deactivate *E. coli* was observed when the bacterium was grown as a co-culture when compared to when the organism was treated as a pure culture. It was interesting to observe the difference in response when the cocultures were first grown together or when grown separately and then combined.

In both cases, the presence of the *Pseudomonas* cells is believed to have shielded the *E. coli cells* against the photodynamic oxidative stress, either by forming aggregates with them when grown together, or by reducing the amount of porphyrin that binds to them, when grown separately.

A similar pattern was observed when the antimicrobial agent used was an antibiotic. The MIC of the mixed cultures for ampicillin showed that when grown together, the cocultures required double the ampicillin concentration for their growth inhibition. And *E. coli,* when cultivated associated with *Pseudomonas*, had its inhibitory concentration increased to a value at least three times higher than when in pure culture. The findings demonstrate the importance of considering the behaviour of mixed microbial communities when designing antimicrobial treatment systems for practical application.

4.5 Immobilisation of the porphyrin

Most antimicrobial photodynamic inactivation studies to date have been carried out with the photosensitisers dissolved in an aqueous medium. In the case of water disinfection, the attachment of the reactive oxygen species (ROS) to an insoluble material would avoid the necessity of recovering the dissolved photosensitiser from the treated water.

Some research groups already investigated the use of immobilised photosensitisers in PDI for water disinfection purposes. Materials like nylon fibres (Bozja, 2003), chitosan (Bonnett *et al.*, 2006), silica (Magaraggia *et al.*,2013) and polystyrene (Nakonechny *et al.*,2013) have already being used.

According to Jimenez-Hernandez *et al.*, (2006), the material used to immobilise the photosensitiser must include the following characteristics: compatibility with the photosensitiser, allowing easy and reproducible immobilisation procedures and avoiding leaching out to water; mechanical strength and stability towards sunlight; good oxygen permeability for efficient reactive oxygen species production and diffusion; high biocompatibility to maximise the interaction between the polymer and the microorganisms; easy commercial availability; and low cost. For these reasons, the immobilisation of TMPyP both to glass beads and to a hydrogel was explored.

When immobilised to the glass beads, the porphyrin was shown to be effective in deactivating the bacteria *E. coli* T37-1 and *P. fluorescens* DSM 50090, with the time required for the inactivation of each of them being increased only by 15 minutes, when compared to the porphyrin free in solution. However, as the porphyrin leached from the beads, its presence in the solutions throughout the experiment was also responsible for inactivating the bacteria.

In order to avoid the porphyrin leaching into the media, a polymer was used for its immobilisation. The polymer chosen was a hydrogel composed of a mixture of two monomers HEMA (2-hydroxyethyl methacrylate) and MAA (methacrylic acid), as described in section 2.2.7. As explained by Brady *et al.* (2007), the MAA monomer provides pendant anionic groups, which creates strong electrostatic interactions with the cationic porphyrin TMPyP, avoiding it leaching into the medium.

The PDI results for the photoinactivation using the polymer-porphyrin matrix were satisfactory, with a 5-log reduction in the number of both bacterial cells being achieved. The different porphyrin concentrations used did not show significant difference in the inactivation rate for *E. coli*, while the concentration of 3.65μM was not effective in inactivating *P. fluorescens* completely.

When comparing the two different systems, suspension and inert, a considerable increase in the light dose was required in order to achieved a 5-log reduction in the number of bacterial cells. For the lowest concentrations of TMPyP, 3.65 and 5 μM, *E.* coli had to be exposed to the light irradiation for additional 120 minutes (157.88 J/cm^2). While for the highest concentration, 10 μM, additional 90 minutes (118.42 J/cm^2) were required to deactivate all the bacteria from the solution. For *P. fluorescens* complete inactivation, the 5 μM concentration, required more 105 minutes (138.1 J/cm^2) of light exposure were and for 10 μM, the time of irradiation had to be 2.5 times longer (90 minutes - 118.42 J/cm^2).

Due to the short lifetime of singlet oxygen, ~10^{-5} second, there is a limited distance, between the initial excitation event and the cytotoxic damage (Brady *et al.*, 2007). This can probably explain the reason the lag (therefore the higher light dose required) that was observed for the bacterial response, since the bacteria probably had to be very close or in contact with the polymeric surface in order to be inactivated. As pointed out by Bayramoglu *et al.* (2013), hydrogels are polymers that have the ability of absorbing water hence gas diffusion, so it is expected that contact between the reactive oxygen species generated by the porphyrin and the bacterial cells will be facilitated in this system.

5. Conclusions and Future Work

Main conclusions

A successful experimental system was designed. The optimal system comprised the porphyrin, TMPyP at a concentration of 5μM, a dichromatic LED lamp (430 and 660nm), glass petri dishes (60 x 15mm) and PBS as the suspending medium. The Gram positive and Gram-negative bacteria (10^5 CFU/ml) investigated were effectively deactivated in the order: vegetative Gram-positive cells > Gram-negative cells > spore forming bacterium.

Interestingly, in the case of the Gram-negative bacteria members of the family *Enterobacteriaceae* were generally more vulnerable to the treatment than the *Pseudomonads. P. fluorescens* and *P. aeruginosa* were the most resistant among the group studied. This resistance towards PDI observed for *Pseudomonads* is attributed to aggregation, which was verified using confocal microscopy. Typically, work investigating the use of PDI for antimicrobial inactivation has been done with pure bacterial cultures. However, in the environment, bacteria are normally found mixed as cocultures and in an attempt to mimic environmental conditions, a coculture comprised of *E. coli* (non-aggregating) and an aggregating culture of *Pseudomonas* was investigated. The responses obtained indicated increased resistance of the bacteria to PDI and also towards antibiotics when grown as cocultures. This increased resistance was attributed to co-aggregation of the cultures and the protective effect of the EPS matrix.

For the practical application of PDI as a polishing step for drinking water disinfection the photosensitiser cannot be used free in solution, and it is therefore necessary to devise a solid support containing the active photosensitiser. To address this issue, the porphyrin was successfully immobilised within a hydrogel. When this hydrogel containing the porphyrin was subsequently assessed for photodynamic inactivation, it showed a good response against the bacteria tested, which indicates the potential of this approach for water disinfection.

Recommendations for future work

The study has highlighted a number of interesting areas for further research:
- Scale-up of the experimental system;
- Studies on additional bacteria to include;

- An investigation of the interaction between the porphyrin and the cell using super-resolution microscopy, as this technique can identify the location of the porphyrin in the cell;

- Further investigations on the response of cocultures.

6. References

Abeledo-Lameiro, M.J., Reboredo-Fernández, A., Polo-López, M.I., Fernández-Ibáñez, P., Ares-Mazás, E., Gómez-Couso, H., (2017) 'Photocatalytic inactivation of the waterborne protozoan parasite Cryptosporidium parvum using TiO2/H2O2 under simulated and natural solar conditions'. *Catalysis Today*, 280, pp.132–138.

Abrahamse, H., Hamblin M.R. (2016) 'New photosensitizers for photodynamic therapy', *Biochemical Journal,* 15;473(4), pp. 347-64.

Acher, A. J., Juven, B. J., (1977) 'Destruction of Coliforms in Water and Sewage Water by Dye-Sensitized Photooxidation', A*pplied and Environmental Microbiology*, 33(5), pp. 1019-1022.

Acher, A. J., Rosenthal, J. (1977) 'Dye-sensitized-photo-oxidation--a new approach to the treatment of organic matter in sewage effluents', *Water Research,* 11, pp. 557-552.

Acher, A., Fischer, E., Tornheim, R., Manor, Y. (1997) 'Sunlight technologies for the photochemical deactivation of organic pollutants in water', in: Becker, M., Bohmer, M. (Eds.), *Solar Thermal Concentrating Technologies*. Muller, Heidelberg, pp. 1403–1413.

Acra, A.; Raffoul, Z.; Karahagopian, Y., (1984) 'Solar Disinfection of Drinking Water and Oral Rehydration Solutions - *Guidelines for Household Application in Developing Countries*. UNICEF, American University of Beirut.

Agostinis, P., K. Berg, K. A. Cengel, T. H. Foster, A. W. Girotti, S. O. Gollnick, S. M. Hahn, M. R. Hamblin, A. Juzeniene, D. Kessel, M. Korbelik, J. Moan, P. Mroz, D. Nowis, J. Piette, B. C. Wilson and J. Golab (2011) 'Photodynamic therapy of cancer: An update'. *CA: A Cancer Journal for Clinicians*, 61, 250–281.

Almeida, A., Cunha, A., Gomes, N. C. M., Alves, E., Costa, L.; Faustino, M. A. F. (2009) 'Phage therapy and photodynamic therapy: low environmental impact approaches to inactivate microorganisms in fish farming plants', *Marine Drugs*, 7(3), pp.268-313.

Alouini. Z and Jemli, M. (2001) 'Porphyrin photodisinfection of secondary waste water, *Journal of Environmental Monitoring*, 41, 429–435.

Alvarez, M.G.; Montes de Oca, M.N.; Milanesio, M.E.; Ortiz, C.S.; Durantini, N. (2014) 'Photodynamic properties and photoinactivation of *Candida albicans* mediated by brominated derivatives of triarylmethane and phenothiazinium dyes'. *Photodiagnosis and Photodynamic Therapy*, 11(2) pp. 148-155.

Alves E., Carvalho C. M. B., Tomé J. P. C., Faustino M. A. F., Neves M. G. P. M. S., Tomé A. C., Neves M. G. P. M. S., Cunha A. (2008) 'Photodynamic inactivation of

recombinant bioluminescent *Escherichia coli* by cationic porphyrins under artificial and solar irradiation'. *Journal of Industrial Microbiology &. Biotechnology,* 35, pp.1447–1454.

Alves, A., Costa, L., Carvalho, C. M., Tomé, J. P., Faustino, M. A., Neves, M. G., Tomé, A. C., Cavaleiro, J. A., Cunha, Â., Almeida, A. (2009) 'Charge effect on the photoinactivation of Gram-negative and Gram-positive bacteria by cationic meso-substituted porphyrins', *BMC Microbiology*, 9, 70.

Alves, E.; Faustino, M.A.F.;Tome, J.P.C.; Neves, M.G.P.M.S.; Tome, A.C. (2011) 'Photodynamic Antimicrobial Chemotherapy in Aquaculture: Photoinactivation Studies of *Vibrio fischeri*', *PLoS ONE,* 6(6). doi:10.1371/journal.pone.0020970.

Alves. E.; Faustino, M.A.F.; Tome, J.P.C.;Neves, M. G. P. M. S.; Tome, A.C.; Cavaleiro, J.A.S.; Cunha, A.; Gomes, N.C.M.;Almeida, A. (2013) 'Nucleic acid changes during photodynamic inactivation of bacteria by cationic porphyrins', *Bioorganic & Medicinal Chemistry*, (21), pp. 4311–4318.

Alves, E., Faustino, M. A. F., Neves, M. G. P. M. S., Cunha, A., Tomé, J. P. C., Almeida, A. (2014) 'An insight on bacterial cellular targets of photodynamic inactivation'. *Future Medicinal Chemistry,* 6 141–164.

Alves, E., Faustino, M. A. F., Neves, M. G. P. M. S., Cunha, A., Nadais, H., Almeida, A. (2015) 'Potential applications of porphyrins in photodynamic inactivation beyond the medical scope'. *Journal of Photochemistry and Photobiology: C Photochemistry,* 22, pp. 34–57.

Ames, B.N., Durston, W.E., Yamasaki, E., Lee, F.D. (1973) 'Carcinogens are mutagens: a simple test system combining liver homogenates for activation and bacteria for detection', *Proceedings of the National Academy of Sciences*, 7, pp.2281–2285.

Amor, B. T., Tronchin, M., Bortolotto, L., Verdiglione, R., Jori, G. (1998) 'Porphyrins and related compounds as photoactivatable insecticides phototoxic activity of hematoporphyrin towards *Ceratitis capitata* and C*actrocera oleae', Photochemistry and Photobiology,* 67(2), pp. 206-211.

Andrews, J. M. (2001), 'Determination of minimum inhibitory concentrations', *Journal of Antimicrobial Chemotherapy,* 48 (1), pp. 5-16.

Ansel, H. C.; Norred, P. W.; Roth, I. L. (1969) 'Antimicrobial Activity of Dimethyl Sulfoxide Against *Escherichia coli*, *Pseudomonas aeruginosa*, and *Bacillus megaterium', Journal of Pharmaceutical Sciences*, 58(7), pp. 836-839.

Anzai, Y., Kim, H., Park, J.-Y., Wakabayashi, H., Oyazu, H., 2000 'Phylogenetic affiliation of the pseudomonads based on 16S rRNA sequences', *International Journal of Systematic and Evolutionary Microbiology,* 50, pp. 1563–1589.

Arenas, Y.; Monro, S.; Shi, G.; Mandel, A.; McFarland, S.; Lilge, L. (2013) 'Photodynamic inactivation of*Staphylococcus aureus* andmethicillin-resistant *Staphylococcus aureus*with Ru(II)-based type I/type II photosensitizers'. *Photodiagnosis and Photodynamic Therapy*, 10, 615—625

Artarsky, S., Dimitrova, S., Bonnett, R., Krysteva, M. (2006) 'Immobilization of Zinc Phthalocyanines in Silicate Matrices and Investigation of Their Photobactericidal Effect on *E. coli', The Scientific World Journal,* 6, pp. 374–382.

Baldursson, S.; Karanis, P. (2011) 'Waterborne transmission of protozoan parasites: reviewofworldwide outbreaks—an update 2004–2010', *Water Research*, 45(20), pp.6603–6614.

Banfi, S.; Caruso, E.; Buccafurni, L.; Battini, V.; Zazzaron,S.; Barbieri, P.; Orlandi, V. (2006) 'Antibacterial activity of tetraaryl-porphyrin *photosensitiser*s: An in vitro study on Gram-negative and Gram-positive bacteria', *Journal of Photochemistry and Photobiology B: Biology*,85, pp. 28–38.

Barbhaiya, H.B., Rao, K. K. (1985) 'Production of pyoverdine, the fluorescent pigment of *Pseudomonas aeruginosa* PAO1', *FEMS Microbiology Letters,* 27(2), pp. 233-235.

Barker-Reid, F., Fox Ellen, M. & Faggian, R. (2010) 'Occurrence of antibiotic resistance genes in reclaimed water and river water in the Werribee Basin, Australia', *Journal of Water and Health*, 8, pp. 521–531.

Batalha, P. N., Gomes, A. T. P. C., Forezi, L. S. M., Costa, L., de Souza, M. C. B. V., Boechat, F. C. S., Ferreira, V. F., Almeida, A., Faustino, M. A. F., Neves, M. G. P. M. S., Cavaleiro, J. A. S. (2015) 'Synthesis of new porphyrin/4-quinolone conjugates and evaluation of their efficiency in the photoinactivation of *Staphylococcus aureus', RSC Adances*, 5, pp. 71228–71239.

Bauer AW, Kirby WMM, Sherris JC, Turk M. (1966) 'Antibiotic susceptibility testing by a standardized single disk method'. *American Journal of Clinical Pathology,* 45: 493–6.

Bayramoglu, A., Kucuk, Urhan, M., Ercan, S., Abacı, O., Guler, H.I., Kucukkaya, Y., Korkmaz, M.C. (2013) 'Hypertension and matrix metalloproteinase-9 enzyme activity', *Journal of Selçuk University Natural and Applied Science,* 3, pp. 60–68.

Bergmans L, Moisiadis P, Huybrechts B, Van Meerbeek B, Quirynen M, Lambrechts P. (2008) 'Effect of photo-activated disinfection on endodontic pathogens *ex vivo'*. *International Endodontic Journal,* 41, pp. 227–39.

Berney M., Weilenmann, H.U., Simonetti, A., Egli, T. (2006) 'Efficacy of solar disinfection of *Escherichia coli, Shigella flexneri, Salmonella Typhimurium and Vibrio cholera', Journal of Applied Microbiology*, 101(4), pp.828-836.

Bertoloni, G.; Rossi, F.; Valduga, G.; Jori, G.; van Lier, J. (1990) 'Photosensitizing activity of water- and lipid-soluble phthalocyanines on *Escherichia coli'*, *FEMS Microbiology Letters,* 71 (1–2), pp. 149–156.

Bhatti, M., MacRobert, A., Meghji, S., Henderson, B. &Wilson, M. (1997) 'Effect of dosimetric and physiological factors on the lethal photosensitization of *Porphyromonas gingivalis* in vitro'. *Photochemistry and Photobiology*, 65, pp.1026–1031.

Bogucka, K., Wojtczak, L. (1966) 'Effect of sodium azide on oxidation and phosphorylation processes in rat-liver mitochondria', *Biochimica et Biophysica Acta*, 122 (3), pp. 81–392.

Boneca I.G., Chiosis, G. (2003) 'Vancomycin resistance: occurrence, mechanisms and strategies to combat it', *Expert Opinion on Therapeutic Targets,* 7, pp. 311–328.

Bonnett, R., Krysteva, A.M., Lalov, I.G., Artarsky, S.V. (2006) 'Water disinfection using photosensitisers immobilized on chitosan', *Water Research*, 40, pp.1269 – 1275.

Bosshard, T., Kotlarski, S., Ewen, T., Schär, C. (2010) 'Spectral representation of the annual cycle in the climate change signal', *Hydrology and Earth System Sciences*, 15, pp. 2777–2788.

Bossier, P., Verstraete, W. (1996) 'Triggers for microbial aggregation in activated sludge?', *Applied Microbiology and Biotechnology,* 45, pp. 1-6.

Bouki, C., Venieri, D., Diamadopoulos, E. (2013) 'Detection and fate of antibiotic resistant bacteria in wastewater treatment plants: a review', *Ecotoxicology and Environmental Safety,* 91, pp. 1-9.

Boye. E., and Moan, J. (1980) 'The photodynamic effect of hematoporphyrin on DNA'. *Photochemistry and Photobiology,* 3, pp. 223-228.

Bozja, J., Sherrill, J., Michielsen, S. and Stojiljkovic, I. (2003) 'Porphyrin-based, light activated antimicrobial materials', *Journal of Polymer Science: Part A Polymer Chemistry*, 41, pp. 2297-2303.

Brady, C., Bell, S. E. J, Parsons, C., Gorman, S. P., Jones, D. S., McCoy, C. P. (2007) 'Novel Porphyrin-Incorporated Hydrogels for Photoactive Intraocular Lens Biomaterials', *The Journal of Physical Chemistry B***,** 111, pp. 527-534.

Braud, A., Je´ze´quel, K., Bazot, S., Lebeau, T., (2009) 'Enhanced phytoextraction of an agricultural Cr-, Hg- and Pb-contaminated soil by bioaugmentation with siderophoreproducing bacteria', *Chemosphere*, 74, pp. 280–286.

Braun, B., Ortner, J., Funken, K.-H., Scha¨ fer, M., Schmitz, C., Horneck, G., Fasdni, M. (1997) 'Dye-sensitized detoxification and disinfection of contaminated water'. In: Becker, M., Bohmer, M. (Eds.), *Solar Thermal Concentrating Technologies*. Muller, Heidelberg, pp. 1391–1413.

Bronshtein I, Afri M, Weitman H, Frimer AA, Smith KM, Ehrenberg B. (2004) 'Porphyrin depth in lipid bilayers as determined by iodide and parallax fluorescence quenching methods and its effect on photosensitizing efficiency'. *Biophysics Journal,* 87(2), pp. 1155–1164

Buchovec, I., Vaitonis, Z. , Luksiene, Z. (2009) 'Novel approach to control *Salmonella enterica* by modern biophotonic technology: photosen-sitization', *Journal of Applied Microbiology,* 106, pp. 748, http://dx.doi.org/10.1111/j.1365-2672.2008.03993.x.

Buchovec, I., Paskeviciute, E., Luksiene, Z. (2010) 'Photosensitization-based inactivation of food pathogen Listeria monocytogenes in vitro and on the surface of packaging material', *Journal of Photochemistry and Photobiology B: Biology*, 99, pp. 9–14.

Caminos, D. A., Spesia, M. B., Pons, P, Durantini, E. N. (2008), 'Mechanisms of *Escherichia coli* photodynamic inactivation by an amphiphilic tricationic porphyrin and 5,10,15,20-tetra(4-*N,N,N*trimethylammoniumphenyl) porphyrin'. *Photochemical and Photobiological Sciences,* 7, pp. 1071–1078.

Caminos, D. A., Spesia, M. B., Durantini, E. N. (2006) 'Photodynamic inactivation of *Escherichia coli* by novel *meso*-substituted porphyrins by 4-(3-*N*,*N*,*N* trimethylammoniumpropoxy)phenyl and 4-(trifluoromethyl)phenyl groups', *Photochemical and Photobiological Sciences*, *5*, pp. 56–65.

Carvalho C. M. B., Alves E., Costa L., Tomé J. P. C., Faustino M. A. F., Neves M. G. P. M. S., et al. (2010) 'Functional cationic nanomagnet – porphyrin hybrids for the photoinactivation of microorganisms'. *ACS Nano*, 4, pp. 7133–7140.

Carvalho, C. M. B., Gomes, A. T. P. C., Fernandes, S. C. D., Prata, A. C. B., Almeida, M. A., Cunha, M. A., Tome, J. P. C., Faustino, M. A. F., Neves, M. G. P. M. S., Tome, A. C., Cavaleiro, J. A. S., Lin, Z., Rainho, J. P., Rocha, J. J. (2007) 'Photoinactivation of bacteria in wastewater by porphyrins: Bacterial b-galactosidase activity and leucine-uptake as methods to monitor the process', *Journal of Photochemistry and Photobiology B: Biology*, 88 (2-3), pp.112-118.

Casteel, M.J.;,Jayaraj, K., Gold, A., Ball, L.M., Sobsey, M.D. (2004) 'Photoinactivation of Hepatitis A Virus by Synthetic Porphyrins', *Photochemistry and Photobiology*, 80: pp. 294-300.

Cetinkaya, I; Flak, P; Mayhall, C. G. (2000) 'Vancomycin resistant enterococci'. *Clinical Microbiology Reviews,* 13, pp. 686-707.

Cevrvia, J.S., Ortolano, G. A.; Canonica, F. P. (2008) 'Hospital tap water: A reservoir of risk from health care-associated infection', *Infectious Diseases in Clinical Practice*, 16, pp. 349-353.

Cézard, C., Farvacques, N., Sonnet, P. (2015) 'Chemistry and Biology of Pyoverdines, *Pseudomonas* Primary Siderophores', *Current Medicinal Chemistry*, 22, pp.165-186.

Chong, M.N., Jin, B., Chow, C.W.K., Saint, C. (2010) 'Recent developments in photocatalytic water treatment technology: a review'. *Water Research*, 44 (10), pp. 2997-3027.

Cossu, R., Lai, T., Sandon, A. (2012), 'Standardization of BOD5/COD ratio as a biological stability for MSW', *Waste Management*, 32 (8), pp. 150-158.

Chopra, I., Roberts, M. (2001), 'Tetracycline antibiotics: mode of action, applications, molecular biology, and epidemiology of bacterial resistance', *Microbiology and Molecular Biology Reviews.*, 65(2), pp. 232-260.

Collins, T.L., Markus, E.A., Hassett, D.J., Robinson, J.B. (2010) 'The effect of a cationic porphyrin on *Pseudomonas aeruginosa* biofilms. *Current Microbiology,* 61(5), pp. 411–416.

Cordeiro, R.M., Miotto, R., Baptista, M.S. (2012) 'Photodynamic efficiency of cationic meso-porphyrins at lipid bilayers: insights from molecular dynamics simulations'.*The Journal of Physical Chemistry B,* 116(50), pp. 14618–14627.

Costa, L., Tomé, J. P., Neves, M. G., Tomé, A. C., Cavaleiro, J. A., Faustino, M. A., Cunha, A., Gomez, N. C. M. & Almeida, A. (2011) 'Evaluation of resistance development

and viability recovery by a non-enveloped virus after repeated cycles of aPDT'. *Antiviral Research,* 91, pp. 278–282.

Cronan J. E. (2003) 'Bacterial membrane phospholipids: where do we stand?' *Annual Review of Microbiology,* 57(1), pp. 203–224.

Dahl, T.A., Middenand, W.R., Hartman, P.E. (1987) 'Pure singlet oxygen citotoxicity for bacteria, *Photochemistry and Photobiology,* 46, pp. 345–352 doi: 10.1111/j.1751-1097.1987.tb04779.x

Dai, T., Huang, Y., Hamblin, M. R. (2009) 'Photodynamic therapy for localized infections – state of the art', *Photodiagnosis Photodynamic Therapy*, 6(3-4), pp.170–188.

Dastgheyb, S.S., Eckmann, D.M., Composto, R.J., Hickok, N.J. (2013) 'Photo-activated porphyrin in combination with antibiotics: Therapies against Staphylococci', *Journal of Photochemistry and Photobiology B: Biology*, 129, pp. 27–35.

Davies, D. (2003), 'Understanding biofilm resistance to antibacterial agents', *Nature Reviews Drug Discov*ery, 2(2), pp.114-122.

Davison, A. (2005). Water safety plan (WHO).

Demidova, T.; Hamblin, M. (2005) 'Effects of cell-*photosensitiser* binding and cell density on microbial photoinactivation', *Antimicrobial Agents* and *Chemotherapy,* 6(49), pp. 2329–2335.

DeRosa, M. C., Crutchley, R.J. (2002) 'Photosensitized singlet oxygen and its applications', *Coordination Chemistry Reviews,* 233—234, pp. 351—71.

diPoto, A., Sbarra, M.S., Provenza, G., Visai, L., Speziale, P. (2009) 'The effect of photodynamic treatment combined with antibiotic action or host defence mechanisms on *Staphylococcus aureus* biofilms'. *Biomaterials,* 30(18), pp. 3158–3166.

Domingues, M. M., Castanho, M.A., Santos, N.C. (2009) 'rBPI21 promotes lipopolysaccharide aggregation and exerts its antimicrobial effects by (hemi) fusion of PG-containing membranes'. *PLoS ONE,* 4(12), pp. 83-85.

Dondji, B., Duchon, S. , Diabate, A. , Herve, J.P. , Corbel , Hougard, V. J.M. , Santus, R. , Schrevel, J. (2005) 'Assessment of laboratory and field assays of sunlight-inducedkilling of mosquito larvae by photosensitizers', *Journal of Medical Entomolpgy,* 42, pp. 652,http://dx.doi.org/10.1603/0022-2585(2005)042[0652:AOLAFA]2.0.CO;2.

Dossell, R., Millioni, R., Puricelli, L., Tessari, P., Arrigoni, G., Franchin, C., Segalla, A., Teardo, E., Redd, E. (2012) 'Molecular targets of antimicrobial photodynamic therapy identified by a proteomic approach', *Journal of Proteomics*, 7 7, pp. 3 2 9 – 3 4 3.

Dougherty, TJ (1998) 'A brief history of clinical photodynamic therapy development at Roswell Park Cancer Institute', *Journal of Clinical Laser Medicine & Surgery,* 14, pp. 219–221.

El Fouly A, Ertle J, El Dorry A, Shaker MK, Dechêne A, Abdella H, Mueller S, Barakat E, Lauenstein T, Bockisch A, Gerken G, Schlaak JF. (2015) 'In intermediate stage hepatocellular carcinoma: radioembolization with yttrium 90 or chemoembolization', *Liver International,* 35(2), pp. 627-35.

Eloff, J. N. (1998) 'Which extractant should be used for the screening and isolation of antimicrobial components from plants?'. *Journal of Ethnopharmacology*, 60, pp. 1–8.

El-Tayeb, T.A., El-Aziz, N.M.A. , Awad, H.H. . (2013) 'A study on the dynamics of Aedescaspius larval uptake and release of novel haematoporphyrin', *African. Entomology,* 21, pp. 15, http://dx.doi.org/10.4001/003.021.0108.

EPA (2002), Water Treatment Manuals Coagulation, Flocculation & Clarification.

EPA (2010), Water Quality in Ireland, 2007-2009.

EPA (2013), Water Treatment Report.

Epand, R. M., Epand, R. F. (2009) 'Lipid domains in bacterial membranes and the action of antimicrobial agents'*, Biochimica et Biophysica Acta (BBA),* 1788(1), pp. 289-294.

Ergaieg, K. and Seux, R. (2009) 'A comparative study of the photoinactivation of bacteria by meso-substituted cationic porphyrin, rose bengal and methylene blue, *Desalination* 246, pp. 353–362.

Ergaieg, K., Chevanne, M., Cillard, J., Seux, R. (2008) 'Involvement of both type I and type II mechanisms in Gram-positive and Gram-negative bacteria photosensitization by a *meso*-substitutedcationic porphyrin', *Solar Energy*, 82, pp.1107—17.

Ericsson, J. M., Sherris, J. C. (1971) 'Antibiotic sensitivity testing: report of an international collaborative study'. *Acta Pathologica et Microbiologica* Scandinavica, 217 (Suppl): pp. 1–90

Farrell, A., Quilty, B. (2002) 'Substrate dependent auto-aggregation of *Pseudomonas putida* CP1 during the degradation of mono-chlorophenols and phenol', *Journal of Industrial Microbiology and Biotechnology*, 28, pp. 316-324.

Ferro, S., Coppellotti, O., Roncucci, G., Ben Amor T. and Jori, G. (2006) 'Photosensitized inactivation of *Acanthamoeba palestinensis* in the cystic stage', *Journal of Applied Microbiology*, 101, pp. 206–212.

Ferro, S., Guidolin, L., Tognon, G., Jori. G. and Coppellotti, O. (2009) 'Mechanisms involved in the photosensitized inactivation of *Acanthamoeba palestinensis* trophozoites', *Journal of Applied Microbiology*, 107, pp. 1615–1623.

Fidai, S., Farmer, S. W., Hancock, R. E.W. (1997) 'Interaction of cationic peptides with bacterial membranes', *Methods in Molecular Biology*, 78, pp. 187– 204.

Fingar, V.H., Wieman, T.J., Karavolos, P.S., Doak, K.W., Ouellet, R., van Lier, J.E. (1993) 'The effects of photodynamic therapy using differently substituted zinc phthalocyanines on vessel constriction, vessel leakage and tumor response'. *Photochemistry and Photobiology,* 58, pp. 251–258.

Foote, C. S. (1991) 'Definition of type I and type II photosensitized oxidation', *Photochemistry and Photobiology*, 54, pp. 659-659

Funes, M. D., Caminos , D., Alvarez , M.G., Fungo, F., Otero, L., Durantini, E. (2009) 'Photodynamic properties and photoantimicrobial action of a electrochemically generated porphyrin polymeric films', *Environmental Science and Technology,* 43, pp. 902–908.

Gerba, C. O., Wallis, C., Melnick, J.L. (1977) 'Disinfection of Wastewater by Photodynamic Oxidation'. *Journal of the Water Pollution Control Federation*), 49(4), pp. 575-583.

Giese, A.C. (1953) 'Protozoa in photobiological research', *Physiological Zoology,* 26, 1.

Giovannetti, R. (2012) 'The Use of Spectrophotometry UV-Vis for the Study of Porphyrins', Macro To Nano Spectroscopy, Dr. Jamal Uddin (Ed.), , InTech, ISBN: 978-953-51-0664-7

Girotti A.W. (2001) 'Photosensitized oxidation of membrane lipids: reaction pathways, cytotoxic effects, and cytoprotective mechanisms', *Journal of Photochemistry and Photobiology: B,* 63, pp. 103–113.

Goble, F.C., Boyd, J.L. . (1959) 'Action of certain tetrapyrrole derivatives in experi-mental *Trypanosoma congolense* infections', *Experimental Biology and Medicine,* 100, pp. 745, http://dx.doi.org/10.3181/00379727-100-24765.

Graf, J., Togouet, S. Z., Kemka, N., Niyitegeka, D., Meierhofer, R. & Pieboji, J. G. (2010) 'Health gains from solar water disinfection (SODIS): evaluation of a water quality intervention in Yaounde, Cameroon'. *Journal of Water Health*, 8, pp. 779– 796.

Grinholc, M., Nakonieczna, J., Fila, G., Taraszkiewicz, A., Kawiak, A., Szewczyk, G., Sarna, T., Lilge, L., Bielawski, K.P. (2015) 'Antimicrobial photodynamic therapy with fulleropyrrolidine: photoinactivation mechanism of *Staphylococcus aureus*, in vitro and in vivo studies', *Applied Microbiology and Biotechnology,* 99, pp.4031–4043.

Gulino, A., Condorelli, G. G., Mineo, P., Fragalà, I. (2005) 'An x-ray photoelectron spectra and atomic force microscopy characterization of silica substrates engineered with a covalently assembled siloxane monolayer', *Nanotechnology,* 16, pp. 10.

Guo, Y., Rogelj, S., Zhang, P. (2011) 'Rose Bengal- decorated silica nanoparticles as photosensitisers for inactivation of gram-positive bacteria', *Nanotechnology*, 21,102–109. http://dx.doi.org/10.1088/0957-4484121/6/ 065102.

Hamblin, M. R., Hasan, T. (2004), 'Photodynamic therapy: a new antimicrobial approach to infectious disease?', Photochemical *and Photobiological Sciences*, 3, pp. 436-450.

Hamblin, M.R. (2012) 'Antimicrobial photodynamic therapy and photodynamic inactivation, or killing bugs with dyes and light', *Photochemictry and photobiology,* 88, pp. 496-498.

Hanakova A, Bogdanova K, Tomankova K, Binder S, Bajgar R, Langova K, Kolar M, Mosinger J, Kolarova H. (2014). Study of photodynamic effects on NIH 3T3 cell line and bacteria. *Biomedical Papers of the Medial Faculty of the University Palacky Olomouc Czech Republic,* 158, pp. 201–207.

Hegge, A.B., Bruzell, E., Kristensen, S., Tønnesen, H.H. (2012) 'Photoinactivation of Staphylococcus epidermidis biofilms and suspensions by the hydrophobic *photosensitiser* curcumin – Effect of selected nanocarrier Studies on curcumin and curcuminoides XLVII', *European Journal of Pharmaceutical Sciences,* 47, pp. 65–74.

Henke, P., Lang, K., Kubat, P., Sykora, J., Slouf, M. And Mosinger, J. (2013), 'Polystyrene nanofiber materials modified with an externally bound porphyrin photosensitiser', *Applied Materials & Interfaces*, 5, pp. 3776−3783

Henne, K., Kahlisch, L., Brettar, I and Hofle, MG. (2012) 'Analysis of structure and composition of bacterial core communities in mature drinking water biofilms and bulk water of a citywide network in Germany', *Applied and Environmental Microbiology*, 78, pp. 3530-3538.

Hijnen, W.A.M., Beerendonk, E.F., Gerriet Medema, G.J. (2006) 'Inactivation credit of UV radiation for viruses, bacteria and protozoan (oo) cysts in water: a review', *Water Res*earch, 40 (1), pp. 3-22.

Holt, J. G., Krieg, N. R., Sneath, P. H. A., Staley, J. T., Williams, S. T. (1994) 'Bergey's manual of determinative bacteriology'. In: Holt *et al.* (1994) *Facultatively anaerobic Gram-negative rods,* 9th edn. Lippincott Williams & Wilkins, Baltimore, Maryland, p 179.

Ibekwe, A.M., Grieve, C.M. (2003) 'Detection and quantification of *Escherichia coli* O157:H7 in environmental samples by real-time PCR', *Journal of Applied Microbiology* 94, pp. 421-431.

Inoué, S. (1990) 'Foundations of confocal scanned imaging in light microscopy', p. 1–17. In J. B. Pawley (ed.), *Handbook of Biological Confocal Microscopy* © Plenum Press, New York.

Jemli, M., Alouini, Z., Sabbahi, S., Gueddari, M., (2002) 'Destruction of faecal bacteria in wastewater by three photosensitisers', *Journal of Environmental Monitoring*, 4, pp. 511-516.

Jiménez-Hernández, M., Manjón, F., García-Fresnadillo, D. and Orellana, G. (2006) 'Solar water disinfection by singlet oxygen photogenerated with polymer supported Ru(11) sensitisers'. *Solar Energy*, 80, pp. 1382-1387.

Johnson GA, Ellis A, Kim H, Muthukrishnan N, Snavely T, *et al.* (2014) 'Photoinduced Membrane Damage of E. coli and S. aureus by the *Photosensitiser*- Antimicrobial Peptide Conjugate Eosin-(KLAKLAK)2'. *Plos One,* 9(3) pp.191-220. doi:10.1371/journal.pone.0091220.

Jori G. (2006) 'Photodynamic therapy of microbial infections: State- of- the-art and perspectives'. *Journal of Environmental Pathology, Toxicology and Oncology*, 25, pp.505–519.

Jori G., Spikes, J. D., (1984) 'Photobiochemistry of porphyrins. In: Topics in Photomedicine'. Smith KC (Ed.) 183-318

Junqueira, J.C., Ribeiro, M. A., Rossoni, R. D., Barbosa, J. O., Querido, S. M. R., Jorge, A. O. C. (2010) 'Antimicrobial Photodynamic Therapy: Photodynamic Antimicrobial Effects of Malachite Green on Staphylococcus, Enterobacteriaceae, and Candida', *Photomedicine and Laser Surgery,* 28(1), pp. 67-72.

Kassab, K., Dei, D., Roncucci, g., Jori, G., Coppellotti, O. (2003) 'Phthalocyanine-photosensitised inactivation of a pathogenic protozoan, *Acanthamoeba palesteninensis'*, *Photochemical and Photobiological Sciences*, 2, pp.668–672.

Kassab, K., Amor, T. B., Jori, G., Coppellotti, O. (2002) 'Photosensitization of *Colpoda inflata* cysts by *meso*-substituted cationic porphyrins'. *Photochemical and Photobiological Sciences*, 1, pp. 560–564.

Kato H, Komagoe K, Nakanishi Y, Inoue T, Katsu T. (2012) 'Xanthene dyes induce membrane permeabilization of bacteria and erythrocytes by photoinactivation'. *Photochemistry and Photobiology,* 88(2), pp. 423–431.

Komagoe K, Kato H, Inoue T, Katsu T. (2011) 'Continuous real-time monitoring of cationic porphyrin-induced photodynamic inactivation of bacterial membrane functions using electrochemical sensors'. *Photochemical and Photobiological Sciences,* 10(7), pp. 1181–1188

Konopka, K. and Goslinski, T. (2007) 'Photodynamic therapy in dentistry', *Journal of Dental Research,* 86, pp. 694–707.

Kossakowskaa, M., Nakoniecznaa, J., Kawiakb, A., Kurlendad, J., Bielawskia, K.P., Grinholc, M. (2013), 'Discovering the mechanisms of strain-dependent response of *Staphylococcus aureus* to photoinactivation: Oxidative stress toleration, endogenous porphyrin level and strain's virulence'. *Photodiagnosis and Photodynamic Therapy*, 10, pp. 348—355.

Krouit, M., Granet, R. and Krausz, P. (2009) 'Photobactericidal films from porphyrins grafted to alkylated cellulose - synthesis and bactericidal properties'*. European Polymer Journal,* 45, 4, 1250-1259.

Kuznetsova, N. A.; Makarov, D. A.; Kalya, O.L. (2007) 'Photosensitized oxidation by dioxygen as the base for drinking water disinfection'. *Journal of Hazardous Materials,* 146, pp. 487–491.

Lambrechts, S. A. G., Aalders, M. C. G., Langeveld-Klerks, D. H., Khayali, Y. & Lagerberg, J. W. M. (2003) 'Effect of monovalent and divalent cations on the photoinactivation of bacteria with meso-substituted cationic porphyrins'. *Journal of Photochemistry and Photobiology*, 79, pp. 297–302.

Lazzeri, D., Rovera, M., Pascual, L and Durantini, E.N. (2004), 'Photodynamic studies and photoinactivation of *Escherichia coli* using meso-substituted cationic porphyrin

derivatives with asymmetric charge distribution. *Photochemistry and Photobiology*, 80, pp. 286 – 293.

Levinson W. (2010), 'Antimicrobial Drugs: Resistance'. Levinson W, ed. *Review of Medical Microbiology and Immunology*. 11th ed. New York: McGraw-Hill; Chapter 11.

Linden, K. G., Shin, G. A., and Sobsey, M. D. (2002) 'Relative efficacy of UV wavelengths for the inactivation of Cryptosporidium paryum.' *Water Science and Technology*, 43,12, pp. 171.

Lucantoni, L., Magaraggia, M. , Lupidi, G. , Ouedraogo, R.K., Coppellotti, O., Esposito, F, Fabris, C., Jori, G., Habluetzel, A. . (2011) 'Novel, meso-substituted cationicporphyrin molecule for photo-mediated larval control of the dengue vector *Aedes aegypt*', *PLoS Neglected Tropical Diseases,* 5, pp. 14-34, http://dx.doi.org/10.1371/journal.pntd.0001434.

Luksiene, Z. (2005) 'New approach to inactivation of harmful and pathogenic microorganisms by photosensitization'. *Food Technology and Biotechnology',* 43, pp. 411-418.

Luksiene, Z., Danilcenko, H., Tarasevi˘ciene, Z. , Anusevicius, ˘Z. , Maroziene, A. , Nivinskas, H. (2007) 'New approach to the fungal decontamination of wheat used for wheat sprouts: effects of aminolevulinic acid', *International Journal of Food Microbiology.* 116, pp. 153, http://dx.doi.org/10.1016/j.ijfoodmicro.2006.12.040.

Luksiene, Z., Peciulyte, D., Lugauskas, A., (2004) ' Photodynamic inactivation of harmfuland pathogenic microorganisms', *Veterinary Medicine and Zootechnology*, 26, 58.

Luksiene, Z., Buchovec, I. , Paskeviciute, E. (2009) 'Inactivation of food pathogen *Bacillus cereus* by photosensitization in vitro and on the surface of packaging material, *Journal of Applied Microbiology,* 107, pp. 20-37, http://dx.doi.org/10.1111/j.1365-2672.2009.04383.x.

Lustigman, S., Berthus, E. (1996), 'Photosensitised inactivation of *Plasmodium falciparum* in human red cells by phthalocyanines', *Transfusion*, 28, pp. 643–648.

Lyons, M.M., Lau, Y.T., Carden, W.E., Ward, J.E., Roberts, S.B., Smolowitz, R., Vallino, J. and Allam, B. (2007) 'Characteristics of marine aggregates in shallow-water ecosystems: implications for disease ecology'. *Ecohealth*, 4, 4, 406 – 420.

Maclean, M., MacGregor, S.J., Anderson, J.G., Woolsey, G.. (2009) 'Inactivation of bacterial pathogens following exposure to light from a 405-nanometer light-emitting diode array', *Applied Environmental Microbiology*, 75, pp.1932–1937.

Magaraggia, M., Faccenda, F., Gandolfi, A., Jori, G. (2006) 'Treatment of microbiologically polluted aquaculture waters by a novel photochemical technique of potentially low environmental impact', *Journal of Environmental Monitoring*, 8 (9), pp.923–931.

Magaraggia, M., Jori,G., Soncin, M., Schofield, C.L., Russell, D. A. (2013) 'Porphyrin–silica microparticle conjugates as an efficient tool for the photosensitised disinfection of water contaminated by bacterial pathogens', *Photochemical and Photobiological Sciences,* 12, pp. 2170.

Mah, T.-F. C., O'Toole, G. A. , (2001) 'Mechanisms of biofilm resistance to antimicrobial agents,' *Trends in Microbiology*, vol. 9, no. 1, pp. 34–39, 2001

Maier, R., Pepper, I., & Gerba, C. (2000) 'Environmental microbiology'. Orlando, Florida: Academic Press.

Mai-Prochnow, A., Bradbury, M., Ostrikov, K., Murphy, A. (2015) '*Pseudomonas aeruginosa* Biofilm Response and Resistance to Cold Atmospheric Pressure Plasma Is Linked to the Redox-Active Molecule Phenazine'. *PLoS ONE,* 10(6)pp. e0130373. doi:10.1371/journal.pone.0130373.

Malato, S., Fernandez-Ibanez, P., Maldonado, M. I., Blanco, J., Gernjak, W. (2009) 'Decontamination and disinfection of water by solar photocatalysis: recent overview and trends,' *Catalysis Today*, vol.147,no. 1, pp.1–59.

Malik, Z., Hannania, J. and Nitzan, Y. (1990) 'Bactericidal effects of photoactivated porphyrins — an alternative approach to antimicrobial drugs', *Journal of Photochemistry and Photobiology B: Biology*, 5 (3–4), pp. 281–293.

Malik, Z., Ladan, H., Nitzan, Y. (1992) 'Photodynamic inactivation of Gram-negative bacteria: problems and possible solutions', *Journal of Photochemistry and Photobiology B: Biology*, 14, pp. 262–266.

Mamone, L.,Di Venosa, G.,Gándara, L., Sáenz, D., Vallecorsa, P., Schickinger, S., Rossetti, M.V., Batlle, A., Buzzola, F., Casas, A. (2014) 'Photodynamic inactivation of Gram-positive bacteria employing natural resources'. J*ournal of Photochemistry and Photobiology B: Biology,* 133, pp. 80–89.

Manjon, F., Garcia-Fresnadillo, D., Orellana, G. (2009) 'Water disinfection with Ru(II)photosensitisers supported on ionic porous silicones', *Photochemical and Photobiological Sciences,* 8, pp. 926‑932.

Manjon, F., Santana-Magana, M, Garcia-Fresnadillo, D., Orellana, G. (2010) 'Singlet oxygen sensitizing materials based on porous silicone: Photochemical characterization, effect of dye reloading and application to water disinfection with solar reactors', *Photochemical and Photobiological Sciences,* 9, pp. 838‑845.

Mavrodi D. V., Parejko J. A., Mavrodi O. V., Kwak Y. S., Weller D. M., Blankenfeldt W., et al. (2013) 'Recent insights into the diversity, frequency and ecological roles of phenazines in fluorescent *Pseudomonas* spp'. *Environmental Microbiology,* 15, pp. 675–686.

Mbakidi, J.P., Herke. K., Alvès, S., Chaleix, V., Granet, R., Krausz, P., Leroy-Lhez, S., Ouk, T.S., Sol, V. (2013) 'Synthesis and photobiocidal properties of cationic porphyrin-grafted paper'. *Carbohydrate Polymers,* 91, pp. 333– 338.

McGuigan, K.G., Conroy, R.N., Mosler, H.J., Preez, M.Du., UbombaJaswa, E., Fernandez-Ibanez, P., (2012) 'Solar water disinfection (SODIS): a review from benchtop to rooftop'*. Journal of Hazardous Materials,* 235–236, pp. 29–46.

Mena K.D., Gerba C.P. (2009) 'Risk Assessment of *Pseudomonas aeruginosa* in Water'. In: Whitacre D. (eds) Reviews of Environmental Contamination and Toxicology Vol 201. *Reviews of Environmental Contamination and Toxicology* (Continuation of Residue Reviews), vol 201. Springer, Boston, MA

Mendez-Vilas A, Ed. Science against Microbial Pathogens: Communicating current research and technological advances, Microbiology Book Series, Vol. 1. Badajoz, Spain, Formatex Research Center Publisherpp. 684-691.

Merchat, M., Spikes, G., Bertoloni, G., Jori, G. (1996) 'Studies on the mechanism of bacteria photosensitization by meso-substituted cationic porphyrins', *Journal of Photochemistry and Photobiology B: Biology,* 35, pp. 149–157.

Mezzatesta, M.L.,Gona,F., Stefani,S. (2012) '*Enterobactercloacae* complex: clinicalimpactandemergingantibioticresistance'. *Future Microbiology,* 7, pp. 887–902. doi: 10.2217/fmb.12.61

Mills, E.M., Takeda, K., Yu, Z.X., Ferrans, V., Katagiri, Y., Jiang, H., Lavigne, M.C, Leto, T.L., Guroff G. (1998) 'Nerve growth factor treatment prevents the increase in superoxide

produced by epidermal growth factor in PC12 cells'. *The Journal of Biological Chemistry,* 273, 22165-8.

Minnock, A., Vernon, D.I. , Schofield, J. ., Griffiths, J., Parish, J.H. ., Brown, S.B. (1996) 'Photoinactivation of bacteria. Use of a cationic water-soluble zinc phthalocyanine to photoinactivate both Gram-negative and Gram-positive bacteria', *Journal of Photochemistry and Photobiology B – Biology*, 32, pp. 159–164.

Minnock, A., Vernon, D.I., Schofield, J., Griffiths, J., Parish, J.H.and Brown, S.B. (2000) 'Mechanism of uptake of a cationic water-soluble pyridinium zinc phthalocyanine across the outer membrane of *Escherichia coli'*, *Antimicrobial Agents Chemotherapy*, 44 (3), pp. 522–527.

Moan J. (1990) 'On the diffusion length of singlet oxygen in cells and tissues'. *Journal of Photochemistry and Photobiology B: Biology*, 6, pp. 343–344.

Moan, J.; Peng, Q. (2003) 'An outline of the history of PDT'. Chapter 1. Published on 31 October 2007 on http://pubs.rsc.org | doi:10.1039/9781847551658-00001.

Montie, T. C. (1998) 'Biotechnology Handbooks 10 – Pseudomonas. Knoxville, Tenesse.

Mortelmans, K. & Riccio, E. S. (2000) 'The bacterial tryptophan reverse mutation assay with *Escherichia coli* WP2'. *Mutation Research/Fundamental and Molecular Mechanisms of Mutagenesis*, 455, (1-2), 61–69, ISSN 0027-5107.

Mortelmans, K. & Zeiger, E. (2000) 'The Ames Salmonella/microsome mutagenicity assay'. *Mutation Research/Fundamental and Molecular Mechanisms of Mutagenesis,* 455, (1-2), 29–60, ISSN 0027-5107.

MWH. (2005) 'Water treatment: principles and design'. 2nd edition. John Wiley and Sons, Hoboken, New jersey.

Naik, A.J.T., Ismail, S., Kay, C.,Wilson, M., Parkin, I . P. (2011) 'Antimicrobial activity of polyurethane embedded with methylene blue, toluidene blue and gold nanoparticles against *Staphylococcus aureus*, illuminated with white light'. *Materials Chemistry and Physics,* 129, pp. 446– 450.

Nakonechny, F., Nisnevitch, M., Nitzan, Y,., Firer, A. (2011) 'New techniques in antimicrobial therapy: scope of application and overcoming drug resistance in nosocomial infections'. In: Nakonechny, F., Pinkus, A., Hai, S., Yehosha, O., Nitzan, Y., Nisnevitch, M. (2013) 'Eradication of Gram-Positive and Gram-Negative Bacteria by *Photosensitiser*s Immobilized in Polystyrene'. *Photochemistry and Photobiology,* 89: pp. 671–678.

Nakonieczna,J., Grinholc, M. (2012) ‘Photodynamic inactivation requires innovative approach concerning numerous bacterial isolates and multicomponent sensitizing agents’. *Photodiagnosis and Photodynamic Therapy*, 9, pp. 359—361.

Nikaido, H. (1990) ‘Permeability of the lipid domains of bacterial membranes’, in *Membrane transport and Information Storage*, ed. R. C. Aloia, C. V. C. Curatin and L. M. Gordon, Alan R. Liss,New York, pp. 165–190.

Nisnevitch M., Nakonechny F., Firer M. and Nitzan Y. (2009) ‘Photodynamic antimicrobial chemotherapy with *photosensitiser*s in liposomes under external and chemoluminescent excitation’. *The Federation of European Biochemical Societies* (FEBS) Journal, 276 S1, 332.

Nitzan, Y., Wexler, H.M., Finegold, S.M. , (1994) ‘Inactivation of anaerobic bacteria byvarious photosensitized porphyrins or by hemin’, *Current Microbiology,* 29, 125, http://dx.doi.org/10.1007/BF01570752.

Nitzan, Y., Balzam-Sudakevitz, A. & Ashkenazi, H. (1998) ‘Eradication of Acinetobacter baumannii by photosensitized agents in vitro’, *Journal of Photochemistry and Photobiology*, 42, pp. 211–218.

Nitzan, Y., Shainberg, B. & Malik, Z. (1989) ‘The mechanism of photodynamic inactivation of *Staphylococcus aureus* by deuteroporphyrin’. *Current Microbiology*, 19, pp. 265–269.

Ohtsuki, A., Hasegawa, T., Hirasawa, Y., Tsuchihashi, H., Ikeda, S. (2009) ‘Photodynamic therapy using light-emitting diodes for the treatment of viral warts’. *Journal of Dermatology,* 36, pp. 525–528.

Oliveira, A., Almeida, A., Carvalho, C.M.B., Tome, J.P.C., Faustino, M.A.F., Neves, M.G.P.M.S., Tome, A.C., Cavaleiro, J.A.S., Cunha, A. (2009) ‘Porphyrin derivatives as *photosensitiser*s for the inactivation of *Bacillus cereus* endospores’. *Journal of Applied Microbiology*, ISSN 1364-5072.

Orlandi, V T., Caruso, E., Banfi S. and Barbieri, P. (2012) ‘Effect of Organic Matter on the In Vitro Photoeradication of *Pseudomonas aeruginosa* by Means of a Cationic Tetraaryl-porphyrin’. *Photochemistry and Photobiology*, 88pp. 557–564.

Orlandi, V T., Caruso, E., Tettamenti, G., Banfi S. and Barbieri, P. (2013) ‘Photoinduced antibacterial activity of two dicationic 5,15-diarylporphyrins’. *Journal of Photochemistry and Photobiology B: Biology,* 127, pp. 123–132.

Orlandi, V. T.; Bolognese, F.; Chiodaroli, L.; Tolker-Nielsen, T.; Barbieri, P. (2015) 'Pigments influence the tolerance of *Pseudomonas aeruginosa* PAO1 to photodynamically induced oxidative stress', *Microbiology,* 161, pp. 2298–2309.

Orlandi, V.T., Bolognese, F., Martegani, E., Cantaluppi, V., Medana, C., Barbieri, P. (2017) 'Response to photo-oxidative stress of Pseudomonas aeruginosa PAO1 mutants impaired in different functions', *Microbiology,* doi: 10.1099/mic.0.000543.

Osifeko, O. L., Nyokong, T. (2014) 'Applications of lead phthalocyanines embedded in electrospun fibers for the photoinactivation of Escherichia coli in water', *Dyes and Pigments,* 111, pp 11-15.

Pandey, R. K., Zheng, G. (2000) 'Porphyrins as *photosensitiser*s in Photodynamic Therapy'. In: The Porphyrin Handbook. Kadish, K.M., Smith, K.M, Gullard, R. Vol.6.

Parakh, P., Gokulakrishnan, S., Prakash, H. (2013) 'Visible light water disinfection using [Ru(bpy)2(phendione)](PF6)2.2H2O and [Ru(phendione)3]Cl2.2H2O complexes and their effective adsorption onto activated carbon'. *Separation and Purification Technology*, 109, pp.9–17.

Pattison, D. I., Rahmanto, A. S., Davies, M.J. (2012) 'Photo-oxidation of proteins', *Photochemical and Photobiological Sciences*, 11, pp. 38-53

Pawley, J. B. (ed.). (1995). Handbook of biological confocal microscopy. Plenum Press, New York.

Pelon, W., Whitman, B.F., Beasley, T.W. (1977) 'Reversion of histidine-dependent mutant strains of *Salmonella typhimurium* by Mississippi River water samples', *Environmental Science and Technology,* 11, pp. 619–623.

Peng, Q., Moan, J., Nesland, J.M., Rimington, C. (1990) 'Aluminum phthalocyanines with asymmetrical lower sulfonation and with symmetrical higher sulfonation: a comparison of localizing and photosensitizing mechanism in human tumor LOX xenografts'. *International Journal of Cancer*, 46, pp. 719–726.

Perlin, M., Mao, J.C.H., Otis, E.R., Shipkowitz, N.L. , Duff R.G., (1987) 'Photodynamic inactivation of influenza and herpes viruses by hematoporphyrin', *Antiviral Research*, 7, 43, http://dx.doi.org/10.1016/0166-3542(87)90038-6.

Plaetzer K, Krammer B, Berlanda J, Berr F, Kiesslich T. (2009) 'Photophysics and photochemistry of photodynamic therapy: fundamental aspects'. *Lasers in Medical Sciences,* 24(2), pp. 259–268.

Pond, K. (2005) 'Water recreation and disease infections: Plausibility of associated acute effects, sequelae and mortality'. London: IWA Publishing, World Health Organization.

Preuß, A., Saltsman, I., Mahammed, A., Pfitzner, M., Goldberg, I., Gross, Z., Röder, B. (2014) 'Photodynamic inactivation of mold fungi spores by newly developed charged corroles'. *Journal of Photochemistry and Photobiology B: Biology,* 133, pp. 39–46.

Preuβ A, Zeugner L, Hackbarth S *et al*. (2013) 'Photoinactivation of *Escherichia coli* (SURE2) without intracellular uptake of the photosensitizer', *Journal of Applied Microbiology.* 114(1), pp. 36–43

Pudziuvyte, B., Bakiene, E., Bonnett, R., Shatunov, P.A., Magaraggia, M., Jori, G. (2011) 'Alterations of *Escherichia coli* envelope as a consequence of photosensitization with tetrakis(*N*-ethylpyridinium-4-yl)porphyrin tetratosylate'. *Photochemocal and Photobiological Sciences,* 10(6), pp. 1046–1055.

Qin, Y., Luan, X., Bi, L., He, G., Bai, X., Zhou, C., Zhang, Z. (2008) 'Toluidine blue-mediated photoinactivation of periodontal pathogens from supragingival plaques'. *Lasers in Medical Sciences,* 23, pp.49–54.

Raab, O. (1900) 'Ueber die Wirkung fluorizierender Stoffe auf Infusorien,' Z. Biol. 39, 524–546.

Raetz, C. R. H. (1978) 'Enzymology, Genetics, and Regulation of Membrane Phospholipid Synthesis in *Escherichia coli'. Microbiological Reviews*, p. 614-659.

Reddi, E., Ceccon, M., Valduga, G., Jori, G. ., Bommer, J.C., Elisei, F., Latterini L., Mazzucato, U. (2002) 'Photophysical properties and antibacterial activityof *meso*-substituted cationic porphyrins', *Photochemistry and Photobiology*, 75 (5), pp. 462–470.

Reginfo-Herrera, J. A.. Sanabria, J.; Machuca, F.; Dierolf, C. F.; Pulgarin, C.; Orellana, G. (2007) 'A Comparison of Solar Photocatalytic Inactivation of Waterborne *E. coli* Using Tris(2,2'-bipyridin)ruthenium(II), Rose Bengal, and TiO_2'. *Journal of Solar Energy Engineering,* 129, pp.135.

Richardson, S.D., Thruston, A. D., Caughran, T.V., Chen, P.H., Collette, T.W., Schenck, K.M., Lykins, B.W., Rav-Acha, C., Glezer, V. (2000) 'Identification of new drinking water disinfection by-products from ozone, chlorine dioxide, chloramine, and chlorine'. *Water Air Soil Pollution*, 123(1)pp.95-102.

Rolim, J.P.M.L., de-Melo, M.A.S., Guedes, S.F., Albuquerque-Filho, F. B., de Souza, J.R., Nogueira, N. A.P, Zanin, I.C.J., Rodrigues, L.K.A. (2012) '*Journal of Photochemistry and Photobiology B: Biology* 106, 40–46.

Rossi, G., Goi, D., Comuzzi, C. (2012) 'The photodynamic inactivation of Staphylococcus aureus in water using visible light with a new expanded porphyrin. *Journal of Water and Health*, 103.

Sabbahi, S.; Ayed, L. B.; Boudabbous, A. (2013) 'Cationic, anionic and neutral dyes: effects of photosensitizing properties and experimental conditions on the photodynamic inactivation of pathogenic bacteria'. *Journal of Water and Health*, pp. 590-599.

Saino, E., Sbarra, M. S., Arciola, C. R., Scavone, M., Bloise, N., Nikolov, P., Ricchelli, F., Visai, L. (2010) 'Photodynamic action of tri-*meso* (*N*-methylpyridyl), *meso* (*N*-tetradecyl-pyridyl) porphine on *Staphylococcus epidermidis* biofilms grown on Ti6Al4V alloy'. *The International Journal of Artificial Organs,* 33(9), pp. 636–645.

Sampaio, R.N., Machado, A.E.H., Piovesan, E., Gonçalves, P.J., De Paula, R., Cavaleiro, J.A.S.,Barbosa Neto, N.M. (2014) 'Influence of the solvent-porphyrin interaction on the UVeVis absorption of free base imidazol cationic porphyrin'. *Dyes and Pigments*, 100, pp. 73 -78.

Schastak, S., Ziganshyna, S., Gitter, B., Wiedemann, P., Claudepierre, T. (2010) 'Efficient Photodynamic Therapy against Gram-Positive and Gram-Negative Bacteria Using THPTS, a Cationic *Photosensitiser* Excited by Infrared Wavelength'. *PLoS ONE,* 5(7)pp. e11674. doi:10.1371/journal.pone.0011674.

Schoenen, D. (2002) 'Role of disinfection in suppressing the spread of pathogenswith drinkingwater: possibilities and limitations',*Water Research*, vol. 36, no. 15, pp. 3874–3888.

Schuitmaker, J.J., Baas, P., van Leengoed, H.L.L.M., van der Meulen, F.W., Star, W.M., van Zandwijk, N. (1996) 'Photodynamic therapy: a promising new modality for the treatment of cancer'. *Journal of Photochemistry and Photobiology B: Biology,* 34, pp. 3-12

Sharman, W.M., Allen, C.M., Van Lier, J.E. (2000) 'Role of activated oxygen species in photodynamic therapy'. *Methods Enzymology, pp.* 319, 376–400.

Silhavy, T.J., Kahne, D., Walker, S. (2010) 'The bacterial cell envelope. *Cold Spring Harbor Perspect. Biology,* 2(5), a000414.

Silva, R.N., Tomé, A.C., Tomé, J.P.C., Neves, M.G.P.M.S., Faustino, M.A.F., Cavaleiro, J.A. S., Oliveira, A., Almeida, A., Cunha, A. (2012) 'Photo-inactivation of *Bacillus* endospores: inter-specific variability of inactivation efficiency'. *Microbiology and Immunology*, 56, pp. 692–699.doi:10.1111/j.1348-0421.2012.00493.x

Sniadecki J. ‘Jerdrzej Sniadecki (1768–1838) On the cure of rickets’ (1822) Cited by W. Mozolowski. *Nature.* 1939;143, pp. 121–124.

Sousa, J.C.F., Silva, M.T., Balassa, G. (1976) ‘An exosporium-like outer layer in *Bacillus subtilis* spores’. *Nature,* 263, pp. 53–54.

Spagnul, C., Turner, L. C., Boyle, R. W. (2015) ‘Immobilized photosensitizers for antimicrobial applications’, *Journal of Photochemistry and Photobiology B: Biology*,150, pp.11‑30.

Spesia, M.B., Lazzeri, D., Pascual, L., Rovera, M, Durantini, E.N. (2005) ‘Photoinactivation of Escherichia coli using porphyrin derivatives with different number of cationic charges’, *FEMS Immunology and Medical Microbiology*, 44, pp. 289–295.

Stojicic S, Amorim H, Shen Y, Haapasalo M. (2013) ‘*Ex vivo* killing of *Enterococcus faecalis* and mixed plaque bacteria in planktonic and biofilm culture by modified photoactivated disinfection’. *International Endodontic Journal*, 46, pp. 649–59.

Stojiljkovic, I., Evavld, B. D., Kumar, V. (2001) ‘Antimicrobial properties of porphyrins’. *Expert Opinion on Investigational Drugs*, 10(2), pp. 309-320.

Strakhovskaya, M., Antonenko, Y.N., Pashkovskaya, A., Kotova, E. A., Kireev V, Zhukhovitsky, V.G., Kuznetsova, N.A, Yuzhakova, O.A, Negrimovsky, V.M, Rubin, A.B. (2009) ‘Electrostatic binding of substituted metal phthalocyanines to enterobacterial cells: its role in photodynamic inactivation’. *Biochemistry (Moscow),* 74(12), pp. 1305–1314.

Street, C.N. and Gibbs, A. (2010) ‘Eradication of the corrosion –causing bacterial strains *Desulfovibrio vulgaris* and *Desulfovibrio desulfuricans* in planktonic and biofilm form using photodisinfection’. *Corrosion Science,* 52(4), pp. 1447-1452.

Sundaresan, M., Yu, Z.X., Ferrans, V.J., Irani, K. & Finkel, T. (1995) ‘Requirement for generation of HO for plate let derived growth factor signal transduction’. *Science,* 270, 2969.

Tardivo, J. P., Del Giglio, A., de Oliveira C.S., Gabrielli, D. S., Junqueira, H. C., Tada, D. B., Severino, D., Turchiello, R. F., Baptista, M. S. (2005) ‘Methylene blue in photodynamic therapy: from basic mechanisms to clinical applications’. *Photodiagnosis and Photodynamic Therapy,* 2(3), pp. 175–191

Tavares, A., Carvalho, C. M. B., Faustino, M. A., Neves, M. G. P. M. S., Tomé, J. P. C., Tomé, A. C., Cavaleiro, J. A. S., Cunha, Â., Gomes, N. C. M., Alves, E. & Almeida, A.

(2010). Antimicrobial photodynamic therapy: study of bacterial recovery viability and potential development of resistance after treatment Mar. Drugs 8, 91–105.

Tavares, A,, Dias, S. R. S., Carvalho, C. M. B., Faustino, M. A. F. , Tomé, J. P. C., Neves, M. G. P. M. S., Tomé, A. C., Cavaleiro, J. A. S. , Cunha, A. , Gomes, N. C. M. , Alves E., Almeida, A. (2011) 'Mechanisms of photodynamic inactivation of a Gram-negative recombinant bioluminescent bacterium by cationic porphyrins', Photochemical and Photobiological Sciences, 10, pp. 1659–1669.

Tegos, G., Anbe, M., Yang, C., Demidova, T., Satti, M., Mroz, P., Janjua, S., Gad, F., Hamblin, M. (2006) 'Protease-stable polycationic *photosensitiser* conjugates between polyethyleneimine and chlorin(e6) for broad-spectrum antimicrobial photoinactivation'. *Antimicrobial agents and Chemotherapy,* pp. 1402–1410.

Thandu, M., Commuzi, C., Goi, D. (2015) 'Phototreatment of Water by Organic Photosensitizers and Comparison with Inorganic Semiconductors'. *International Journal of Photoenergy*, Article ID 521367, 22 pages http://dx.doi.org/10.1155/2015/521367.

Thompson, C.N, Duy PT, Baker S (2015) 'The Rising Dominance of *Shigella sonnei*: An Intercontinental Shift in the Etiology of Bacillary Dysentery'. *PLoS Neglected Tropical Diseases,* 9(6): e0003708. https://doi.org/10.1371/journal.pntd.0003708

Tolba, O., Loughrey, A., Goldsmith, C., Millar, B. C., Rooney, P. J. & Moore, J. E. (2008) 'Survival of epidemic strains of healthcare (HA-MRSA) and community-associated (CA-MRSA) meticillin-resistant Staphylococcus aureus (MRSA) in river-, sea- and swimming pool water. *International Journal of Hygiene and Environmental Health,* 211, pp. 398–402.

Tosk, J., Sherif, A., Hall, R., Lau, B. (1986) 'Phototoxicity of hematoporphyrin derivative in larvae of *Culex quinquefasciatus*', *Proceedings and Papers of the Annual Conference of the California Mosquito Control Association, 54*, 70.

Tota-Maharaj, K., Meeroff, D.E. (2013) 'Evaluation of Solar Photosensitised River Water Treatment in the Caribbean'. *International Journal of Photoenergy*, Article ID 487890, 10 pages.

Tümmler, B.,Wiehlmann, L., Klockgether, J., Cramer, N., (2014) 'Advances in understanding Pseudomonas'. *F1000prime reports*. 6 p. 9.

Usacheva, M. N., Teichert, M.C., Biel, M.A. (2003) 'The role of the methylene blue and toluidine blue monomers and dimers in the photoinactivation of bacteria'. *Journal of Photochemistry and Photobiology B: Biology*, 71, pp. 87–98.

Usacheva, M. N., Teichert, M. C., Sievert, B. A. C. E., Biel, M. A. (2006) 'Effect of Ca2þ on the Photobactericidal Efficacy of Methylene Blue and Toluidine Blue Against Gram-Negative Bacteria and the Dye Affinity for Lipopolysaccharides', *Lasers in Surgery and* Medicine, 38, pp.946–954.

Usacheva, M. N., Buddhadev, L., Saif, S. R. N., Swayam, P. (2006) 'Nanoparticle-Mediated Photodynamic Therapy for Mixed Biofilms', *Journal of Nanomaterials, 2016*, Article ID 4752894.

Vilela, S.F.G., Junqueira, J.C., Barbosa, J.O., Majewski, M., Munin, E., Jorge, A.O.C. (2012) 'Photodynamic inactivation of Staphylococcus aureus and Escherichia coli biofilms by malachite green and phenothiazine dyes: An in vitro study'. *Archives for oral Biology,* 57, pp. 704 – 710.

Villanuena, A. (1993) 'The cationic meso-substituted porphyrins: an interesting group of photosensitizers', *Journal of Photochemistry and Photobiology B: Biology,* 18, pp. 295-298.

Vollmer, W., Seligman, S.J. (2010) 'Architecture of peptidoglycan: more data and more models'. *Trends in Microbiology,* 18(2), pp. 59–66.

Wagner, A. B. V. Water resource management in an interdisciplinary perspective, (1997).*Euro-Mediterranean Sciences and Technology Cooperation*, ed. M. Kayamanidou, Ballière Tindall, London, pp. 44–46.

Weaste, R. C. (1975), Handbook of Chemistry and Physics, 56th Edition, Ed. (1975). CRC Press, Cleveland.

WHO (2008). Water treatment and pathogen control.

WHO (2011). Cause-specific mortality: regional estimates for 2008. Geneva, World Health Organization.

WHO (2011). Guidelines on drinking water.

WHO/UNICEF (2010), Joint Monitoring Programme for Water Supply|| Sanitation and Hygiene (JMP).

Wohllebe, S., Richter, R., Richter, P., Häder, D.P. (2009) 'Photodynamic control ofhuman pathogenic parasites in aquatic ecosystems using chlorophyllin andpheophorbid as photodynamic substances', *Parasitology Research*, 104, 593,http://dx.doi.org/10.1007/s00436-008-1235-6.

Yu, K.G., Li, D.H., Zhou, C.H. and Diao, J.L. (2009) ‘Study on the synthesis and antimicrobial activity of novel cationic porphyrins’. *Chinese Chemical Letters,* 20, pp. 411–414.

Zhang, B., Yu, Q., Jia, C., Wang, Y., Xiao, C., Dong, Y., Xu, N., Wang, L., Li, M. (2015) ‘A synthetic Mn_4Ca-cluster mimicking the oxygen-evolving center of photosynthesis’, *Science,* 6235, pp. 690-693.

Appendix I

TMPyP concentration in the glass beads

Using the linear equation obtained from the calibration curve between TMPyP solution absorbance and concentration (Figure 3.2), the amount of porphyrin coating the glass beads could be calculated.

Using the equation: $0.226 = 71541.\mathrm{x} + 0.0087$

Where x is the concentration (mol/L) wanted and y is the known absorbance (0.226 AU), which obtained by UV-visible spectroscopy of the glass petri dish where the beads were immersed in TMPyP solution (10μM). Therefore,

$$0.226 = 71541.\mathrm{x} + 0.0087, \text{ so}$$

$$\mathrm{x} = 0.00000304 \ \frac{mol}{L}$$

The concentration of the porphyrin in the glass beads surface is approximately 0.00000304 mol/L or 3.04μM.

Extinction coefficient (ε) calculation

For the ε calculation the following equation (Weast *et al.,* 1975).

$$\varepsilon = \frac{A_\lambda}{c.L}$$

Where, A_λ is the compound absorbance at a specific wavelength, *c* is the compound concentration (mol/L) and *L* is the light path length, in centimetres (always adjusted to 1cm in laboratory spectrophotometers).

The values for the absorbance and concentration, which were used to obtain the calibration curve, are in table AI.

Table AI – TMPyP absorbance and respective concentration in PBS at 422nm.

Absorbance (AU)	Concentration (μM)	Concentration (M)
0	0	0
0.1902	2.5	0.0000025
0.2779	3.65	0.00000365
0.3754	5	0.000005
0.5128	7.5	0.0000075
0.7248	10	0.00001

Therefore,

$$\varepsilon = \frac{0.2779}{3.65.10^{-6}.1} = 76{,}000\ M^{-1}.cm^{-1}$$

Singlet oxygen quantum yield calculation

The singlet oxygen quantum yield of TMPyP in PBS was calculated using the equations shown in item 2.2.1.2 - Near-infrared spectroscopy - singlet oxygen generation, and the values obtained from the graph and used on the calculations are shown below:

First, the unwanted area was calculated:

$$Z = 149\left(\frac{83.26 + 130.5}{2}\right)$$

$$Z = 15{,}925$$

Then the integrated area of TMPyP emission:

$$I = 71{,}436 - 15{,}925$$

$$I = 55{,}519$$

And finally, the quantum yield was calculated:

$$\Phi_{TMPyP} = 0.22 \,.\, \frac{55.519}{25{,}262} . \frac{0.20}{0.13} = 0.74$$

Appendix II

Publications and conferences

Journal articles

Passos, T. M., Marconato, J. C., Martins-Franchetti, S. M. (2015) 'Biodegradation of films of low density polyethylene (LDPE) poly(hydroxibutyrate-co-valerate) (PHBV), and LDPE/PHBV (70/30) blend with Paecilomyces variotii', *Polímeros,* doi.org/10.1590/0104-1428.1432.

Goddard, A.R., Pérez-Nieto, S.; Passos, T. M., Quilty, B.; Carmichael, K., Irvine, D. J.; Howdle, S. M. (2016) 'Controlled polymerisation and purification of branched poly (lactic acid) surfactants in supercritical carbon dioxide', *Green Chemistry*. doi: 10.1039/c6gc00745g.

Oliveira, R. N., Moreira, A. P.D., Mancini, M. C., Oliveira, F. C. S., Passos, T. M., Quilty, B., Thiré, R. M. S. M., McGuinness, G. B. (2016) 'FTIR analysis and quantification of phenols and flavonoids of five commercially available plants extracts used in wound healing', *Revista Matéria,* 11743, pp.767-779.

Keogan, D. M., Fagan, L. E., Passos, M. P.; Müller-Bunz, H., Quilty, B.; Griffith, D. M. (2016) 'Synthesis of polymeric bismuth chlorido hydroxamato complexes, X-ray crystal structure and antibacterial activity of a novel Bi(III) salicylhydroxamato complex', *Inorganica Chimica Acta*. doi: https://doi.org/10.1016/j.ica.2016.09.021.

Oliveira, R. N., Moreira, A. P.D., Thiré, R. M. S. M., Quilty, B., Passos, T. M., Simon, P., Mancini,M. C., McGuinness, G. B. (2017) 'Absorbent polyvinyl alcohol–sodium carboxymethyl cellulose hydrogels for propolis delivery in wound healing applications' *Polymer Engineering and Science.* doi: 10.1002/pen.24500.

Conferences

Oral presentation:

Passos, T. M., Pryce, M., Quilty, B. (2017). 'Antimicrobial photodynamic inactivation of *Pseudomonad* strains'. Oral presentation at the 17th Congress of the European Society for Photobiology. Pisa, Italy, 4th to 8th of September.

Poster presentations:

Passos, T. M., Pryce, M., Quilty, B. (2015). An innovative approach for the photodisinfection of water using photosensitisers. Paper presented at the School of Biotechnology 7th Annual Research Day, Dublin City University, Dublin, 30th of January.

Passos, T. M., Pryce, M., Quilty, B. (2015). An innovative approach for the photodisinfection of water using photosensitisers. Paper presented at the 1st Brazil Ireland Science Week, Dublin Castle, Dublin, 23rd to 26th of February.

Passos, T. M., Pryce, M., Quilty, B. (2015). Photodynamic Inactivation - a novel approach to water disinfection. Paper presented at the 5th Irish Environmental Researchers Colloquium (Environ 2015), IT Sligo, Sligo, 8th to 10th of April.

Passos, T. M., Pryce, M., Quilty, B. (2015). Application of TMPyP in Bacterial Photodynamic Inactivation for Water Disinfection. Paper presented at the 115th General Meeting – American Society for Microbiology, New Orleans Ernest N. Memorial Convention Center. New Orleans, 30th of May to 2nd of June.

Passos, T. M., Pryce, M., Quilty, B. (2016). Application of TMPyP in Bacterial Photodynamic Inactivation for Water Disinfection. Paper presented at the 26th Irish Environmental Researchers Colloquium (Environ 2016), University of Limerick, Limerick, 22nd-24th March.

Passos, T. M., Pryce, M., Quilty, B. (2017). Effectiveness of photodynamic inactivation of microorganisms monitored by culturable and non-culturable techniques. Paper presented at the Microbiology Society Annual Conference, Edinburgh International Conference Centre, Edinburgh, 3rd-6th April.

Passos, T. M., Pryce, M., Quilty, B. (2017). Influence of bacterial cell aggregation on water disinfection with photodynamic inactivation. Paper presented at the 10th International Conference in Biofilm Reactors, University College Dublin, Dublin, 9th – 12nd May.